CHARACTERIZATION OF CELLULAR IMMUNE RESPONSES DURING LASSA VIRUS INFECTION IN MICE AND HUMANS

VORGELEGT DEM
FACHBEREICH 2 (BIOLOGIE/CHEMIE) DER
UNIVERSITÄT BREMEN
ALS DISSERTATION
ZUR ERLANGUNG DES GRADES EINES DOKTORS
DER NATURWISSENSCHAFTEN
(DR. RER. NAT.)

ANGEFERTIGT IN DER ABTEILUNG VIROLOGIE AM
BERNHARD-NOCHT-INSTITUT
FÜR TROPENMEDIZIN, HAMBURG

VORGELEGT VON
DAVID MAXIMILIAN WOZNIAK

HAMBURG, 2019

DATUM DER DISPUTATION: 23.08.2019

GUTACHTER DER DISSERTATION:

1. PROF. DR. RER. NAT. ANDREAS DOTZAUER
   UNIVERSITÄT BREMEN, FB 2

2. PROF. DR. MED. STEPHAN GÜNTHER
   BERNHARD-NOCHT-INSTITUT FÜR TROPENMEDIZIN, HAMBURG

Table of Contents

List of Abbreviations

actB: beta-actin
ADCC: antibody dependent cellular cytotoxicity
alv.: alveolar
ANOVA: analysis of variance
APC: antigen presenting cell
-APC: -allophycocyanin
AST: Aspartate aminotransferase
B cell: B lymphocyte
Ba366: Bantou 366 (strain)
BALT: bronchus-associated lymphoid tissue
BNITM: Bernhard-Nocht-Institute for Tropical Medicine
BSL: Biosafety Level
BUV: Brilliant Ultraviolet
BV: Brilliant Violet
Ca: calcium
CARD: caspase-recruitment domain
CD: Cluster of differentiation
CD40L: CD40 ligand
cDC: conventional DC
C-domain: constant domain
CFSE: carboxyfluorescein succinimidyl ester
CTLA-4: cytotoxic T lymphocyte associated protein 4
Cy: Cyanine
DC: dendritic cell
D-domain: diversity domain
DMEM: Dulbecco's Modified Eagle's Media
DMSO: Dimethyl sulfoxide
DNA: desoxyribonucleic acid
dpi: days post infection
EBOV: Ebola virus
EDTA: Ethylenediaminetetraacetic acid
ESCRT: endosomal sorting complex required for transport
FACS: fluorescence-activated cell sorting
FCS: fetal calf serum
FFU: focus forming unit
FITC: fluoresein isothiocyanate
G1: gap 1
GA391: Lassa virus strain GA391
GMEM: Glasgow minimum essential medium
GOT: Glutamic Oxaloacetic Transaminase
GP: glycoprotein
GPC: Glycoprotein precursor
H-2K^{b}: specific murine MHC Class I allele
HBSS: Hank's Balanced Salt Solution
HHD: human HLA-A2.1 murine H-2Db fusion receptor
HLA-DR: Human Leukocyte Antigen - serotype; DR
i.n.: intranasal
i.p.: intraperitoneal
i.v.: intravenous
Iba-1: ionized calcium-binding adapter molecule 1
IC_{50}: half maximal inhibitory concentration
IFA: Immunofocus Assay
IFN: Interferon
IFNAR: interferon alpha/beta receptor
IFNAR^{BL6}: bone marrow-chimeric IFNAR knock-out mice with C57BL/6 bone marrow
IgG: Immunoglobulin Class G
IgM: Immunoglobulin Class M
IGR: intergenic region
IKKε: IκB kinase ε
IL: Interleukin

IRF3: interferon regulatory factor 3
ISTH: Irrua Specialist Teaching Hospital
ITIM: immunoreceptor tyrosine-based inhibitory motif
JAK: Janus kinase
J-domain: junction domain
JUNV: Junin virus
kb: kilobase
kDa: kilodalton
KLRG1: cell lectin-like receptor subfamily G, member 1
L: L protein (arenaviral polymerase)
LAMP1: Lymphosomal-associated membrane protein 1
LASV: Lassa virus
LCMV: lymphocytic choriomeningitis virus
LF: Lassa fever
Lin: Lineage markers
L-segment: Large segment
LuJV: LuJo virus
Ly5.1: natural allelic isoform of CD45 known as CD45.1
***M. natalensis*:** *Mastomys natalensis*
MACS: Magnetic-activated cell sorting
MACV: Machupo virus
MALT: mucosa-associated lymphoid tissues
MAVS: mitochondiral antiviral signaling protein
MDA5: Melanoma differentiation-associated protein 5
MHC: major histocompatibility complex
MOI: multiplicity of infection
MORV: Morogoro virus
Mx: myxovirus resistance
MΦ: macrophage
NFAT: nuclear factor of activated T cells
NF-κB: nucelar factor kappa-light-chain-enhancer of activated B cells
NHP: non-human primate
NIR: near infra-red
NK cell: natural killer cell
NP: nucleoprotein
OT-I: ovalbumin-specific TCR 1
PAMP: pathogen-associated molecular pattern
PBMC: periphal blood mononuclear cell
PBS: Phosphate buffered solution
PCR: Polymerase chain reaction
PD-1: programmed cell death protein 1
pDC: plasmacytoid DC
PD-L1: PD-1 ligand
-PE: -phycoerythrin
PerCP: Peridinin-chlorophyll-protein complex
PMA: Phorbol myristate acetate
PRR: pattern-recognition receptor
qPCR: quantitative polymerase chain reaction
RAG: recombination associated gene
RBC: red blood cell
RIG-I: retinoic acid inducible gene I
RNA: ribonucleic acid
RNP: ribonucleoprotein
RT-PCR: reverse transcript polymerase chain reaction
SCID: Severe Combined Immune Deficiency
SD: standard deviation
SCS: single cell suspensions
SKI-1/S1P: Subtilisin Kexin Isozyme-1 / Site-1 Protease
SLEC: short-lived effector cell

S-segment: Small segment
STAT: Signal Transducer and Activator of Transcription proteins
T cell: T lymphocyte
TACV: Tacaribe virus
T_{CM}: central memory T cell
TCR: T cell receptor
T_{eff}: effector T cell
T_{EM}: effector memory T cell
TLR: toll-like-receptor
TMB: 3,3',5,5'-Tetramethylbenzidine
TNF: tumor necrosis factor
TSST-1: toxic shock syndrome toxin 1
U: enzyme unit
UTR: untranslated region
vcRNA: viral copy RNA
V-domain: variable domain
vmRNA: Viral mRNA
vRNA: viral RNA
WHO: World Health Organization
Z: Z protein (arenaviral matrix protein)
α-: anti-

1. Introduction

Lassa fever (LF) is a viral hemorrhagic fever disease endemic to West African countries. Estimations of yearly infection rates range up to 300,000 people each year with estimated 5,000 fatalities [1]. Many parts of Lassa fever pathogenesis are not yet fully understood, leaving humans vulnerable to outbreaks since no approved vaccines or specific treatments exist. This gives strong precedence to increase our research and deepen our knowledge of this disease.

1.1 Discovery of Lassa fever and outbreaks

The first reported cases of Lassa fever (LF) occurred in 1969 in Nigeria on the Jos plateau. After treating local patients, the nurses Laura Wine, Lily Pinneo and Harry Elyea at the Jos Mission Hospital sequentially fell ill of a back then unknown disease [2]. Laura Wine died from this unknown combination of symptoms, while Lily Penny Pinneo and Harry Elyea were able to be evacuated to the USA, where they slowly recovered from the Lassa fever. The *Lassa mammarenavirus* (LASV) itself was first isolated by a research team around Dr. John Frame at Yale University.

Since then various countries ranging from Guinea, Sierra Leone, Liberia to Nigeria are reporting outbreaks of LF, while reports of singular cases can also be found throughout other West African countries [3-5].

In the past, outbreaks of LF usually occurred on a small locally contained scale, but with increasing mobility and rising population density in West Africa the chance of an uncontrolled epidemic spread increases. At the same time slowly rising standards of living and hygienic standards in West Africa partially reduce the chance of transmission. However, import of this disease via aircraft passengers makes LF also a global concern. As a disease with major health system impact and epidemic potential LF was prioritized by the WHO in their Research and Development Blueprints from 2015 on [6].

LASV infections occur mostly during the local dry season each year. Potential explanations for this include that the natural reservoir host of LASV, *Mastomys natalensis*, lives closer to humans, because of natural food shortages during the dry season [7]. It is also hypothesized, that due to increased stability of LASV at low relative humidity, virus particles could also be transmitted via aerosolized dust from *Mastomys* urine [8], leaving LF a wide spread health risk in West Africa.

1.2 Epidemiology

Most laboratory confirmed cases of LF in the last years have been reported from Nigeria. Nevertheless, LF cases were also reported by other West African countries like Guinea, Sierra Leon, Liberia, Mali, Benin and Togo [4, 9, 10] during the last decades. Broad serological antibody studies of humans point towards a geographical spread of Lassa virus (LASV) in countries like Côte d'Ivoire, Burkina Faso and Ghana [11]. These serological studies also revealed regionally high seroprevalence of anti-Lassa antibodies in native people, indicating that the overall morbidity and mortality rates of Lassa virus infection are lower than the hospitalization and case fatality rates suggest. However, past nosocomial outbreaks still reached case fatality rates as high as 65% [12].

Other viral diseases like influenza infections often show complicated disease progression in immune compromised people like children and elderly [13]. LF cases however are seen in all age groups and prominent in healthy adults (20-50 years), which are usually considered to be in prime physiological condition. It remains not fully understood if strong immunological reactions favor LF disease progression or if adults are more prone to LASV infection, because of behavioral and sociological aspects.

1.3 Natural reservoir host *Mastomys natalensis*

The natural transmission route of LASV occurs from animal to human, marking LF as a zoonosis [14]. The natural reservoir hosts of LASV are small rodents, mostly the multimammate mouse *Mastomys natalensis,* but LASV has also been detected in other rodent species like *Mastomys erytholeucus* and *Hylomyscus pamfi* [15].

Like the majority of small rodent species, *M. natalensis* is highly reproductive. The mice are distributed over wide areas of Sub-Saharan Africa (Figure 1 [16]), nevertheless LASV has only been found in West African *Mastomys* sp. [17]. The wide geographical spread, high reproductivity and the feeding habits of an adaptive generalist make the eradication of *M. natalensis* and consequentially of LASV by conventional vermin-control practically impossible.

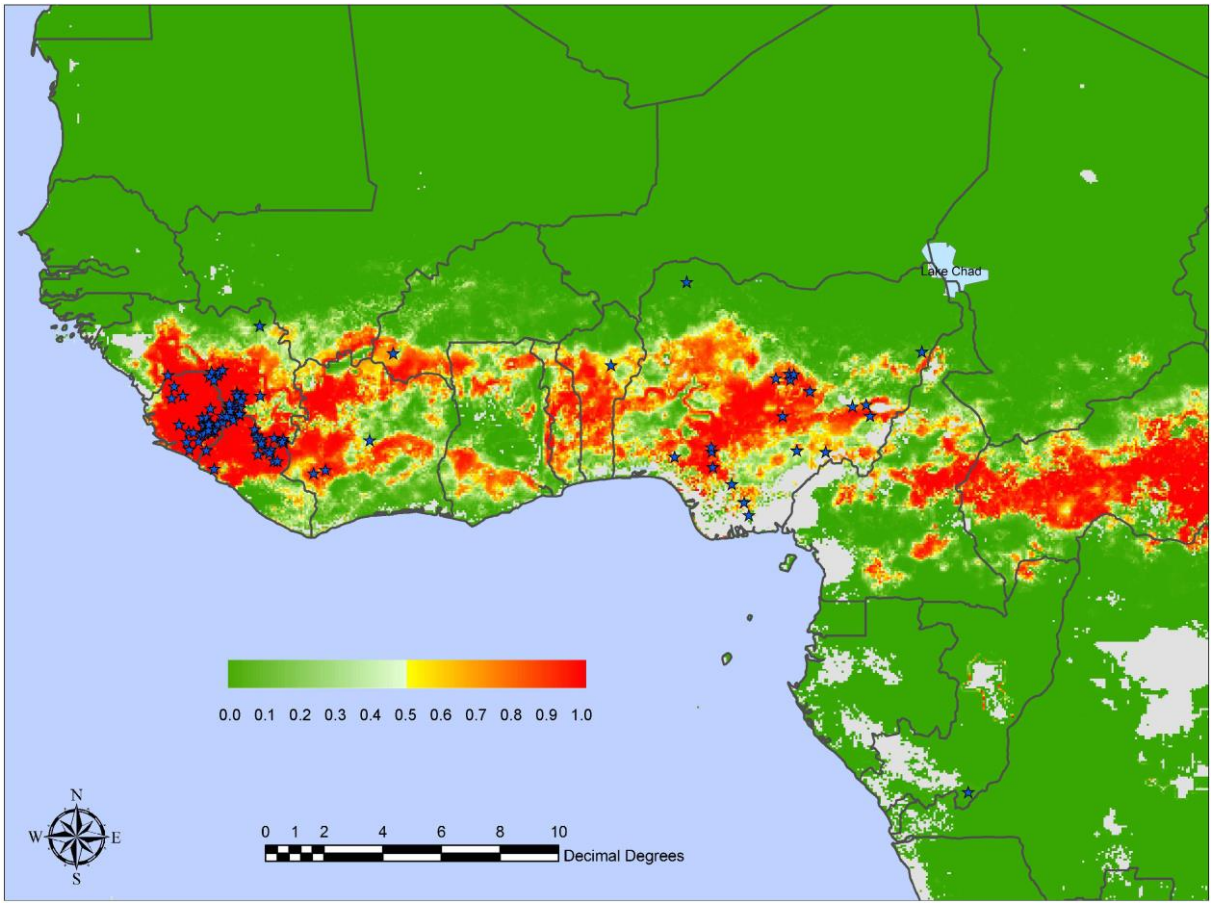

Figure 1 Mean predicted Lassa risk map for West Africa based on *Mastomys natalensis* habitat spread. Probability scale range from 0.0 (green) to 1.0 (red). Blue stars indicate LASV localities. Grey areas are excluded from predictions due to insufficient satellite imagery (cloud coverage) or environmental conditions are outside the model's limit. Image: Fichet-Calvez & Rogers 2009 [16] CC BY.

1.4 Possible transmission routes of LASV

M. natalensis is considered vermin in West African countries. These rodents can often be found close to human dwellings, foraging for food in human storages. It is speculated, that transmission therefore mostly occurs via food contaminated with urine or feces of *M. natalensis* [18, 19]. Other sources of transmission could include direct contact with the infected rodents' blood during killing or contact due to hunting, trading, preparation and consumption of *M. natalensis* as bush meat [20].

While most LF cases occur through spillover events from the rodent reservoir, human to human transmissions, especially in hospital settings have been reported. LASV infected people excrete LASV RNA in all bodily fluids including saliva, urine, feces, blood and semen [21]. Historically, these nosocomial outbreaks rear the highest lethality rates. It remains unclear if the disease course is worsened, because of higher inoculation titers in human-to-human-transmission or if viral codon-adaption through human host

passage could be responsible for the increased pathogenicity as it is being hypothesized [22].

1.5 Symptoms of Lassa fever

The clinical symptoms of Lassa fever are ambiguous and are often mistaken for other common tropical febrile illnesses like malaria, typhoid fever or influenza. Common symptoms include: fever, sore throat, cough, headache, malaise, chest and muscle pain, vomiting and diarrhea [23]. Less frequent symptoms are oral ulcers, purulent pharyngitis, facial oedemas, petechiae and intestinal hemorrhage. These less frequent symptoms are specific for viral hemorrhagic fevers, but are also indicators of a severe disease progression. Additional complications of LF can arise in late infection or early reconvalescent stages with sensorineural hearing loss [24]. In studies from the 1980s LF in humans was associated with a leukopenia in the early symptomatic time frame, while late severe course are marked especially by granulocytosis and expansion of lymphocytes [25]. Levels of transaminases like AST/GOT (Aspartate aminotransferase) are elevated in patient serum during LF, exceeding AST levels of >200 U/L in severe cases. Another common complication of severe Lassa fever is kidney failure, marked by rising blood urea nitrogen and creatinine levels. Early detection of renal failure allows for intervention with dialysis, possibly increasing the patient's chance of survival [26].

The chain of events leading to death in severe LF cases is not completely understood. Most pathological symptoms of LF can be replicated with the help of different animal models. Studies in mice and non-human primates (NHPs) helped elucidate connections of sensorineural hearing loss in LASV infections with T cell infiltration [27, 28]. Experiments in chimeric mice could rule out vascular leakage syndrome as a singular cause of death by use of the fibrin-derived signaling peptide FX-06 (Oestereich et al. information in publishing), but also showing a CD8 T cell connection with induction of vascular leakage [29]. Even though the enrollment of animal models gives important insights into the pathology of LASV infections, the definitive cause for lethality in LF remains unclear; leaving cytokine storm and multi organ failure still as the major descriptors of death [30, 31].

The described broad symptomatic and severe complications that can arise during LASV infection make rapid and reliable diagnostic of the disease most valuable tools in correct treatment and prevention of spread.

1.6 Diagnostics, Treatment and Vaccines

In the past, specific proof of viral infections has been slow and labor-intensive, since the virus had to be cultivated on mammalian cells to be amplified for visual conformation using electron microscopy. The indirect detection of Lassa-specific IgM and IgG in patient sera is another diagnostic tool, but with limited use in acute infection as the disease can rapidly progress to lethal complications even before antibodies are produced by the patient. The need of a progressed infection status with humoral immune reaction makes this method thereby suboptimal for early detection and medical intervention in newly infected patients. Direct and indirect detection methods can also be prone to cross-reactions with other viruses [32, 33]. Nowadays, the fastest, most sensitive and specific detection method for Lassa fever diagnostics is considered to be reverse transcription polymerase chain reaction (RT-PCR). Quantitative reactions (RT-qPCR) even can provide an approximated predictor of outcome, because high viremia correlates with low survival rate [34]. Testing of sequential samples via RT-qPCR also allows a broad categorization into the infection stages: increasing viremia, peak viremia or clearance/reconvalescence phase. However, due to the high interstrain variability of LASV, PCRs should be performed with variable primer sequences [35].

No generally approved drug against LASV exists; therefore, treatment is restricted to supportive and intensive medical care and the off-label use of Ribavirin (a ribonucleic analogon), which has shown positive effects on outcome, when administered early during infection [36]. Researchers are screening several existing antiviral drugs for new uses against LASV [37]. One promising and further tested drug candidate against LASV is Favipiravir (T-705), a broad-spectrum ribonucleic analogon, licensed in Japan as an Influenza flu medication. This compound has been shown to reliably reduce viremia of LASV and increase survival in an *in vivo* mouse model and NHPs [38, 39].

Up to this point there is also no licensed vaccine against LASV infections. Neutralizing antibodies against LASV arise only late after reconvalescence and have been shown to impart protection against LF as shown in NHP experiments, if applied in high doses [40]. Dependent on the targeted antigen epitope antibodies can be very strain specific and can allow for escape mutants to arise if antibodies of a singular clone are used. Development of an effective vaccine is a topic of ongoing research employing different virus platforms [41, 42], focusing on inducing both a humoral and cellular immune response. It is known, that immunity against LASV is generally possible, *in vivo* experiments with attenuated reassortant virus ML29 conveyed protection against LASV

infection [42, 43]. Absence of reports from reinfection of people, who survived Lassa fever despite ongoing exposure risk, indicates similar protection in humans. Anecdotal reports even provide data of long lasting specific IgG antibody production 40 years after the last possible exposure to LASV [44].

1.7 Lassa virus

1.7.1 Lassa virus structure

LASV is a negative stranded enveloped RNA virus without a capsid and belongs to the family of Arenaviridae. It has a variable size ranging from 60-300 nm [45, 46] and contains electron-dense granule structures that gave the Arenaviridae its name (Latin *arena*: sand). The genome of LASV is segmented and its four viral genes are encoded in an ambisense manner. Each virion is comprised of two single stranded RNA genome segments (S- & L-segment) as well as ofall four encoded viral proteins - NP, L, GPC& Z proteins. The lipid envelope of the virions is host membrane derived and internally incorporates ribosomes of the host ('sandy' electron-dense granules) (see Figure 2).

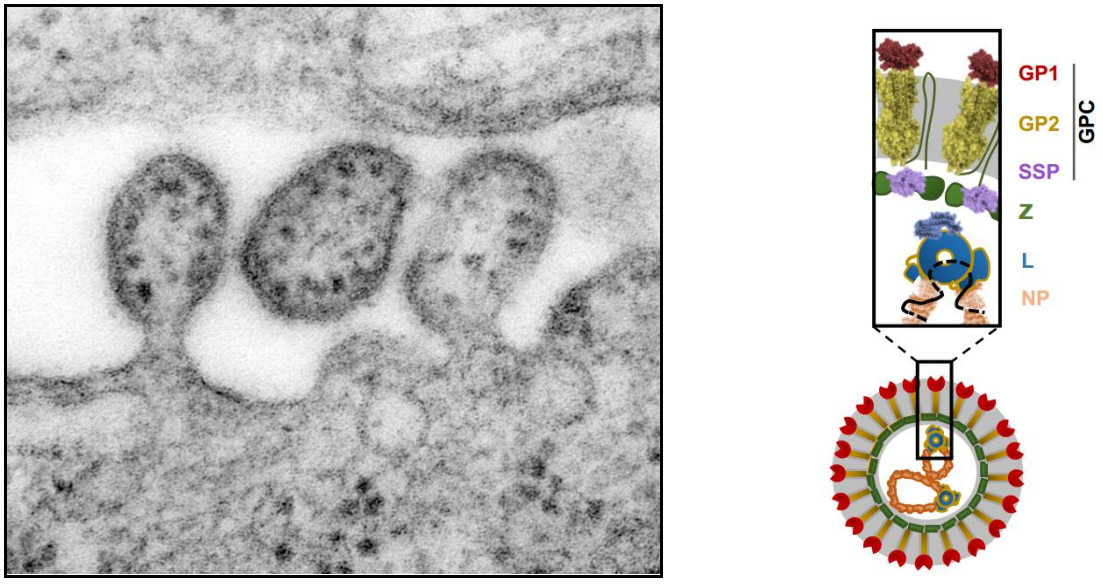

Figure 2 Structure of Lassa virus (LASV). Left: Electron-microscopic image of LASV budding from a cell. Right: Schematic of the structural protein composition of a LASV virion including the S- & L-segment RNPs. Image: C. S. Goldsmith, D. Auperin public domain; Structure schematic: adapted from Kerber et al. 2015 **[47]**.

Each of the virus proteins is multifunctional. They do not only represent the building blocks of the virus replication and budding machinery, but also directly interfere with host cell processes (see 1.12 LASV mechanisms against the immune system).

The viral RNA-dependent RNA polymerase (L protein; *L: large*) is the biggest of the LASV proteins (~ 250 kDa) [48]. It is responsible for viral genome transcription and replication [49]. The L protein utilizes a cap-snatching mechanism enabling host-derived cap-structures to be transferred to viral RNA [50, 51] in order to initiate translation and to protect its viral mRNA from intracellular degradation. The L protein is the least abundant protein in the LASV virion and is usually bound to the ends of the RNA genome segments.

The nucleoprotein NP binds to the single stranded vRNA and stabilizes it in a ribonucleoprotein (RNP) complex [52]. High abundance of NP negatively regulates the viral replication by degrading dsRNA and thereby probably delaying the immunological detection via RIG-I-like-receptors [53].

The RNP and L protein together are the minimum requirement for the viral genome replication machinery [54].

The glycoprotein precursor (GPC) of *Arenaviridae* forms the viral receptor for cell surface adhesion, cell entry and late endosomal egress. LASV pre-GPC is cleaved during virus assembly by the host subtilase SKI-1/S1P into glycoprotein 1 and glycoprotein 2 (GP-1 & GP-2), which form the functional multimeric virus receptor and the stable-signaling peptide, which stays associated to the receptor [55].

The smallest of the encoded viral proteins is the matrix protein Z. Not only is it the structural matrix protein of the virion and important for budding from the cell surface, it is also known to directly interfere with the Type I Interferon (IFN) response of the host cell, by inhibiting the signaling of intracellular host receptors for viral RNA structures (e.g., RIG-I, MDA5) [56].

1.7.2 LASV genome

The bisegmented genome of LASV consists of the S-segment with a length of ~3.4 kb and the L-segment ~7 kb in length. Each segment carries two open reading frames with one protein being encoded in genomic orientation and the other in antigenomic orientation. This coding strategy is also referred to as ambisense coding. The S-segment encodes the NP and GPC protein, while the L-segments encodes the L and Z

protein. Both open reading frames of each segment are separated by a predicted hairpin-loop structure forming sequence, the intergenic region (IGR), which topologically terminates transcription (see Figure 4). The 5' and 3' ends of each RNA genome segment additionally carry untranslated regions (UTRs), which are important cis-acting elements [54]. Since the L protein and the NP protein, which are essential for the viral replication machinery, are coded in negative strand orientation, LASV is categorized as a negative single strand RNA virus by origin like the phylogenetically related segmented negative stranded *Bunyaviridae* and *Orthomyxoviridae* [57].

1.7.3 Old World and New World arenaviruses

Up to this date the family *Arenaviridae* contains 41 virus species [57], subclassified into mammarenaviruses, reptarenaviruses and newly classified hartmaniviruses. Mammarenaviruses are classically subdivided into Old and New World arenaviruses based on their geographical distribution (Figure 3). Representatives of the Old World arenaviruses are e.g., lymphocytic choriomeningitis virus (LCMV), LASV, LuJo virus (LuJV) and Morogoro virus (MORV). Representatives of the New World arenaviruses are e.g., Junin virus (JUNV), Machupo virus (MACV) and Tacaribe virus (TACV). Both the Old and New World complexes are comprised of human pathogenic and apathogenic viruses. A selection of the arenavirus complexes and the corresponding diseases is listed in Table 1.

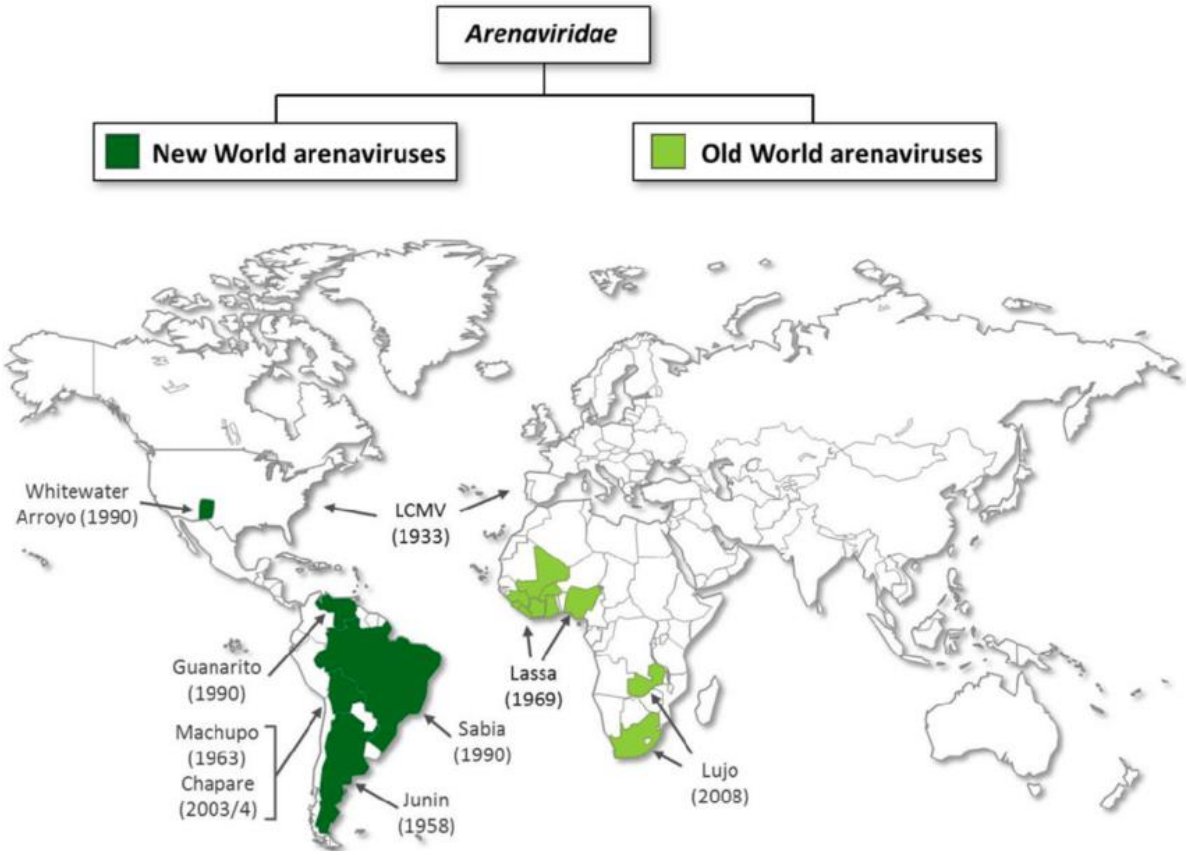

Figure 3 Continental separation of the Old and New World Arenavirus complexes with prominent agents of disease and their first discovery. Image: Fehling, Lennartz & Strecker 2012 [58] CC BY 3.0

Table 1 Selected pathogenic and apathogenic Arenaviruses. Adapted from Maeset al. 2018 and Fenner's Veterinary Virology (Fifth Edition) **[57, 59]**

Species	Virus	Geographic Occurrence	Human Disease	Natural Host
Genus *Hartmanivirus*				
Hartmaniviruses				
Haartman hartmanivirus	Haartman Institute snake virus (HISV)	captive boid snakes	none	uncertain
Genus *Reptarenavirus*				
Reptarenaviruses				
California reptarenavirus	CAS virus (CASV)	captive boid snakes	none	uncertain
Giessen reptarenavirus	University of Giessen virus 1 (UGV-1)	captive boid snakes	none	uncertain
Golden reptarenavirus	Golden Gate virus (GOGV)	captive boid snakes	none	uncertain
Ordinary reptarenavirus	tavallinen suomalainen mies virus 2 (TSMV-2)	captive boid snakes	none	uncertain
Rotterdam reptarenavirus	ROUT virus (ROUTV)	captive boid snakes	none	uncertain

Species	Virus	Geographic Occurrence	Human Disease	Natural Host
Genus *Mammarenavirus*				
Old World Arenaviruses				
Lymphocytic choriomeningitis mammarenavirus	lymphocytic choriomeningitis virus (LCMV)	Worldwide	flu-like disease, meningitis, meningoencephalitis	*Mus musculus*
Ippy mammarenavirus	Ippy virus (IPPYV)	Central African Republic	Infection, no disease	*Arvicanthus spp.*
Lassa mammarenavirus	Lassa virus (LASV)	West Africa	Hemorrhagic fever (Lassa fever)	*Mastomys natalensis*
Lujo mammarenavirus	Lujo virus	Southern Africa	Hemorrhagic fever (Lujo fever)	unknown
Mobala mammarenavirus	Mobala virus (MOBV)	Zambia	Infection, no disease	*Praomys jacksoni*
Mopeia mammarenavirus	Mopeia virus (MOPV)	Southern Africa	Infection, no disease	*Mastomys natalensis*
Morogoro mammarenavirus	Morogoro virus (MORV)	South East Africa (Tanzania)	no disease	*Mastomys natalensis*
New World Arenaviruses				
Argentinian mammarenavirus	Junín virus (JUNV)	Argentina	Hemorrhagic fever (Argentine hemorrhagic fever)	*Calomys musculinus, C. laucha, Akodon azarae*
Brazilian mammarenavirus	Sabiá virus (SABV)	Brazil	Hemorrhagic fever (Brazilian hemorrhagic fever)	unknown
Cali mammarenavirus	Pichindé virus (PICHV)	Colombia	none	*Oryzomys albigularis*
Chapare mammarenavirus	Chapare virus (CHAPV)	Bolivia	Hemorrhagic fever	unknown
Guanarito mammarenavirus	Guanarito virus (GTOV)	Venezuela	Hemorrhagic fever (Venezuelan hemorrhagic fever)	*Zygodontomys brevicauda, Oryzomys spp.*
Machupo mammarenavirus	Machupo virus (MACV)	Bolivia	Hemorrhagic fever (Bolivian hemorrhagic fever)	*Calomys callosus*
Tacaribe mammarenavirus	Tacaribe virus (TCRV)	Trinidad	none, except for one laboratory-acquired case systemic disease	unknown, possibly *Artibeus spp.* bats
Whitewater Arroyo mammarenavirus	Whitewater Arroyo virus (WWAV)	United States	Hemorrhagic fever	*Neotoma albigula*

1.7.4 LASV replication cycle

LASV, like every virus, is dependent on host cells for replication. Entering a host cell is hereby the first important step of the infection cycle. The most commonly used host ligand enabling LASV to bind to a cell is α-dystroglycan. Cell infections in the absence of α-dystroglycan have also been shown, indicating that alternative entry ligands exist [60]. To enter a cell, the Lassa virion binds α-dystroglycan via GP1, which induces a clathrine-dependent non-classical endocytosis of the virion. Internal pH changes in the late endosome results in a intercellular receptor switch to the host receptor LAMP1 and conformational changes of the GP-trimer, bringing virus envelope and endosome membrane into membrane fusion distance [61]. This process releases the contents of the LASV virion into the host cell cytoplasm, where viral transcription and replication occurs.

At first, only the L protein and NP can be transcribed into mRNA restricted by the ambisense coding strategy. Only after the antigenomic strand is produced during genome replication, the Z protein coding gene and GPC gene are in the correct 3' to 5'-orientation for their transcription to occur (Figure 4).

After translation by host ribosomes virus assembly occurs at the plasma membrane, where viral RNPs, consisting of L, NP and the viral RNA are transported to. GPC is transported via the endoplasmatic reticulum and is maturation cleaved, while Z is interacting with the ESCRT (endosomal sorting complex required for transport) machinery. This induces cell membrane protrusion and finally budding of the virion [62, 63].

This non-cytolytic replication cycle of LASV induces low to no cytopathic effects in most cell lines [64].

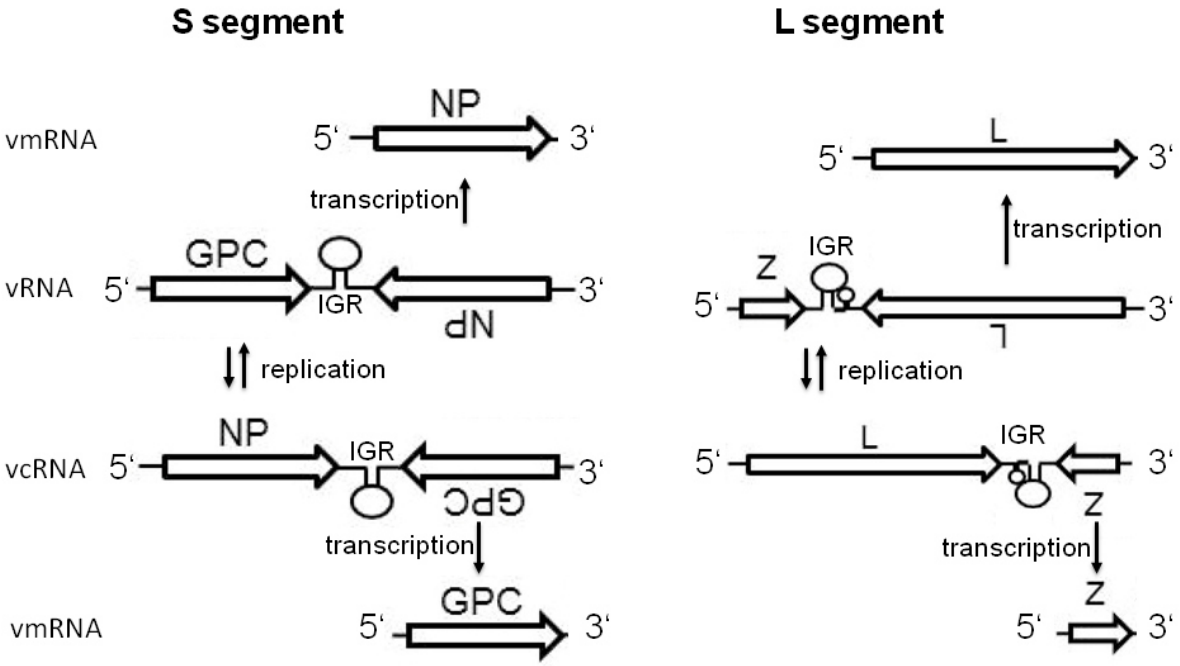

Figure 4 Replication and Transcription Mechanism of the ambisense Arenavirus genomes. Viral mRNA (vmRNA) from the NP and L genes can be directly transcribed from the genome with transcription termination by the intergenic region (IGR). Transcription of the GPC and Z genes can only occur in the same fashion once a viral copy RNA (vcRNA) strand is replicated from the vRNA genome template. Modified from Urata & Yasuda 2012 [65] CC BY 3.0.

1.8 Immunology

After life existed in a sufficient density on this planet, parasitism as a survival strategy became highly viable. Being able to fend off parasitic pathogens of all kinds thereby became an important evolutionary advantage. From unicellular bacteria, archaea and eukarya to the big multicellular organisms of the eukarya each branch of life developed its own kind of pathogen defense. The unison of the different pathogen defense reactions of an organism is called the immune system. In the following basic concepts of the mammalian immune systems will be described.

1.8.1 Hematopoiesis

Multicellularism allowed for specialization of singular cells, which also led to extensive specialization of cells whose main purpose is the immune defense. The majority of these specialized immune cells is generated by the bone marrow in a process called hematopoiesis. Hematopoiesis (Greek: *hemato-*: blood; *poiesis*: to make) generates all cell types of the blood: from erythrocytes and platelets to all different types of leukocytes (Figure 5). The diverse types of leukocytes are overall subdivided into

myeloid cells and lymphoid cells dependent on their progenitor cell and fulfill different important roles.

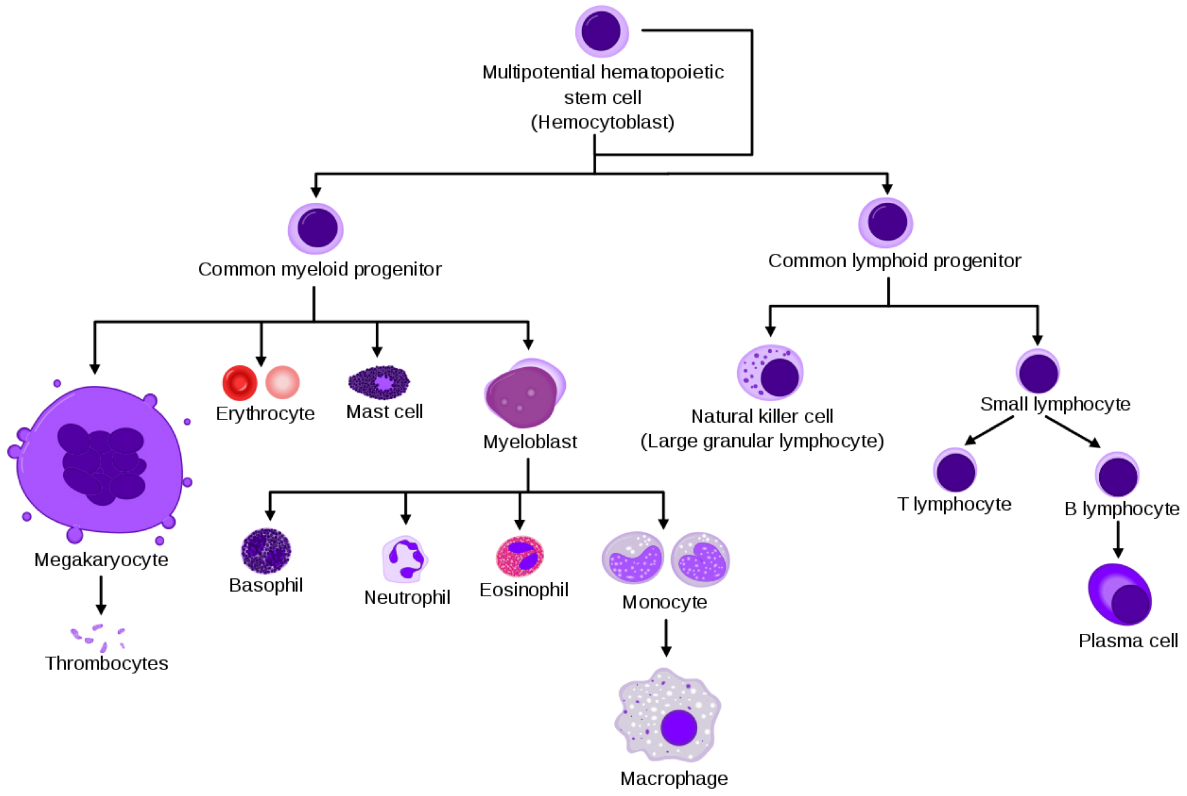

Figure 5 Simplified hematopoietic cell lineages. Cells of the blood are separated in to myeloid and lymphoid progenitor descendants. The main constituent of the blood, the erythrocyte is of myeloid origin, while cells of the adaptive immune system like T and B lymphocytes belong to the lymphoid compartment. Modified from Mikael Häggström modified from A. Rad CC BY SA 3.0

1.8.2 The innate and the adaptive immune system

The myeloid leukocyte compartment is comprised of monocytes, macrophages, dendritic cells (DCs), mast cells as well as different kinds of granulocytes. It is categorized as part of the innate immune system, meaning that cells of this compartment mostly recognize pathogens via evolutionary selected, conserved pattern-recognition receptors (PRR) targeted against various pathogen-associated molecular patterns (PAMPs). These cells combat pathogens by phagocytosis, release of soluble antimicrobial proteins from granules or expulsion of DNA to form extracellular traps killing pathogens [66, 67].

In contrast, most of the lymphoid immune compartment is categorized as the adaptive part of the immune system and consists of various T lymphocytes (T cells) and B lymphocytes (B cells) subtypes as well as natural killer cells (NK cells). B- and T cells recognize pathogens via variable receptors, which are genetically newly recombined

during each lymphocyte's maturation. This makes the system adaptive against a tremendous range of structures the organism might encounter [68].

Once a lymphocyte contacts a pathogen or foreign structure that fits its specific receptor, it proliferates and can also produce long-lived memory cells. Memory cells allow for rapid targeted immunological response should the same structure be encountered again in the future.

The types of responses between B and T cells hereby differ strongly. While B cells begin the production of antibodies, that can neutralize, block or mark the encountered specific antigens, T cells on the other hand are capable of directly inducing cell death in cells presenting their specifically recognized antigen in a major histocompatibility complex (MHC).

NK cells – the third type of lymphocyte – classically act more in an innate immunity manner, based on germline-encoded invariant receptors. NK cells are, therefore, also known as innate lymphocytes. In recent years however, evidence of adaptive receptor regulation and memory reactions of NK cells has surfaced [69, 70], which further blurs the lines between innate and adaptive immunity.

Both the innate and adaptive immune systems are interacting with each other and are critical for efficient protection against pathogens. For example monocytes, macrophages and dendritic cells, cells of the innate immune system, hold roles of professional antigen presenting cells (APCs). APCs are capable of processing and afterwards presenting phagocytosed extracellular antigens on their surface via MHCs, where T cells of the adaptive immune system can sense them. In this way APCs can prime T lymphocytes or elicit the help of T helper cells for the stimulation and maturation of the APC itself by provided ligand interaction or cytokine production [71].

1.8.3 Immunological Messengers: Cytokines

Cytokines are important signaling molecules of the immune system. 66 different cytokines are described for humans [72]. Cytokine types vary strongly in their molecular structure and the associated responses. The responses to cytokines are overall divided into proinflammatory and anti-inflammatory responses. Proinflammatory cytokines regulate the expression of antimicrobial agents up, induce immune cell proliferation, recruit other immune cells to the site and inhibit cellular metabolism. All in order to attack foreign structures, inhibit pathogen replication, induce apoptosis in cells and to

prevent pathogen spread. Important proinflammatory cytokines are e.g. IFNα IFNβ, IFNγ, TNFα, IL-2 (interleukin-2), IL-6 and IL-8. Anti-inflammatory cytokines on the other hand inhibit these proinflammatory responses in order to avoid undesired damage induced by indiscriminate run-away processes of inflammation. Anti-inflammatory cytokines facilitate antibody production, inhibit immune responses to harmless foreign antigens and facilitate cell regeneration. Important anti-inflammatory cytokines are e.g., IL-4, IL-10, and IL-13. Both, proinflammatory and anti-inflammatory cytokines, are needed for a well regulated immune response and the correct development and maturation of immune cells [73, 74].

1.9 Mechanisms against intracellular pathogens/viruses

1.9.1 Intracellular PRRs

Evolutionary, the innate immune system is the older part of the immune system and allows for cells to recognize pathogen structures via conserved PRRs.

One family of PRRs are the toll-like-receptors (TLRs). Different receptors of this family are able to bind to structurally conserved molecules of pathogens. The TLR2-TLR6 heterodimer for example can recognize bacterial and fungal cell wall components, β-glucans, while TLR4 can sense bacterial lipopolysaccharides. This allows for a first cellular reaction against the pathogen including alterations of the cell metabolism or secretion of chemo- and/or cytokines into the cell surroundings. Also intracellular PRRs play an important role to fend off cell invading pathogens. TLR3, RIG-I and MDA5 are examples of intracellular receptors recognizing double stranded RNA molecules that occur during replication of RNA viruses [75, 76]. These receptors are situated at the beginning of signaling cascades that lead to activation of transcription factors like NFκ-B (nuclear factor kappa-light-chain enhancer of activated B-cells) and IRF3 (interferon regulatory factor 3), which induce secretion of Type I interferons (IFNα & IFNβ) from the host cell to itself and to adjacent cells (Figure 6).

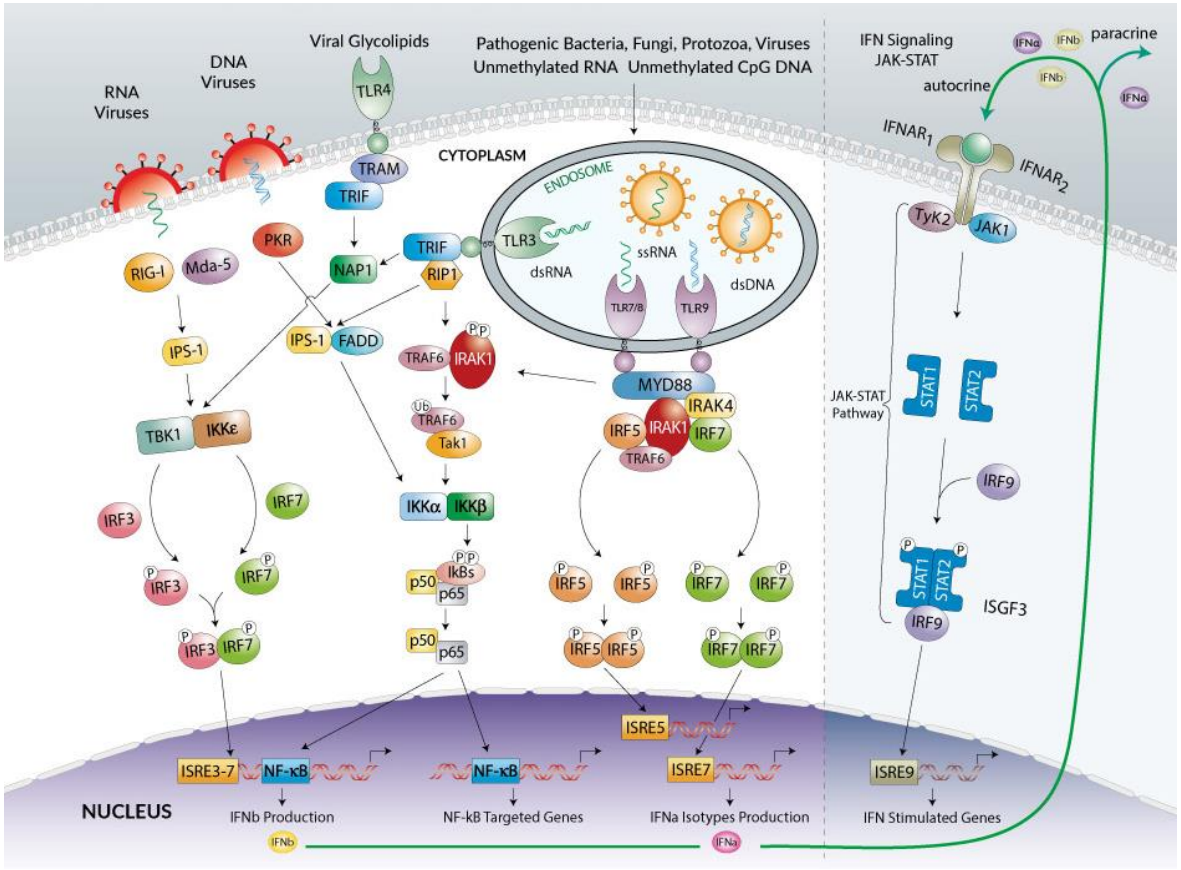

Figure 6 Pathway of Type I IFN Production and Signaling. RIG-I & MDA-5 dsRNA detection (left) with subsequent IFNβ production. Type I Interferon recognition (right) by the Interferon α/β receptor (IFNAR) with translocation of phosphorylated STAT1/STAT2 dimers and resulting transcription of interferon stimulated genes (ISG). Copyright ©InvivoGen. All Rights Reserved. https://www.invivogen.com/

1.9.2 The Type I IFN response

IFNα and IFNβ are important messenger molecules in the early immune response. When IFNα or IFNβ bind to the extracellular domain of the membrane anchored interferon alpha/beta receptor (IFNAR), the JAK/STAT-signaling pathway is engaged (Figure 6), shifting the cell into an antiviral state. The antiviral state includes the production of protective Mx-proteins [77] and increases the production of MHC molecules and proteins of the antigen processing machinery [78, 79]. While the MHC I molecule is already expressed by cells in a steady-state, its expression can be further increased to present more peptides of degraded intracellular proteins on the cell's surface to cells of the adaptive immune system. Should a cell harbor foreign proteins, e.g. because it has been infected, the foreign proteins also get indiscriminately processed by the antigen-presentation machinery and are then presented on the cell surface. Cytotoxic CD8 T cells, which recognize MHC-I-presented peptides with their peptide-specific T cell receptor (TCR), then can induce apoptosis of the infected cell.

Thus the upregulation of MHC I molecules increases the chance of detection of the infected cell by T lymphocytes.

1.9.3 Induced apoptosis

One of the most basal evolutionary perks in the metazoan tree of life is the controlled apoptosis of single cells, either throughout development [80] and maturation checkpoints [81, 82], or induced by other cells or pathogens [83]. To clear pathogens from the intracellular space, infected host cells are readily sacrificed in a controlled self-destruct sequence (apoptosis) for the greater good of the organism. This chosen and orderly cell death denies obligate intracellular pathogens their replication niche. In plants this reaction is a very common reaction since they inherited no cellular immune system and the cell-cell-contacts are very restricted by their cell walls leaving non-motile pathogens usually isolated and limited in further propagation [84].

Also mammalian cells can undergo apoptosis once viral infections are sensed by the cell itself via RIG-I and MDA5 [83, 85], which can be counteracted by other anti-apoptotic signaling or by viral proteins. Another common apoptosis is induced during an infection directly by other pathogen-surveying cells, e.g., NK cells and T cells. NK cells are capable of surveying for pathogen-induced changes of cell surface markers (down regulation of MHC I) on other cells or are capable of binding to antibody-opsonized cells via a FcγIIIA receptor (CD16) in a process called antibody dependent cellular cytotoxicity (ADCC) [86]. T cells on the other hand specifically survey for pathogen-specific peptides that are presented in MHC complexes on cells. Contact-induced apoptosis can be executed by these cells via several pathways. Fas ligand on the effector cells, for example, can bind to the Fas receptor on the recipient cell, setting further signal transduction into action and activating caspase 8. Caspase 8 in turn activates other downstream caspases and induces apoptosis [87]. Furthermore direct inducers of apoptosis can be released in the immunological synapses between effector and target cells by the cytotoxic T cell. These pro-apoptotic caspase-pathway-inducing granzymes are shuttled via the membrane pore-forming protein perforin into target cells [88], which starts the self-disassembly process in the receiving cell.

1.10 T lymphocytes

1.10.1 The T cell receptor and T lymphocyte maturation

T cells like all hematopoietic cells are generated in the bone marrow, but unlike cells of the innate immune system, T cells leave the bone marrow in an immature state. They migrate to the thymus (T lymphocyte = Thymus lymphocyte) to complete their maturation. The reason for this elaborate maturation process is the highly adaptive nature of the TCR. It can be virtually recombined to ~10^{15} possible clonotypes of the receptor [72, 89, 90], but in reality much lower numbers have to be considered at single points in time. This adaption through recombination is of a semi-random nature and working receptors have to be selected for. The TCR consists of four domains (V, D, J, C) each with various differing gene duplications. Genetic recombination of the domains by the host recombinases RAG1 & RAG2 (recombination associated gene) rebuilds the TCR randomly in each T cell with one gene for each domain. The recombined TCR is tested on the epithelium of the thymus, if it can bind either MHC I or MHC II. T cells at this stage express both of the CD4 and CD8 co-receptors. Only TCRs able to bind the MHCs get positively selected, while all T cells with a dysfunctional TCR undergo apoptosis.

The thymus is a specialized immune organ needed for T cell maturation. Cells of its cortex express proteins, which are normally only found in other specialized tissue cells. These proteins are degraded by the antigen-presentation machinery for presentation on the epithelial cells of thymus cortex.

T cells with a MHC-binding TCR will survey the thymal epithelia cells and, if strong binding of the new TCR to such a self-antigen loaded MHC occurs, the T cells receives signaling to undergo apoptosis. This way, the negative TCR selection in the thymus inhibits the existence of T cells, which react to self-antigens (auto-reactive) and could thereby induce autoimmune reactions.

T cells, which survived both the positive as well as the negative selection steps during maturation are released into the body as naïve T cells where they circulate until they encounter their specific TCR antigen epitope.

1.10.2 CD4 T cells

In the beginning of their maturation process T cells harbor both the CD4 as well as the CD8 co-receptor on their surface. After positive selection to either MHC I with the CD8 co-receptor or MHC II with the CD4 co-receptor, they will start to exclusively express only the one relevant co-receptor splitting them into a $CD4^+$ and a $CD8^+$ T cell population [91], which fulfill different roles in the organism.

CD4 T cells, also commonly named T helper cells, survey for specific antigen loaded onto MHC II on APC surfaces. During the cell-cell interaction CD4 T cells provide APCs with cell activation/maturation signals in form of cell-ligand interactions and additional cytokine production (e.g., IFNγ) enhancing their responses [92]. Another important key signal in the activation of APCs is the ligation of cell-surface receptors with other cell surface ligands e.g., the APC's CD40 interacting with CD40 ligand (CD40L) expressed on CD4 T cells.

APCs that have been 'licensed' this way are more effective in priming CD8 T cells under low inflammatory circumstances and show enhanced cross-presentation of antigens [93, 94].

Additionally, CD4 T cell help is an important factor in the proper function of $CD8^+$ cytotoxic T cells. Not only can CD4 T cells release chemokines to attract CD8 T cells [95], the paracrine production of IL-2 by CD4 T cells is also critical for CD8 T cells to pass proliferation check points during low antigen, low inflammation conditions, thereby avoiding activation induced non-responsiveness [96]. Instances of cell-contact mediated help of CD4 to CD8 T cells via CD40-CD40L stimulation also have been described, but seems to be majorly facilitated by APCs [97].

CD4 T cells not always supplement and enhance the functions of other immune cell types. Specialized regulatory T cells can also suppress the effector functions of immune cells in order to prevent overshooting or reactions and induce immune tolerance (T regulatory cells), which in some cases is to the detriment of pathogen clearance [98-100].

1.10.3 CD8 T cells

As soon as a pathogen is able to invade a host cell, it becomes untargetable by many eradication mechanisms of the immune system, which are only targeting the extracellular space. An important cell type against threats, which subvert extracellular

immune responses, are cytotoxic CD8 T cells. When an activated CD8 T cell senses peptides of non-self origin on a MHC I complex, they actively induce apoptosis via formation of an immunological synapse with the presenting cell (see 1.9.3 Induced apoptosis). CD8 T cells like other cells of the adaptive immune system can be discriminated on basis of their differentiation and activation status. T cells, which have not yet encountered their specific antigen, are considered antigen naïve T cells ($CD44^-$, $CD62L^+$). Once activated via priming through APCs, the now primed T cells proliferate and produce further differentiated cell progeny. Several putative models for the mode of differentiation into effector and memory subtype haven been proposed and are still highly debated for the past decade [101-103]. During acute infection, the most prominent subtype are the short lived effector cells (SLECs). Characterized by expression of cell surface markers like KLRG1 (killer cell lectin-like receptor subfamily G, member 1), CD44, the downregulation of CD62L and the expression of effector proteins like granzymes, perforins as well as IFNγ and TNFα. These cells are able to produce strong effector functions and are terminally differentiated losing most their proliferative capabilities. Once an infection is cleared the SLEC population contracts, leaving back only long-lived memory cells [104]. CD8 memory T cells are distinguished by the expression of anti-apoptotic markers like the IL-7 receptor (CD127) and are subdivided into effector memory (T_{EM}) and central memory T cells (T_{CM}). Memory cells are responsible for rapid recall reactions should the antigen be encountered again, this includes effector functions as well as high proliferation responses. T_{EM} are usually tissue resident, surveying the periphery and strong effector responses. T_{CM} on the other hand remain in a lymphoid homing preferential status ($CD62L^{hi}$) waiting for antigens to be encountered and reacting by rapid proliferation to generate new effector cells.

1.10.4 KLRG1, CTLA-4 & PD-1: immune receptors with tyrosine-based inhibitory motifs (ITIM) and different functions

KLRG1, CTLA-4 (cytotoxic T lymphocyte associated protein 4) and PD-1 (programmed cell death protein 1) have been identified to have inhibitory effects on the immune responses of the expressing cells. These immune receptors share a tyrosine-based inhibitory motif (ITIM), marked by a S/I/V/LxYxxI/V/L-motif in the cytoplasmic tail of the receptor, that recruits phosphatases inhibiting the Akt (Protein Kinase B)-signaling

pathway [105]. Still, the extent of their inhibitory function and their use as phenotypic markers varies greatly between the three receptors.

Several inhibitory effects of KLRG1 on NK cells and T cells have been presented over the last years, including inhibition of the NFAT signaling-pathway (nuclear factor of activated T cells) as well as reduction of T cell proliferation and Ca^{2+} influx (reviewed in [106]). Inhibition by KLRG1 occurs spatially restricted together with TCR engagement when KLRG1's ligand E-, R- or N-cadherin is also expressed on the surveyed cell. However in experimental LCMV infections *in vivo* it was a shown that KLRG1 does only have a negligible physiological role on CD8 T cells as infected KLRG1-deficient mice clear the infection [107]. None the less, KLRG1 is a powerful predictor to discriminate SLECs ($KLRG1^{hi}$ $CD127^{lo}$) and CD8 T cells that a predisposed to become memory T cells ($KLRG1^{lo}$ $CD127^{hi}$) [108].

The inhibitory receptor, CTLA-4, has been the topic of avid research in the past decade, as CTLA-4-agonists or CD28-antagonists show potential in immune modulatory therapy of autoimmune diseases and in transplantation settings [109]. Monoclonal CTLA-4 antagonists on the other hand can be employed against melanoma [110]. CTLA-4 is expressed on T cells and functions as a competitor to stimulation of CD28. CD28 is expressed on T cells and transduces co-stimulating signals when bound to CD80 or CD86 on APCs during priming events. Not only does CTLA-4 has a higher avidity to CD80 than CD28 does and, thereby, reducing co-stimulatory potential, it also carries an ITIM further propagating inhibitory signals instead of CD28's stimulatory ones. The expression of CTLA-4 is transient on the cell surfaces after the activation of T cells [111]. It strongly limits T cell proliferation and effector functions and is important for proper regulatory T cell (T_{reg}) function. CTLA-4 KO mice for example die within 3-4 weeks after birth of lymphoproliferative autoimmune responses [112]. In late stages of the immune response CTLA-4 is especially upregulated on anergic or exhausted CD8 effector T cells [113] e.g. after high dose antigen stimulation or chronic stimulation. CTLA-4 is thus often considered as a marker of inhibited T cell populations. However, CTLA-4 can also mark normal function as it is in the case of CD4 T regulatory cells. Additionally, CTLA-4 is also transiently upregulated after early T cell receptor engagement [111, 114, 115].

Similar to CTLA-4, PD-1 expression is also transiently upregulated upon antigen stimulation of T cells [116] and on exhausted T cells after chronic stimulation [113, 117]. The PD-1 ligands PD-L1 and PD-L2 are differentially expressed on cells. PD-L2 can be

induced on APCs while PD-L1 is constitutively found on a wide variety of cells from non-hematopoietic cells like neurons and endothelial cells to immune cells like T cells and APCs. PD-1, like CTLA-4, is also a highly researched topic and has been the target of several now licensed cancer treatments. Antagonizing PD-1's inhibitory effects on effector T cells can reactivate T cells and thereby improve anti-cancer responses [118, 119]. Thus PD-1 is generally considered to be an inhibitory marker of effector T cells and especially found on dysfunctional exhausted T cells during chronic infection or stimulation. Additionally LCMV infection experiments have shown, that a block of PD-1 during early and late time points of infection leads to faster clearance of the infection [116], presenting another potential scope of important PD-1 interactions during early immune responses.

1.11 Macrophages and dendritic cells

Asalready mentioned; monocytes, macrophages and dendritic cells are highly important interaction partners for the adaptive immune responses. The ability of these cells to phagocytose antigens and process them, allows APCs to effectively prime CD4 T cells via MHC II and CD8 T cells via cross-presentation on MHC I. Monocytes, macrophages and dendritic cells exist in different subtypes with partly very different functions. Macrophages are a prime example of producers of inflammation (subtype M1) by strong secretion of inflammatory cytokines (e.g., IFNγ and TNFα), in contrast the M2 macrophage subtype is also important for healing and tissue regeneration [120]. Similarly, discussions are held over the manifold subsets of dendritic cells [121]. To functionally differentiate the most important, only conventional DCs (cDCs) and plasmacytoid DCs (pDCs) will be discussed here.

cDCs with CD141 expression in humans and CD8 in mice are functional considered as antigen-cross-presenting APCs capable of effectively priming CD8 T cells [122]. pDCs with their expression of CD123/CD303/CD304 in humans and B220 in mice are, on the other hand often described for their antiviral functions through secretion of high levels of type I interferons, IFN-α & -β [123].

It is hypothesized, that in particular APCs might play a critical role in several diseases as they are early infection targets of some pathogens [124]. Migration of the activated APCs would thereby facilitate the dissemination of the pathogens to the lymphatic system [125, 126].

The duality of APCs providing essential co-stimulation and cytokine milieus to T lymphocytes, but also escalating the infection by disseminating it, marks another example of the double-edged nature of immunological responses. Therefore, the study of adaptive immune responses always also has to consider the innate immune cell responses.

1.12 LASV mechanisms against the immune system

The most important evolutionary trait of every virus besides replication is the evasion or delay of immune responses of its host cell to avoid early and total eradication of the own genetic information before propagation. For this purpose LASV has a range of immune suppressive tools within its small genome. Two of the most prominent immune evasion aspects are conveyed by secondary functions of the viral NP and the Z protein. The highly abundant NP protein, e.g., suppresses replication activity by degrading dsRNA [53]. Studies performed with LCMV also showed capabilities of arenaviral NP to directly inhibit IκB kinase ε (IKKε) and the resulting IRF3 induction [127]. Also the translocation of NF-κB is efficiently inhibited in a dose-dependent manner by NP of pathogenic arenaviruses [128]. The Z protein of LASV on the other hand is capable of directly inhibiting signaling from PRR-induced Type I interferon pathways through the blockade of the double-stranded RNA sensor proteins RIG-I and MDA-5 from transducing. The Z protein competitively blocks the CARD (caspase-recruitment domain) of MAVS at the mitochondrial membrane [56], effectively interrupting the signaling cascade of RIG-I and MDA-5. The ability to quench Type I interferon response before Type I interferons are abundantly produced is a trait found throughout the pathogenic arenaviruses.

1.13 The balancing act of immunological responses

Many immunological mechanisms from antibody- or complement-opsonization to direct induction of apoptosis by cytotoxic T cells result in destruction of cells, which is beneficial and wanted if it occurs on a small and organized scale. Immunological responses are tightly regulated feedback mechanisms acting under a general Goldie-locks principle. The immune reaction need not be too weak as it would allow pathogens to overrun the host or enable a chronic infection. An immune response that is too strong

or directed against harmless or self-antigens is on the other hand just as critical, since the resulting cell damage from the reaction can be worse than the infection itself and in worst cases can even lead to death. Strong examples are toxins that indiscriminately overstimulate the immune system like *Staphylococcus*' superantigen TSST-1 (toxic shock syndrome toxin 1), which can induce T cell-dependent cytokine storms with multiorgan failure [129]. Another point of immune overstimulation constitutes the anaphylactic shock by antibody-dependent basophile and mast cell degranulation that shut down vital function critically within very short time frames, easily resulting in the death of the organism [130]. In case of viral infections, cytokine storm have been reported as a severe complication often with fatal outcome as in Influenza virus infections [131, 132]. Cytokine storms and accompanying vascular permeability syndromes are also considered to be a key hallmark in fatal pathologies of hemorrhagic fever viruses like Dengue virus, Ebola virus and Lassa virus [133, 134]. Fatal cases of Lassa fever show an increased expression of proinflammatory cytokines like IFNγ, IL-6, IL-8 and the immune inhibitory IL-10 [135] (Oestereich et al. in preparation), but the simultaneous expression and complex functional redundancies of the different cytokines make pinpointing of specific effects difficult.

These immune pathological cases demonstrate the power the system inherits in order to normally protect the host. Immune dysregulations are therefore an important research topic, creating a possibility for better understanding of tight immune regulation frame works. More and more immune modulatory therapies are introduced for cancer and autoimmune diseases based on receptor-ligand-blocking antibodies or cytokine application [136, 137]. Future capabilites to artificially modulate immune response might enable medical sciences to control immune reactions in a defined manner to better avoid adverse pathological effects. Harnessing of the power of the most versatile and naturally complex defense mechanism that has been produced by evolution, which is effective against bacteria, virus, fungi, parasites and cancers could solve future fears of a post-antibiotic era.

1.14 Thesis Aim

Previous depletion experiments of T cells have shown a strong involvement of CD8 T cells in the severity of symptoms in the IFNAR^{BL6} bone marrow chimeric mouse model for LASV [29]. Observed hospitalization rates of humans at our study site cluster around

the age groups of young adults and adults, which could indicate a putative involvement of detrimental immune overreactions in the clinical symptoms of Lassa fever. Even though a high quantity and quality of immunological research regarding arenaviral LCMV infection exists, knowledge about immune reactions to LASV is sparse. Except for the general antiviral response mechanisms it is unknown if the genetic and taxonomic proximity of LASV to LCMV could allow for a direct transfer of knowledge. While the natural co-evolved host for LCMV is *Mus musculus*, LASV is not adapted to mice and humans. This difference might result in differing inflammation signatures *in vivo*, which in turn can lead to differences in T cell differentiation and response [138].

This thesis aims on further characterizing immune cell responses especially CD8 T cell responses in an established small animal disease model for Lassa fever, in order to compare the results with analyses performed on blood collected at the Irrua Teaching Hospital in Nigeria of Lassa fever study patients. This approach could provide valuable insight into immune cell responses associated with the manifestation of severe LF.

2. Materials and Methods

2.1 Materials and instruments

2.1.1 Disposable Materials and reagents

Disposable materials and materials for molecular biological and microbiological applications were sourced from Sarstedt, Eppendorf, Thermo Scientific, Greiner, Invitrogen, Qiagen, New England Biolabs, and Fermentas.

Disposable materials and materials for cell culturing purposes were manufactured by Sarstedt, PAA, Life Technologies, PAN Biotech, Greiner Bio One, and Biochrom/TPP and STEMCELL Technologies.

2.1.2 Viruses

Virus strain	Source
LASV Ba366	BNITM, Virology
Morogoro-Virus (MORV)	BNITM, Virology
EBOV Zaire	BNITM, Virology

2.1.3 Cell lines

Cell line		Source
Vero E6 FM	Vero cell line (Kidney cell line from green lemurs)	Friedrich-Loeffler Institut; Frankfurt am Main
Vero E6 76	Vero cell line (Kidney cell line from green lemurs)	ATCC
L929	Murine fibroblast cell line	BNITM, diagnostic department

2.1.4 Mouse lines

Cell line	Source
B6(Cg)-*Ifnar1*$^{tm1.2Ees}$/J (IFNAR-/-)	BNITM
B6.SJL-*Ptprc*^{a}*Pepc*^{b}/BoyJ (Ly5.1 /CD45.1)	BNITM
C57BL/6J	BNITM
B6.129S7-*Rag1*^{tm1Mom}/J	BNITM / HPI

2.1.5 Reagents

Reagent	Manufacturer/Distributor
Acridine Orange/Propidium Iodide	Logos biosystems
Antibody Labeling Kit Alexa 647	Thermo Fisher Scientific
BD Cytofix/Cytoperm Plus Golgi Plug Kit	BD
CFSE[1] Cell Division Tracker Kit	biolegend
Collagenase D*(from Clostridium histolytica)*	Roche
DNase I (from bovine pancreas)	Sigma-Aldrich (Merck)
EDTA[2]	Roth
Formaldehyde (37%) stabilised with methanol	Roth
Immuno*blot* TMB[3]substrates	Mikrogen
Lymphoprep	STEMCELL Technologies
Mix-n-Stain Antibody Labeling Kits; CF405S & CF633	Biotium/Sigma-Aldrich (Merck)
PrimeFlow Probe Sets mouse β-actin& LASV GA391 NP	Invitrogen
PrimeFlow RNA Assay Kit	Invitrogen
Red Blood Cell Lysis Buffer (BD Pharm Lyse)	BD
Triton X-100	Roth
Trypan blue solution (0.4%) – Gibco™	Thermo Fisher Scientific

2.1.6 Pharmaceuticals

Name	Manufacturer
Enrofloxacin, Baytril™(2.5%)	Bayer AG
T-705 (Favipiravir), biochemical grade	BOC Science

2.1.7 Buffers and solutions

Name	Composition	
10x PBS[4], pH 7,5	NaCl	1,37 M
	Na_2HPO_4	0,17 M
	KCl	0,03 M
	KH_2PO_4	0,017 M

[1]Carboxyfluorescein succinimidyl ester
[2]Ethylenediaminetetraacetic acid
[3]3,3',5,5'-Tetramethylbenzidine
[4]Phosphate buffered solution

Name	Composition	
Cell culture medium with 5% FCS	DMEM[5]	500 mL
	FCS[6]	25 mL
	Penicillin/Streptomycin (100x)	5 mL
	L-Glutamine (100x)	5 mL
	Non-essential amino acids (100x)	5 mL
	Pyruvate (100x)	5 mL
Infection/Titration media (2% FCS)	DMEM or GMEM	500 mL
	FCS	10 mL
	Penicillin/Streptomycin (100x)	5 mL
	L-Glutamine (100x)	5 mL
	Non-essential amino acids (100x)	5 mL
	Pyruvate (100x)	5 mL
Methylcellulose solution for overlay media	Methylcellulose	16.8 g
	dH_2O	600 mL
	autoclaved; stirred for 24 hours	
Overlay medium for immunofocus assays	Cell culture media with 10% FCS	400 mL
	Methylcellulose solution	200 mL
Collagenase D stock solution (20 mg/mL)	Collagenase D	20 mg
	1x PBS	1 mL
DNaseI stock soltution (5 mg/mL)	DNase I	5 mg
	1x PBS	1 mL
Heparin stock solution 20 U/mL	Heparin (5,000 U/mL)	200 µl
	HBSS[7]buffer	49.8 mL
Heparin working solution	HBSS buffer	450 mL
	Heparin stock solution 20 U/mL	50 mL

[5] *Dulbecco's Modified Eagle's Media*
[6] *Fetal Calf Serum*, FCS
[7] *Hank's Balanced Salt Solution*

2.1.8 Materials for animal experiments

Material	Manufacturer
0.9% sodium chloride solution	Fresenius Kabi
BD Micro-Fine 0.5 mL, cannula diameter: 0,3 mm, length 8 mm	BD
BD Micro-Fine 0.5 mL, cannula diameter: 0.3 mm, length 12.7 mm	BD
BD Microtainer K2E Tubes	BD
BD Microtainer SST Tubes	BD
Cell Strainer 70 µm, Nylon	Greiner Bio-One& Sarstedt
Clini Tray	KLINIKA Medical
FACS tubes, 5 mL, 75x12 mm, PS	Sarstedt
Fuji DRI-CHEM AST(GOT[8]) test chips	Fuji
Lysing Matrix D	MP Biomedicals
MACS MS separation columns	Miltenyi Biotec
Mouse restrainer diameter 28.5 mm	Bioseb
Pan T cell Isolation Kit II, mouse	Miltenyi Biotec
Reflotron® GOT test strips	Roche
Roche Reflotron® Clean + Check test strips	Roche
Sarstedt Microvette K2E Tubes	Sarstedt
Sarstedt Microvette LiHep-Gel Tubes	Sarstedt
Sarstedt Microvette Z-Gel Tubes	Sarstedt
Screwcaptube2 mL	Sarstedt
Sodium Heparin 25000 I.U./5mL	Braun
Stainless steel balls 5 mm	Qiagen
Sterile cellulose swabs Pur-Zellin	Hartmann
Surgical blades (Carbon Steel Sterile No. 11)	Swann-Morton
Syringe 1 mL	Braun
Syringe 5 mL	Braun

2.1.9 Immunofocus assay antibodies

Reagent		Manufacturer
Mouse α-LASV mAB	2F1	BNITM, Virology
Mouse α-LASV/MORV mAB	5D6	BNITM, Virology
Sheep Anti-Mouse IgG, Peroxidase-conjugated		Jackson Immuno Research

[8]Glutamic Oxaloacetic-Transaminase, also known as Aspartate Aminotransferase (AST)

2.1.10 Flow cytometric reagents

Reagent	Manufacturer
LIVE/DEAD® Fixable Blue Dead Cell Stain Kit	Life Technologies
Dextramer SIINFEKL-PE	Immudex
Dextramer H-2 Kb/INHKFCNL-APC	Immudex
Dextramer H-2 Kb/INHKFCNL-PE	Immudex
Dextramer H-2 Kb/KSFLWTQSL-APC	Immudex
Zombie NIR Live/Dead Cell stain	BioLegend

2.1.11 Cell stimulation reagents

Reagent	Manufacturer
Phorbol myristate acetate (PMA)	Sigma-Aldrich (Merck)
Golgi Stop (Brefeldin A)	BD
Ionomycin	Sigma-Aldrich (Merck)
Peptide KSFLWTQSL-NH2	Peptides & elephants
Peptide LTYSQLMTL-NH2	Peptides & elephants
Peptide QAVNNLVEL-NH2	Peptides & elephants
Peptide QSAGFTAGL-NH2	Peptides & elephants
Peptide RALLNMIGM-NH2	Peptides & elephants
Peptide SAGVYMGNL-NH2	Peptides & elephants
Peptide SGYNFSLAGA-NH2	Peptides & elephants
Peptide SGYNFSLSA-NH2	Peptides & elephants
Peptide YQPSNGQYI-NH2	Peptides & elephants

2.1.12 Anti-mouse antibodies

Antigen	Fluorophore	Clone	Class	Manufacturer
CD3	APC	17A2	Rat IgG2b, κ	biolegend
CD3	FITC	17A2	Rat IgG2b, κ	biolegend
CD3	PE/Cy7	145-2C11	Armenian Hamster IgG	biolegend
CD3	Alexa 700	17A2	Rat IgG2b, κ	biolegend
CD3	BV785	17A2	Rat IgG2b, κ	biolegend
CD3	PerCP/Cy5.5	17A2	Rat IgG2b, κ	biolegend
CD3	BV785	17A2	Rat IgG2b, κ	biolegend
CD4	FITC	GK1.5	Rat IgG2b, κ	biolegend
CD4	PE	GK1.5	Rat IgG2b, κ	eBioscience
CD4	BUV737	GK1.5	Rat IgG2b, κ	BD
CD8	BV650	53.6.7	Rat IgG2a, κ	biolegend
CD8	BUV395	53-6.7	Rat IgG2a, κ	biolegend
CD8a	APC/Cy7	53.6.7	Rat IgG2a, κ	biolegend
CD8a	BV421	53-6.7	Rat IgG2a, κ	biolegend
CD11a	eFluor 450	M17/4	Rat IgG2a, κ	eBioscience
CD11b	BV510	M1/70	Rat IgG2b, κ	biolegend
CD11b	BV650	M1/70	Rat IgG2b, κ	biolegend
CD11c	PE	HL3	Armenian Hamster IgG_1, λ2	BD
CD11c	BV785	N418	Armenian Hamster IgG	biolegend
CD11c	PE/Cy7	N418	Armenian Hamster IgG	biolegend
CD16/32 FACS Block TruStainX	-	101320		biolegend
CD38	Alexa 488	90	Rat IgG2a, κ	biolegend
CD44	BV510	IM7	Rat IgG2b, κ	biolegend
CD45	APC	30-F11	Rat IgG2b, κ	biolegend
CD45.1	PE	A20	Mouse IgG2a, κ	biolegend
CD45.1	Alexa 700	A20	Mouse IgG2a, κ	biolegend
CD45.2	APC	104	Mouse IgG2a, κ	biolegend
CD45R/B220	BV650	RA3-6B2	Rat IgG2a, κ	biolegend
CD45R/B220	BV785	RA3-6B2	Rat IgG2a, κ	biolegend
CD45R/B220	PerCP/Cy5.5	RA3-6B2	Rat IgG2a, κ	biolegend
CD45R/B220	PE/Cy7	RA3-6B2	Rat IgG2a, κ	biolegend
CD45R/B220	FITC	RA3-6B2	Rat IgG2a, κ	biolegend
CD62L	APC	MEL-14	Rat IgG2a, κ	biolegend
CD62L	FITC	MEL-14	Rat IgG2a, κ	biolegend

Antigen	Fluorophore	Clone	Class	Manufacturer
CD62L	BV421	MEL-14	Rat IgG2a, κ	biolegend
CD103	PerCP/Cy5.5	2,00E+07	Armenian Hamster IgG	biolegend
CD103	PE-Dazzle	2,00E+07	Armenian Hamster IgG	biolegend
CD103	BV421	2,00E+07	Armenian Hamster IgG	biolegend
CD127	PerCP/Cy5.5	A7R34	Rat IgG2a, κ	biolegend
CD152 (CTLA-4)	PE	UC10-4B9	Armenian Hamster IgG	eBioscience
CD152 (CTLA-4)	APC	UC10-4B9	Armenian Hamster IgG	biolegend
CD161b/c (NK1.1)	FITC	PK136	Mouse IgG2a, κ	biolegend
CD161b/c (NK1.1)	PerCP/Cy5.5	PK136	Mouse IgG2a, κ	biolegend
CD279 (PD-1)	PerCP/Cy5.5	RMP1-30	Rat IgG2b, κ	biolegend
CD279 (PD-1)	APC/Cy7	29F.1A12	Rat IgG2a, κ	biolegend
CD279 (PD-1)	BV605	29F.1A12	Rat IgG2a, κ	biolegend
F4/80	PerCP/Cy5.5	BM8	Rat IgG2a, κ	biolegend
F4/80	PE	BM8	Rat IgG2a, κ	biolegend
GrzmB	PerCP/Cy5.5	QA16A02	Mouse IgG1, κ	biolegend
IFNγ	FITC	XMG1.2	Rat IgG1, κ	biolegend
KLRG1 (MAFA)	PE	2F1/KLRG1	Syrian hamster, IgG	biolegend
KLRG1 (MAFA)	PE/Cy7	2F1/KLRG1	Syrian hamster, IgG	biolegend
LASV GP	CF 633	1B3	-	BNI/NewYork
LASV GP	CF 633	Nanobody02	Llama nanobody	Florian Krammer, Mount Sinai
LASV NP	CF 633	2B5	-	BNI
Ly6C	APC/Cy7	HK1.4	Rat IgG2c, κ	biolegend
Ly6C	BV510	HK1.4	Rat IgG2c, κ	biolegend
Ly6G	PE/Cy7	1A8	Rat IgG2a, κ	biolegend
Ly6G	BV785	1A8	Rat IgG2a, κ	biolegend
MHC II (I-A/I-E)	eFluor 450	M5/114.15.2	Rat IgG2b, κ	eBioscience
MHC II (I-A/I-E)	Pacific Blue	M5/114.15.2	Rat IgG2b, κ	biolegend
Siglec-F	PE	E50-2440	Rat IgG2a, κ	BD
TNFα	PE/Cy7	MP6-XT22	Rat IgG1, κ	biolegend

2.1.13 Anti-human antibodies

Antigen	Fluorophore	Clone	Class	Manufacturer
CD1c	BV421	L161	Mouse IgG1, κ	biolegend
CD3	BV650	OKT3	Mouse IgG2a, κ	biolegend
CD3	Pacific Blue	SK7	Mouse IgG1, κ	biolegend
CD3	BV785	OKT3	Mouse IgG2a, κ	biolegend
CD3	BV510	OKT3	Mouse IgG2a, κ	biolegend
CD4	PerCP/Cy5.5	OKT4	Mouse IgG2b, κ	biolegend
CD4	BV650	OKT4	Mouse IgG2b, κ	biolegend
CD4	Alexa 488	OKT4	Mouse IgG2b, κ	biolegend
CD8a	Alexa 488	RPA-T8	Mouse IgG1, κ	biolegend
CD8a	BV510	RPA-T8	Mouse IgG1, κ	biolegend
CD8a	Alexa 700	RPA-T8	Mouse IgG1, κ	biolegend
CD11c	PerCP/Cy5.5	Bu15	Mouse IgG1, κ	biolegend
CD14	PE/Cy7	HCD14	Mouse IgG1, κ	biolegend
CD15	BV510	W6D3	Mouse IgG1, κ	biolegend
CD16	BUV395	3G8	Mouse IgG1, κ	BD
CD16	BV711	3G8	Mouse IgG1, κ	biolegend
CD19	BV650	HIB19	Mouse IgG1, κ	biolegend
CD19	BV785	HIB19	Mouse IgG1, κ	biolegend
CD19	PerCP/Cy5.5	HIB19	Mouse IgG1, κ	biolegend
CD16/32 FACS Block TruStainX	-	-		biolegend
CD38	BV510	HB-7	Mouse IgG1, κ	biolegend
CD40L (CD152)	FITC	24-31	Mouse IgG1, κ	biolegend
CD45RA	BV711	HI100	Mouse IgG2b, κ	biolegend
CD56	BV605	5.1H11	Mouse IgG1, κ	biolegend
CD56	BV650	HCD56	Mouse IgG1, κ	biolegend
CD62L	PE/Dazzle594	DREG-56	Mouse IgG1, κ	biolegend
CD69	BUV737	FN50	Mouse IgG1, κ	BD
CD86	APC	IT2.2	Mouse IgG2b, κ	biolegend
CD103	BV 421	Ber-ACT8	Mouse IgG1, κ	biolegend
CD123	BV510	6H6	Mouse IgG1, κ	biolegend
CD141	PE	M80	Mouse IgG1, κ	biolegend
CD152 (CTLA-4)	PE	L3D10	Mouse IgG1, κ	biolegend
CD152 (CTLA-4)	PE/Cy7	BNI3	Mouse IgG2a, κ	biolegend
CD178 (FasL)	BV421	NOK-1	Mouse IgG1, κ	biolegend
CD197 (CCR7)	BV421	G043H7	Mouse IgG2a, κ	biolegend
CD279 (PD-1)	APC	EH12.2H7	Mouse IgG1, κ	biolegend
CD303	PE/Cy7	201A	Mouse IgG2a, κ	biolegend
CD304	PE/Cy7	12C2	Mouse IgG2a, κ	biolegend

Antigen	Fluorophore	Clone	Class	Manufacturer
CD370	PE	8F9	Mouse IgG2a, κ	biolegend
GrzmB	PerCP/Cy5.5	QA16A02	Mouse IgG1, κ	biolegend
HLA-DR	BV785	L243	Mouse IgG2a, κ	biolegend
HLA-DR	PE/Cy7	L243	Mouse IgG2a, κ	biolegend
HLA-DR	Alexa 488	L243	Mouse IgG2a, κ	biolegend
IFNγ	FITC	4S.B3	Mouse IgG1, κ	biolegend
KLRG1 (MAFA)	PE	SA231A2	Mouse IgG2a, κ	biolegend
KLRG1 (MAFA)	BV605	2F1/KLRG1	Syrian hamster, IgG	biolegend
KLRG1 (MAFA)	PE	2F1/KLRG1	Syrian hamster, IgG	biolegend
Perforin	BV711	dG9	Mouse IgG2b, κ	biolegend
TNFα	PE/Cy7	MAb11	Mouse IgG1, κ	biolegend

2.1.14 Instruments/Apparatuses

Name of the Instrument	Manufacturer
Cell counter LUNA-FL	Logos Biosystems
Flow cytometer Fortessa	BD
Flow cytometer LSR II	BD
Flow cytometer Guava12	EMD Millipore (Luminex)
Scale	Kern
Precision Scale	Sartorius
Refrigerated centrifuge; swing buckets 15& 50 mL (Rotina 420R)	Hettich
Refrigerated centrifuge;1.5 - 2 mL (5417R)	Eppendorf
Thermocouple with rectal probe (BIO-TK8851 & BIO-BRET-3)	Bioseb
Fast-Prep-24 - Tissue homogenator	mpbio
Reflotron® Chemistry Analyzer	Roche
DRI-CHEM NX500 Chemistry Analyzer	Fuji
TissueLyzer – Tissue homogenator	Qiagen
Isoflurane vaporizer Univentor 410 and inhalation chamber	UNO BV

2.1.15 Software

Software	Application
FACS DIVA BD	Settings and recording with BD flow cytometers
FlowJo X	Analyzes of flow cytometric data
Graphpad Prism 6 & 7	Generation of graphs & statistical analyses
Microsoft Excel 2011 for Mac Microsoft Excel 2007 Windows	Table calculation
Microsoft PowerPoint 2011 for Mac	Creation of diagrams and plots
Microsoft Word 2011 for Mac Microsoft Word 2007 Windows	Text editor
Thomson Reuters EndNote X7	Literature database manager

2.2 Methods

2.2.1 Immunofocus Assay (IFA)

In order to titrate potential infectious virus concentrations in samples, Vero E6 cells grown in 24-well cell culture plates (~4.2x10^4 cells per well; seeded the previous day) in supplemented DMEM were infected with the samples of interest for one hour at 37 °C under a 5% CO_2 atmosphere. Each sample underwent a previous serial dilution in approximated half logarithmic steps within a 96-well polypropylene U-bottom plate. This was achieved by transferring 60 µL of each dilution into 130 µL of fresh medium DMEM or GMEM (2% FCS), mixing the sample at least six times. 200 µL of the full logarithmic dilution steps (every second dilution step) from 10^0 up to 10^{-5} dilutions were used to infect the cells. The infectious inoculum was removed after 1 hour. Afterwards each well was filled with about 1 mL of 6.6% FCS DMEM culture medium thickened with 0.933% methylcellulose (two parts 10% FCS DMEM culture medium with 1 part methylcellulose (2.8% in PBS)) and incubated for five days at 37 °C under a 5% CO_2 atmosphere.

Five days after the infection, the culture overlay medium was removed by inversion of the plates and the 24-well plates were submerged in 4% formalin at room temperature to inactivate the virus and fixate the cells, enabling the export out of the BSL-4 facility.

After fixation the plates were washed three times in a bucket with running tap water. 300 µL of 0.5% Triton-X100 in PBS were added to each well and incubated for 30 minutes at room temperature to permeabilize the cells. Afterwards, the plates were washed again with water and incubated with 300 µL of blocking solution (5% FCS in PBS) for 1 hour on a laboratory rocker. The supernatant was discarded and 200 µL of primary antibody 1:30 (1:100 dilution when 4 °C overnight) in 2% FCS PBS was overlaid for another incubation period of 1 hour at room temperature. Then, the plates were again thoroughly washed with tap water three times before applying 200 µL of peroxidase coupled sheep anti-mouse-IgG detection antibody (1:1,000 dilution) in 2% FCS PBS for another hour of incubation on a rocker. Three subsequent washings with water followed and later 220 µL TMB was added (1:3 dilution with PBS). The conversion of TMB by the coupled horse radish peroxidase resulted in the development of blue colored antigenic foci. The foci were counted manually, and titers calculated based on the dilution steps displaying between 20 to 100 foci. In order to present data in a logarithmic manner, results below the limit of detection were entered as ⅓ of the detection limit.

2.2.2 Generation of the chimeric mouse model

To generate a LASV susceptible immunocompetent mouse model for LASV infection, 6-8-week-old IFNAR$^{-/-}$ (B6(Cg)-*Ifnar1*$^{tm1.2Ees}$/J) recipient mice were transplanted with C57BL/6 Ly5.1 (B6.SJL-*Ptprc*^{a}*Pepc*^{b}/BoyJ) wildtype bone marrow as previously described [29].

In short: Recipient mice were gamma-irradiated with 4 Gray (~150 seconds) two times with a time spacing of 4 hours for a total of 8 Gray. The bone marrow of Ly5.1 mice was extracted under sterile conditions from femurs and tibiae. After red blood cell lysis, straining (70 µm) and PBS washing the cells were manually counted. 3x10^{6} bone marrow cells were intravenously transplanted within 50 µL PBS into the twice irradiated recipient mice via the retro-orbital vein plexus. For the procedure the mice were kept under short time isoflurane anesthesia. Transplanted mice received enrofloxacin (Baytril, Bayer) treated drinking water (0.1 mg/mL) for 6 weeks post transplantation.

Eight weeks post transplantation; blood was sampled from the chimeric mice to verify transplantation efficiency via flow cytometry with a CD45.1-PE CD45.2-APC staining. Animals with >85% CD45.1^{+} PBMCs were used for infection experiments.

2.2.3 Animal housing

Work with and housing of experimental animals was subject to the German animal welfare laws “Tierschutzverordnung” and were conducted with the permission of the science administration “Behörde für Wissenschaft, Forschung und Gleichstellung, Hamburg”, department “Lebensmittelsicherheit und Veterinärwesen” under approval number 31/17. Animals were bred and reared in the animal facilities of the BNITM. *One week before the start of the experiment,* mice were transferred in individually ventilated cages (IVCs) into the BSL4 laboratory with pellet chow and water *ad libitum*. As symptoms of infection arose around day 8 post infection (dpi), all animals additionally received pre-wetted food pellets on height of the bedding. Cages and water were changed on a weekly basis.

2.2.4 Infection of animals

Animals were infected with virus stocks of LASV strain Bantou 366 (LASV Ba366; Accession: KP339063.1) or MORV (Accession: NC_013057.1-58.1) stored at -80 °C

and harvested from infected Vero E6 cell supernatant. Infection was performed with virus diluted in PBS to 100 or 1000 FFU per animal. Intraperitoneal infection (i.p.) was conducted with BD Micro-fine syringes in 100 µL volume. Intranasal (i.n.) infection was performed under short time isofluran anesthesia with 25 µL of inoculum carefully and slowly being pipetted onto one nostril for aspiration.

2.2.5 Organ tissue dissociation

In order to dissociate tissue and cells for virus titration 10-200 mg of the organs were ball-milled within culture media. The organ input was weighed and afterwards 1 mL of DMEM was added. Milling occurred with either using the ceramic lysing matrix D (MP Biomedical) in conjunction with the Fast-Prep-24 for twice 30 seconds at 6 m/s^2 or using the TissueLyzer (Qiagen) with a single 5 mm steel ball at 50 Hz for two times 6 minutes. The samples were afterwards centrifuged at 10,000 x g for 10 minutes to remove debris, then the supernatant was titrated.

2.2.6 Blood sampling

Small volume blood sampling of mice was performed by puncture (transversal puncture) of the *vena caudalis mediana*. Falling blood droplets were collected dependent on the application in either EDTA tubes (BD microtainer/ Sarstedt Microvette) or LiHep tube (Sarstedt Microvette) for flow cytometric analysis, SST tubes (BD microtainer), LiHep-Gel tubes or Z-gel tubes (Sarstedt) for analysis of serum parameters, or HBSS+heparin (2 IU/mL) prefilled reaction tubes for virus titration from full blood. The bleeding was stopped by applying sterile cellulose swabs (Hartmann Pur-Zellin) with pressure to the puncture for 20-30 seconds.

Larger volumes of blood were collected by heart puncture with a syringe (BD micro-fine) as a final bleeding step upon sacrifice of the animal after overdose isoflurane inhalation anesthesia.

Patient blood samples were drawn with full consent of the patients by health care professionals at the ISTH as part of the Lassa pathology study. The National Committee of Ethics in Medical Research of Nigeria, as well as the Ethics Committee of the Medical Association of Hamburg, approved the use of diagnostic leftover samples and the corresponding patient data for this study as well as the collection of samples for the

pathogenesis study of confirmed patients (permits ISTH/HREC/20171208/45, ISTH/HREC/2017128/43 and PV3186 respectively).

2.2.7 Preparation of single cell suspensions (SCS) from mouse organs for flow cytometric analysis

Mouse spleens and lungs were temporarily explanted in to cold PBS until processing. Organs were cut into ~1 mm^3 pieces within 1.5 mL DNAse I/Collagenase D DMEM media (final concentration: 50 Kunitz-Units/mL DNAse I, 400 U/mL Collagenase D). The suspension was incubated at 37 °C for 25 minutes under constant agitation (1000 rpm). Afterwards 30 µL of 0.5 M EDTA was added and incubated for 5 minutes to inhibit further digestion by Ca^{2+} dependent enzymes. The organ suspension was minced through pre-wetted 70 µm cell strainers with sterile syringe plungers. Strainers were then washed with PBS. The cell suspension was centrifuged at 300 x g for 5 minutes at 4 °C. The supernatant was discarded and the cell pellet resuspended in 5 mL red cell lysis buffer (BD Pharm Lyse) to be incubated at room temperature for 5-10 minutes, after which 15 mL PBS were added to osmotically stabilize the suspension. The cells were washed twice with PBS and resuspended in 1 mL PBS.

2.2.8 Blood biochemistry analyzes

Biochemical parameters from mouse sera (SST or Z-gel tubes) were acquired using the Roche Reflotron system and corresponding test strips (AST, ALT, etc.). Human plasma parameters were acquired from EDTA-plasma (purple cap) using the SpotChem platform (Axon Lab).

Sera from mice, starting 2018, were collected in LiHep-Gel tubes and analyzed with test strips from Fuji on the DRI-CHEM NX500. If samples were out of the upper measuring range, they were diluted with 0.9% NaCl.

2.2.9 Cell counting

Concentrations of single cells in suspension were determined by manual counting within a Neubauer counting chamber and Trypan blue stainings or by the use of an automatic

fluorescent cell counter LUNA-FL (Logos Biosystems) with Acridine Orange/Propidium Iodide cell discrimination stain.

2.2.10 T cell purification

Mouse T cells were purified using the Pan T cell isolation Kit II from Miltenyi Biotec following the manufacturer instructions with MACS MS columns (Miltenyi Biotec). Input cells originated from sterile spleen SCSs, which were prepared as described above. Identical procedures were used for purification of T cells from human lymphocyte samples from blood following the manufacturer instructions with the human T cell isolations kits from Miltenyi.

2.2.11 CFSE labeling

If needed purified T cells were labeled with carboxyfluorescein succinimidyl ester (CFSE) staining according to Biolegend's "CFSE Cell Division Tracker Kit", but using an excess of a 15 µM solution of CFSE instead of 5 µM to account for higher labeled cell concentrations.

2.2.12 Verification of purified T cells

10-20 µL of purified T cells were stained with antibodies against CD3, CD4, CD8, and CD45.1 or in case of OT-I T cells against CD3, CD4, CD8 and B220 to verify the cell purity. The same panels were applied to track the T cell repopulation within the blood of transplanted animals over time.

2.2.13 Adoptive transfers

Single cell suspensions of spleen or MACS purified CD3 T cells were transplanted in receiver mice within 100 µL PBS through a BD Micro-Fine syringe intraperitoneally. Transfer of OT-I T cell was done intravenously (i.v.) via the retro-orbital vein plexus in a volume of 50 µL with BD Micro-Fine syringes.

2.2.14 Peptide stimulation

In silico determined MHC-I restricted LASV peptides were ordered from Peptides & Elephants. Peptide pools of 31 different peptides were reconstituted in water with 20-40% DMSO as a stock solution for stimulation assays of human leukocytes. Dilutions of these stock solutions to their final concentration were generated with the respective culturing media.

The cells were incubated at 37 °C with concentrations of 5-10 µg/mL per single peptide for 6-24 h. Brefeldin A (1:1,000) was added during the last 6 h of incubation. Unspecific positive stimulation controls were generated with PMA (50 ng/mL), Ionomycin (2 µg/mL) and Brefeldin A.

2.2.15 Freezing and thawing of PBMCs

Human peripheral blood mononuclear cells (PBMCs) were concentrated at the study site in Nigeria within a biosafety glove box. The purification procedure of the PBMCs consisted of centrifugation and red blood cell lysis (biolegend RBC lysis (10x); BD Pharm Lyse) including several centrifugal washing steps with PBS.

From 2018 on PBMCs were purified using Lymphoprep (STEMCELL) gradient centrifugations in SepMate-15 tubes (STEMCELL) according to manufacturer's protocol.

PBMC pellets were resuspended in fetal bovine serum with 10% (v/v) DMSO and frozen at a constant rate of -1°C·min^{-1} down to -80 °C to be exported on dry ice to Germany for further processing and analysis.

Thawing of the cells was conducted following the protocol of Steinberg and colleagues from 1999 [139] as developed for sensitive hepatocytes, as its since then has been retested as one of the best procedures in an comparative study [140]. The protocol was later changed to the thawing method evaluated by Hønge and colleagues analyzes on thawing of PBMCs in 2017 [141], describing the biggest cell viability factor during thawing being a rapid thawing process with warmed media. This was adapted for our samples with the addition of DNAse (50 Kunitz-Units/mL) within thawing and washing media to reduce cell clumping.

2.2.16 Flow cytometric staining of cells

Previous to live-dead staining, RBCs were lysed or Lymphoprep-purified PBMCs were resuspended in PBS. For live-dead staining cells were incubated with fixable dead cell permeable amine-reactive cross-linker fluorophore couplers (LIVE/Dead fixable Dye thermoFisher, or Zombie dyes biolegend) for 10-15 minutes at room temperature in the dark. Afterwards the cells were washed with serum-supplemented FACS buffer to react left-over amine-reactive couplers prior to addition of antibodies. The cells were pelleted at 300 x g for 5 minutes to be then resuspended in 20 µL unlabeled Fcγ-receptor blocking antibodies anti-CD16/CD32 (1:100 predilution) (TruStainX biolegend, mouse or human) for 10 minutes at room temperature. Finally 30 µL of 1.66-fold fluorescent staining antibody mix were added and incubated at 4° C for one hour or 30 min at room temperature to be then washed with FACS buffer and resuspended in 400 µL fixation/permeabilization buffer (BD Cytoperm/Cytofix) with additional 4% (v/v) formaldehyde supplemented for fixation and inactivation of viruses. The cells were fixed for 1 hour at room temperature before being washed with FACS buffer twice or with BD Perm/Wash if intracellular staining was to be performed. Intracellular staining antibodies were diluted in 50 µL BD Perm/Wash buffer and incubated with the samples for 30 minutes at room temperature. Afterwards the cells were washed twice with Perm/Wash buffer to be afterwards resuspended FACS staining buffer. FACS gatings were applied under exclusion of dead cells and doublets (Gating Strategies: murine T cells (Supplemental figure S1); murine myeloid cells in lung (Supplemental figure S2); murine myeloid cells in spleen and blood (Supplemental figure S3); human T cells (Supplemental figure S5); human myeloid cells (Supplemental figure S5); human DCs (Supplemental figure S6).

2.2.17 Cell count extrapolation per organ

Cell counts were calculated in two different ways. Blood samples were extrapolated to cells·mL^{-1} by recording the volume of the blood used for staining as well as defined volumes of counting beads (biolegend precision counting beads).

For spleen and lungs cell concentrations were determined prior to staining using a cell counter (Luna-FL). Total volumes of single cells suspensions as well as the volume of suspension used for staining were noted. Counting beads were used to assess the cell loss occurring in the staining procedure and recording of cells.

2.2.18 PrimeFlow RNA hybridization assay

PrimeFlow RNA hybridization assays were performed on LASV Ba366 infected murine L929 cells (MOI 0.01 harvested 4 dpi) according to manufacturer's instructions. Slight protocol adaptations were required for inactivation and fixation of pathogenic samples. After the first RNA fixation and subsequent washing steps with RNA permeabilization buffer with added RNAse inhibitors, the cells were spun down at 800 x g for 5 minutes at 2-8 °C to be resuspended in BD Cytofix/Cytoperm fixation buffer supplemented with additional 4% formaldehyde, and incubated for 60 minutes at room temperature. After the inactivation step the cells were spun down again and were washed twice with PrimeFlow permeabilization buffer with RNAse inhibitors before continuing with intracellular staining and the standard manufacturer instructions. LASV GA391 NP hybridization probes were used for detection together with murine β-actin probes as a positive control probes to verify successful signal amplification reactions. Uninfected L929 cells were used as negative control samples.

2.2.19 Software based analysis

Flow cytometric analyses were recorded using BD FACS Diva and analyzed in FlowJo 10.6 (FlowJo,LLC).

Graphical and statistical analysis was performed using Prism Versions 6 and 7 (Graphpad)

Data organization and clean up was performed using Excel 2011 Mac (Microsoft)

Bibliographic management was executed using Endnote X7 (Thomson Reuters).

3. Results

3.1 Immunological analysis of T cell reaction in the IFNAR^{BL6} mouse model for LF

Immunological data on LASV infection is sparse due to the complexity, efforts and costs of BSL4 experimentation. A few small animal models for LF exist, e.g. guinea pigs models, which have to be infected with passage adapted strains of LASV or immune incompetent mouse models showing defects in Type I immune responses are employed. This bears problems in studying immune cells and their responses during LASV infection, because immune incompetent mice do not reflect natural phenotypes and many immunological tools are not available for guinea pigs. Oestereich and colleagues established a model to study fatal LF in hematopoietic competent bone-marrow chimeric IFNAR$^{-/-}$ mice with C57BL/6 bone marrow, showing a link of α-CD8-antibody treatment with significant alleviation of symptom severity despite absence of any virus clearance [29]. In order to further the insights into this topic, focus of this study was concentrated on the role of CD8 T cells in this model including their phenotypes and their influence.

3.1.1 Infection via the intranasal route effectively infects IFNAR^{BL6} mice

In the published infection model for LASV, IFNAR^{BL6} mice were infected via a intraperitoneal route (i.p.) [29]. To mimic a more natural transmission route in humans, mice in this study were infected intranasally with LASV (i.n.), causing an exposition of the mucosal membranes of the nasal passage and the pharyngotracheal space. Additional exposition of the esophagus and digestive tract could also not be excluded as i.n. application sometimes triggered swallowing reflexes. Intranasal MORV infection was chosen as a comparison to LASV, as MORV is a human non-pathogenic closely related arenavirus also found in *M. natalensis*. Differences between both infections might reveal LASV-specific immune pathogenic reactions.

Mice infected with 1,000 FFU LASV i.n. displayed the identical disease symptoms as previously published for i.p. infected mice. Abort criteria were reached between nine to ten days post infection, which following were defined as end time points.

Following the infection, the body weight of LASV infected animals started to decrease by 6 dpi until euthanasia criteria were reached at 9 dpi and 10 dpi, the analysis end points (Figure 7 A). No significant loss of body weight occurred in the MORV or mock infected groups. Mice infected with LASV showed elevated body temperature at day seven post infection with a subsequent drop at 9 dpi or 10 dpi in moribund stages (Figure 7 B). Body temperatures of MORV and mock infected individuals did not change over the course of infection. Serum AST concentrations started to rise at 7 dpi only in LASV infected individuals, rising until sacrifice in the late stages of disease (Figure 7 C). By 7 dpi all LASV infected animals showed pronounced viremia in blood at approximately 10^4 FFU/mL (Figure 7 D). Detection of viral titers in MORV infected animals in blood and organs was less consistent. Only individual animals displayed detectable MORV infections. Viremia in blood for MORV was only detectable for one animal at day seven post infection (Figure 7 D). Additionally, high MORV organ burden of $>10^4$ FFU/g was only encountered in spleen and lung of a single individual at 9 dpi, while samples of other MORV positive animals only had titers of approximately 10^3 FFU/g (Figure 8). In the organs of LASV infected animals low titers of infectious virus became detectable in some mice earliest at the sacrifice time point at 5 dpi while all LASV-infected animals sacrificed at 7 dpi were positive in spleen, lung and liver. LASV titers reached 10^5 FFU/g and more in spleen and lung tissue (Figure 8).

Taken together, using the intranasal route for the infection of the $IFNAR^{BL6}$ model has proven effective in productively infecting $IFNAR^{BL6}$ mice and recapitulating the LF disease symptoms also seen in the i.p. infection of the model. However, using the i.n. infection route greatly reduced the detectable infection efficiency of MORV compared to LASV in this model.

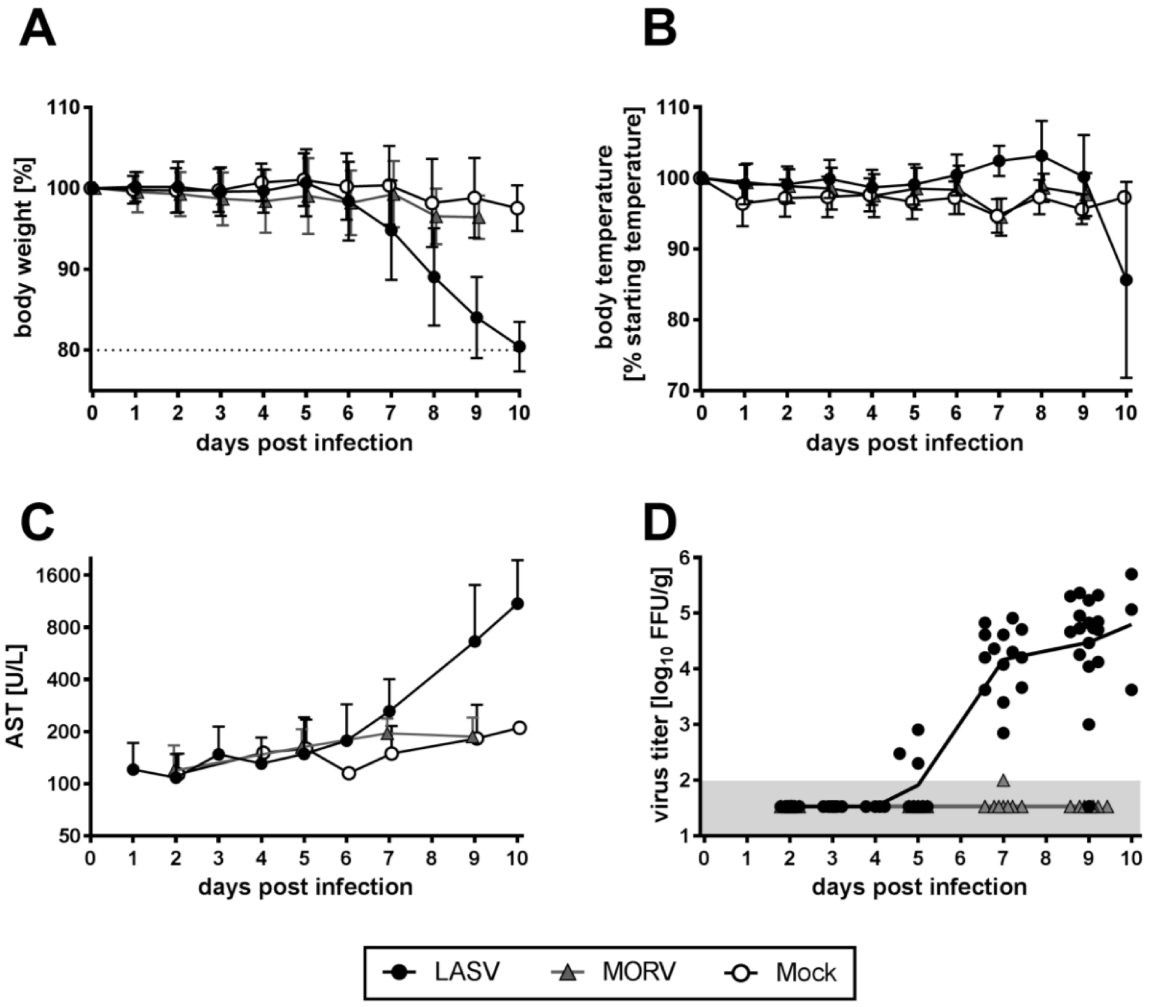

Figure 7 Physiological mouse parameters during LASV and MORV infection. IFNAR^{BL6} were inoculated i.n. with LASV or MORV or mock infection (1,000 FFU). Animals were sacrificed at predestined time points 3, 5, 7, 9 and 10 dpi. (A) Body weight of LASV or MORV infected animals, only LASV-infected mice lose weight beginning 6 dpi. (B) Body temperature of LASV-infected mice is elevated after 5 dpi with a critical temperature drop at 10 dpi. (C) LASV infected mice show elevated AST serum levels at late time points indicating tissue damage. (D) Titration of infectious virus particles in the blood show first detection of LASV at 5 dpi and increasing viremia with time progression; MORV infections mostly remain below the detection limit in the blood. Pooled data of 4 experiments; *Data shows mean ±SD (+replicates).*

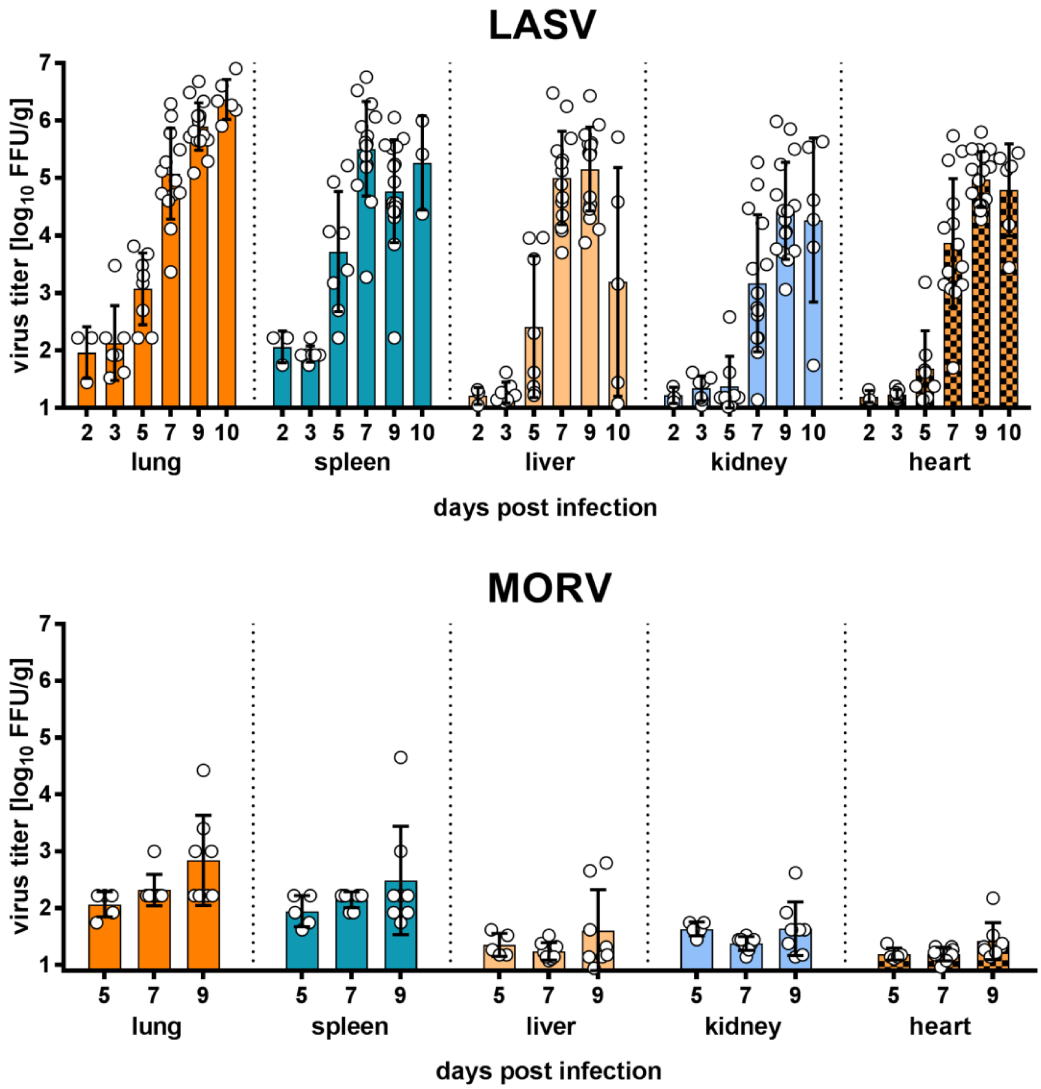

Figure 8 Viral organ burden of LASV- and MORV-infected IFNAR^{BL6} mice.
I.n. infected mice (1,000 FFU) were sacrificed at specific time points 2, 3, 5, 7, 9 & 10 dpi. Determination of viral titers (IFA) with high viral burden after 5 dpi throughout lung, spleen, liver, kidney and heart; only very low or undetectable viral titers during MORV infection. *Data shows mean ±SD (+replicates).*

3.1.2 Characterization of CD8 T cell responses in bone-marrow chimeric IFNAR^{BL6} mice to LASV and MORV infections

Previous experiments of Oestereich and colleagues indicated an involvement of CD8-positive cell populations in immune pathological processes, as depletion with α-CD8-antibody significantly reduced the observed LF symptomatology in the IFNAR^{BL6} mouse model. Under the hypothesis of a potential causation of the pathology through CD8 T cells during the LASV infection, any involvement of CD8 T cells had to be reflected within their immunological phenotype. Therefore potential activation and inhibition statuses of T cells were analyzed using flow cytometry. Immunological reactions of IFNAR^{BL} mice to i.n. LASV inoculation were compared against the reactions to the non-pathogenic MORV and mock infected control animals at early (3 & 5 dpi), intermediate (7 dpi) and late (9 & 10 dpi) time points of infection.

Flow cytometric analyses of the activation markers over the course of infection revealed the appearance of a strongly defined (>70%) CD8 T_{eff} cell ($CD44^+$ $CD62L^-$) population (Figure 9 A) in the spleen and lung nine days post infection. The activation phenotype of CD8 T cells was delayed compared to the onset of symptoms with weight loss starting seven days post infection but coincided the emergence of severe symptoms of the disease. Infection with MORV did not induce an increase in the CD8 T_{eff} population at 9 dpi compared to the mock control (Figure 9 B). The calculated total number of CD3 T cells in the lung was decreased at 9 dpi compared with the mock control and might have had a trend of returning towards mock levels in the moribund stages at 10 dpi (Figure 9 C). At the same time, an overall trend of T cell reduction from the spleen was observed even though it remained unclear, whether this was due to exfiltration or apoptotic cell loss. The measured reduction of T cells in the organs indicated that the occurrence of the prominently activated $CD44^+$ $CD62L^-$ CD8 T cell population could have arisen either from an overall phenotypic shift of the CD8 T cells or from an expansion of LASV-specific CD8 T cells with a simultaneous exfiltration or cell loss of unspecific T cells.

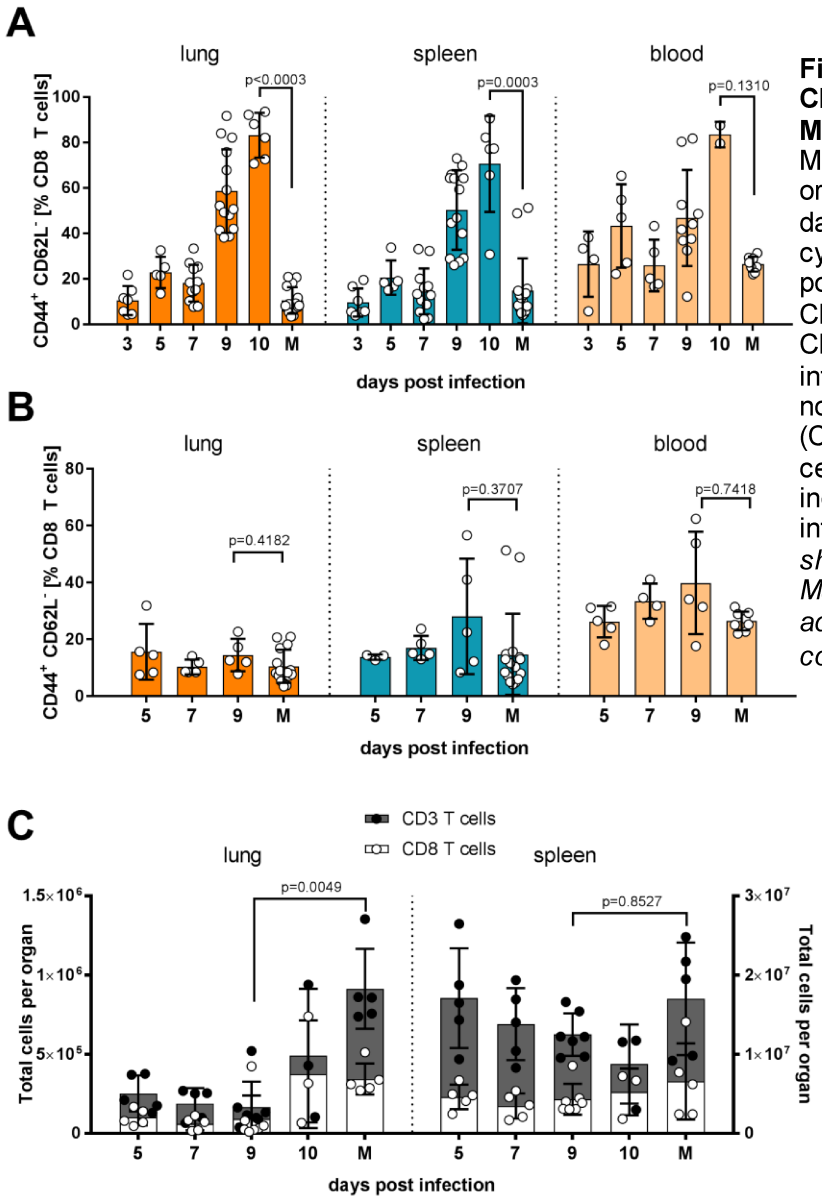

Figure 9 Activation status of CD8 T cells during LASV and MORV infection.
Mice infected i.n. with LASV, MORV or mock-inoculum were sacrificed at days 3, 5, 7, 9 & 10 dpi. (A) Flow cytometry of organs at different time points reveal a significant shift of CD8 T cells towards a $CD44^+$ $CD62L^-$ T_{eff} phenotype during LASV infection.(B) MORV infection does not induce a significant T_{eff} cell shift. (C) Total number of CD3 and CD8 T cells in lung and spleen rather indicate cell reduction during LASV infection instead of expansion. *Data shows mean ±SD (+replicates). Mann-Whitney-test, two-tailed, adjusted p-values with Dunn's correction.*

Inflammatory T cell responses usually are characterized by strong expansion of specific T cells, leading to the generation of terminally differentiated SLECs, which make up the majority of the cells undergoing apoptosis in the contraction phase of the immune response.

In this mouse model, approximately a third in lung and a fourth in spleen of the CD8 T cell population expressed KLRG1 by day nine post infection with LASV (Figure 10 A&B), identifying these cells as SLECs.

Additionally, research for Ebola had shown that fatal cases of Ebola virus disease correlated with a significant increase in the expression of the inhibitory markers PD-1 and CTLA-4 on CD8 T cells [142].

In the investigated i.n. infection with LASV the proportion of CD8 T cells expressing the inhibitory surface marker PD-1 rapidly increased with the occurrence of the shift to the T_{eff} and SLEC phenotypes at 9 dpi. The proportion of CD8 T cell expressing PD-1 even further escalated in the lung up to 10 dpi (Figure 10 A&B). PD-1 was co-expressed on $KLRG1^+$ CD8 T cells indicating the possibility of effector functions ceasing and exhaustion in these cells. The expression pattern of KLRG1 and PD-1 co-expression was more pronounced in the lungs (Figure 10 C) with 9.0% (±7.2 SD) of CD8 T cells co-expressing KLRG1 together with PD-1 at 9 dpi and 16.8% (±7.1 SD) at ten days post infection (Figure 10 A&B). The emergence of the T cell inhibitory marker CTLA-4 reflected the same progression as already seen for PD-1. CD8 T cells started CTLA-4 expression by day seven post infection. Up to day ten post infection the majority of CD8 T cells (77.7% ±21.6 SD) were expressing CTLA-4 (Figure 10 D), while only 4.2% (±1.0 SD) of CD8 T cells were CTLA-4 positive in the lung during early infection (5 dpi) or in mock infected controls. CD8 T cells of the spleen reacted very similar with 31.3% (±20.2 SD) of CD8 T cells expressing CTLA-4 at 9 dpi and 71.7% (±26.3 SD) by day ten of the LASV infection, displaying that this reaction was not locally confined.

The T cell reactions of MORV infected animals did not vary as greatly over the course of the infection (Supplemental figure S7). While MORV infection also led to an activation of CD8 T cells in lung and blood, only a minor induction of CTLA-4 in the spleen was observed. Interestingly PD-1 was only transiently expressed on CD8 T cell at 7 dpi. In LASV infection, however, strong shifts of CD8 T cells to a highly activated SLEC together with the expression of co-inhibitory factors like CTLA-4 and PD-1 point towards a possible overstimulation and subsequent inhibitory regulation of this cell type. Despite the expression of inhibitory factors on the CD8 T cells in the late stages of disease the observed pathology in the mice still progressed on until abort criteria were reached.

Knowing the extent of the overall CD8 T cell response, it was important to fully grasp the nature of the reactions of LASV-specific cytotoxic T cells. Unfortunately however, all attempts to characterize the phenotypes of LASV-specific CD8 T cells via the use of tetramers loaded with the oligopeptide KSFLWTQSL (part of GPC sequence: good *in silico* binding prediction IC_{50}: 56.54 nM (artificial neural network: IEDB)) and the oligopeptide INHKFCNL (part of NP sequence: immunogenic in IFNγ-ELISPOT) showed insufficient and unspecific staining, thereby not allowing for direct answers on the role of LASV-specific CD8 T cells during the infection.

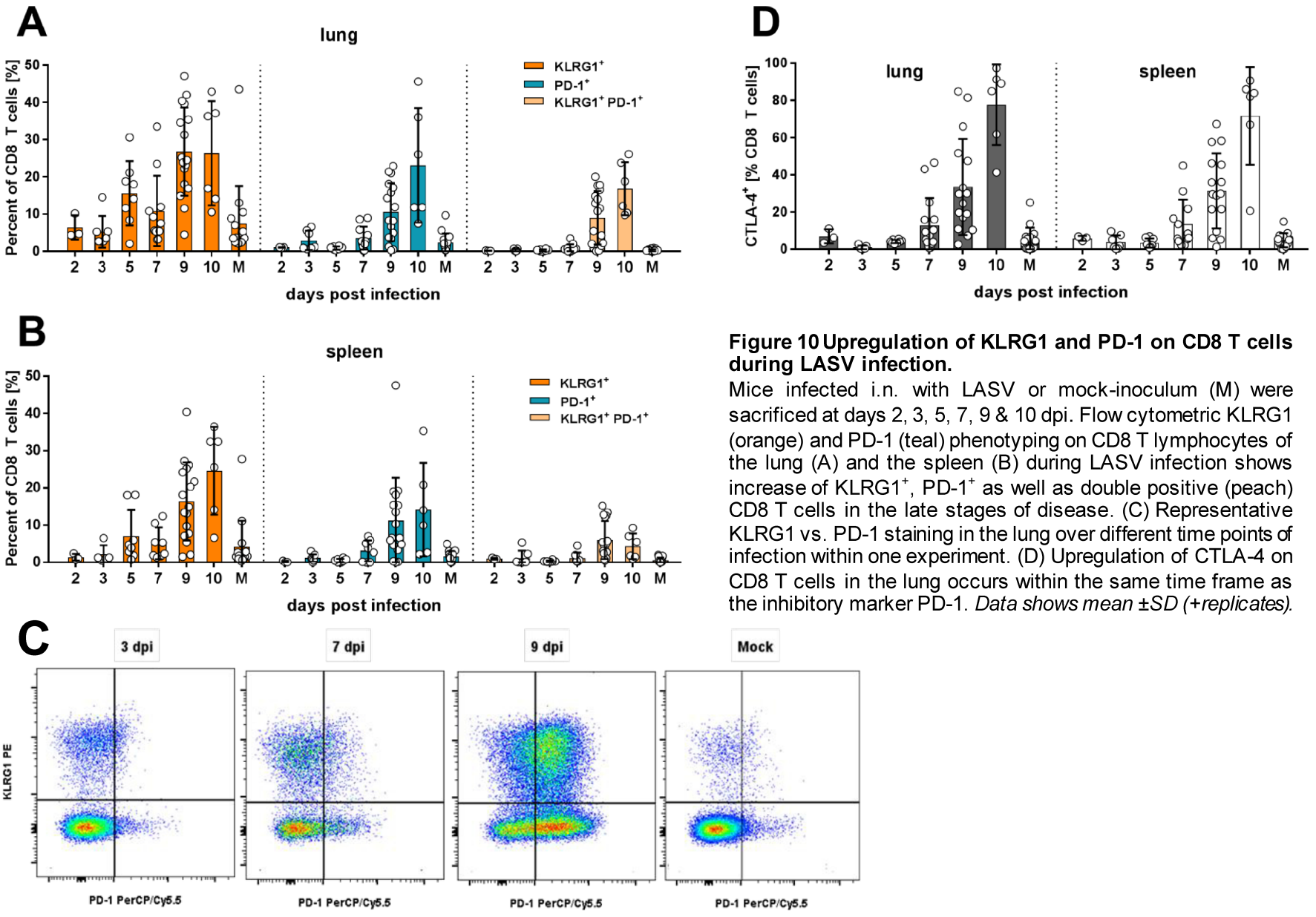

Figure 10 Upregulation of KLRG1 and PD-1 on CD8 T cells during LASV infection.

Mice infected i.n. with LASV or mock-inoculum (M) were sacrificed at days 2, 3, 5, 7, 9 & 10 dpi. Flow cytometric KLRG1 (orange) and PD-1 (teal) phenotyping on CD8 T lymphocytes of the lung (A) and the spleen (B) during LASV infection shows increase of KLRG1$^+$, PD-1$^+$ as well as double positive (peach) CD8 T cells in the late stages of disease. (C) Representative KLRG1 vs. PD-1 staining in the lung over different time points of infection within one experiment. (D) Upregulation of CTLA-4 on CD8 T cells in the lung occurs within the same time frame as the inhibitory marker PD-1. *Data shows mean ±SD (+replicates).*

3.1.3 LASV-unspecific CD8 T cells show only miniscule bystander activation *in vivo*

Failing to directly stain LASV-specific T cells with tetramers lead to an approach of characterizing the opposite. Guaranteed LASV-unspecific T cells of transgenic OT-I T cells were to be characterized in two different animal model approaches to fathom the involvement of unspecific bystander activation of cells during the infection.

OT-I mice only express a single transgenic T cell receptor specific for the MHC I (H-2K^{b})-restricted SIINFEKL peptide, which is part of ovalbumin. OT-I T cells therefore cannot directly react to LASV infection and are thus guaranteed LASV-unspecific. Should activation of OT-I T cells in IFNAR^{BL6} still occur, is this an indicator for unspecific bystander activation of T cells by the environmental inflammatory milieu during the infection.

In the first approach chimeric IFNAR^{BL6} mice were provided i.v. with 1.3x10^{7} adoptively transferred MACS purified OT-I CD3 T cells one day prior to the infection with LASV. The second approach employed the use OT-I mouse bone marrow in the generation of multi-bone-marrow-chimeric mice generating chimeric IFNAR$^{BL6+OT-I}$ mice. After repopulation, the generated mice harbor matured T cells of three different genotypes: wild type (Ly5.1) T cells, SIINFEKL-restricted OT-I T cells and a small leftover minority of immune impaired IFNAR$^{-/-}$ T cells. All three genotypes could be distinguished based on phenotypic markers. Hematopoietic wild type cells expressed CD45.1, while cells of OT-I and IFNAR$^{-/-}$ did not. Additionally, OT-I T cells could be identified by SIINFEKL-tetramer staining.

The introduction of additional OT-I T cells to the established IFNAR^{BL6} animal model via adoptive transfer shifted the disease induced weight loss by half a day ahead within this small sample size (n=5) (two-way ANOVA of cubic regression models) compared to the normal INFAR^{BL6} mice or IFNAR$^{BL6+OT-I}$ mice, which both did not differ from each other. (Figure 11 A) (Supplemental table S1).

Prior to the adoptive transfer into the recipients, OT-I T cells were labeled with CFSE staining enabling flow cytometric tracking of the adoptively transferred OT-I T cells and estimations of the number of cell divisions they underwent since labeling. To test for infection unrelated influences on the adoptively transferred T cells, one recipient mouse was solely mock-infected.

Within the inflammatory milieu of LASV-infected mice, transferred OT-I T cells showed enhanced proliferation compared to the steady-state milieu of an uninfected mouse

(Figure 11 B). Based on SIINFEKL-loaded tetramer staining even OT-I T cell could be identified, which had proliferated sufficiently to dilute the CFSE signal for identification.
Of the adoptively transferred OT-I T cells a smaller fraction expressed the SLEC marker KLRG1 (22.5% ±13 SD) in the lung compared to the CD45.1 wild type CD8 T cells in the same mouse (32.7% ±5.2 SD) (Figure 11 C&D). While the extent of KLRG1-postive CD8 T cells in the blood (Supplemental figure S8 A) behaved similar to the lung (OT-I: 17.7 ±10.4 SD; CD45.1: 31.7% ±10.9 SD), OT-I T cells of the spleen showed virtually no induction KLRG1 expression (OT-I 1.5% ±0.4 SD; CD45.1: 25.1% ±9.8 SD) (Supplemental figure S8 B). A smaller portion of the OT-I T cells downregulated CD62L compared to $CD45.1^{+}$ CD8 T cells in the lung (OT-I: 44.6%±10.2 SD; CD45.1: 18.5%±7.9 SD). Downregulation of CD62L on the transferred OT-I T cells, however, was still stronger compared to immune incompetent $IFNAR^{-/-}$ T cells (Figure 11 C). High percentages of OT-I T cells did express Granzyme B in the lung (77.0% ±17.0 SD) as did the CD45.1 WT CD8 T cells (58.2% ±11.3 SD), while the $IFNAR^{-/-}$ CD8 T cells within every animal remained mostly Granzyme B negative (3.9% ±3.0 SD) in the late stages of infection (Figure 11 E).
Interestingly, retesting for bystander activation within $IFNAR^{BL6+OT-I}$ mixed bone marrow chimeras led to different results. In $IFNAR^{BL6+OT-I}$ mixed bone marrow chimeras, CD8 T cells of each of the three different genotypes matured in the identical environment and were not manipulated *ex vivo* minimizing externally induced influences. The disease progression of LASV infection in $IFNAR^{BL6+OT-I}$ behaved identical to normal $IFNAR^{BL6}$ bone marrow chimeras (Figure 11 A (grey triangle)), and yielded far greater recoveries of OT-I T cells during flow cytometric analysis than the previous adoptive transfer experiment. The activation of OT-I T cells previously seen during the adoptive transfer experiment did not occur within this experimental setup. OT-I T cells of $IFNAR^{BL6+OT-I}$ mice did neither downregulate CD62L to display a SLEC phenotype (Figure 12 A) nor was KLRG1 expression on OT-I T cells induced (Figure 12 B) during the infection. Meaning that the partial activation observed in the adoptive transfer experiment might have been an artifact due to unknown confound variables introduced by magnetic cell sorting, the CFSE staining and the adoptive transfer of the OT-I T cells.
The results of the $IFNAR^{BL6+OT-I}$ model showed that guaranteed LASV-unspecific endogenously matured OT-I T cells were not activated during a fulminate LASV infection, in which wild type CD45.1 cytotoxic T cells were highly activated. This

unresponsiveness of LASV-unspecific T cells shifted the research focus to the involvement of LASV-specific CD8 T cells.

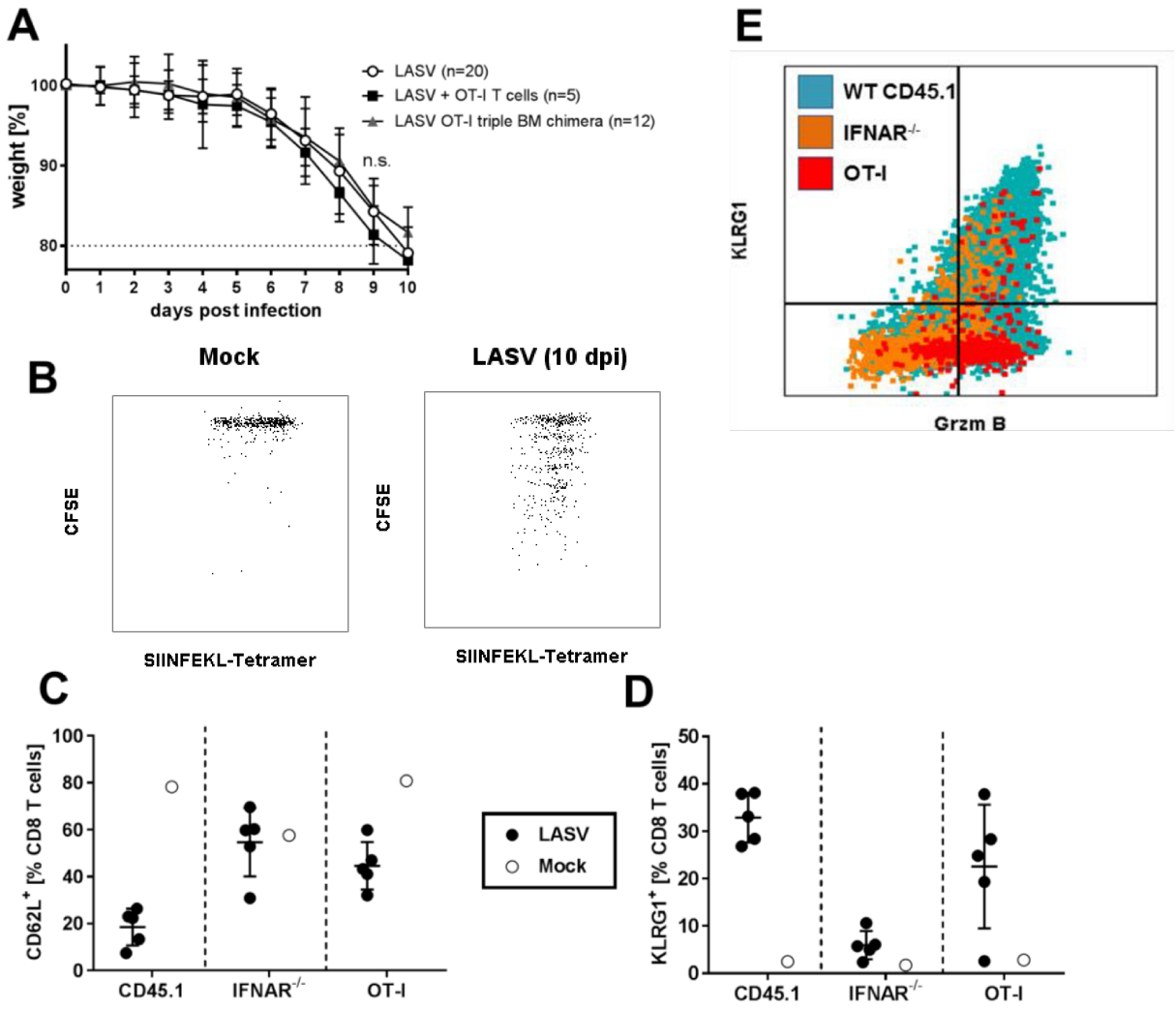

Figure 11 Partial activation of adoptively transferred OT-I T cells in IFNAR^{BL6} split by T cell genotype origin.
(A) Neither transfer of OT-I T cells (solid black square) nor transplantation of OT-I bone marrow (grey triangle) did influence weight loss during infection. (B) OT-I T cells in the lungs of LASV infected animals underwent more cell divisions. (C) CD62L downregulation and (D) KLRG1 upregulation in the lung (9 dpi) depicting differing activation based on genotype after adoptive transfer during infection. (E) Representative CD8 T cell dot plot of an infected animal's lung 10 dpi; (blue) wild type reaction, (orange) IFNAR$^{-/-}$ reaction, (red) OT-I reaction in the same host; *Data shows mean ±SD (+replicates). Multiple t-test (9 dpi), two-tailed, adjusted p-values with Dunn's correction, n.s.: p>0.05.*

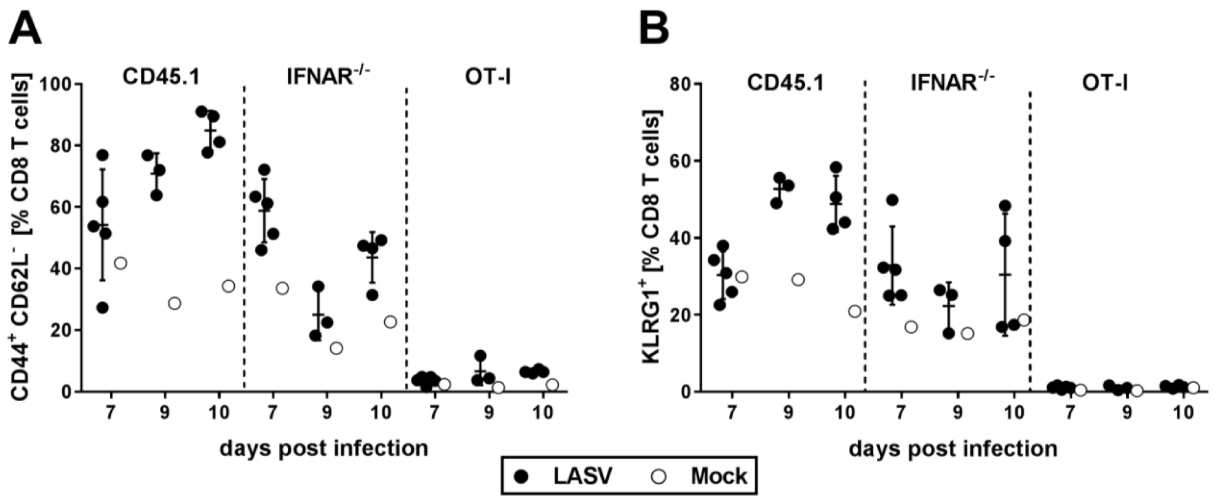

Figure 12 No bystander activation in IFNAR$^{BL6+OT-I}$ bone marrow chimeras.
(A) No induced activation phenotype on endogenously matured OT-I CD8 T cells during LASV infection in the lung (9 and 10 dpi pooled). (B) KLRG1^{+} SLEC phenotype of OT-I T cell previously seen after adoptive transfer is completely diminished despite a fulminant LASV infection being present. *Data shows mean ±SD (+replicates).*

3.1.4 Adoptive transfer of spleen single cell suspension does not induce immune pathologies in immune incompetent RAG1$^{-/-}$ mice

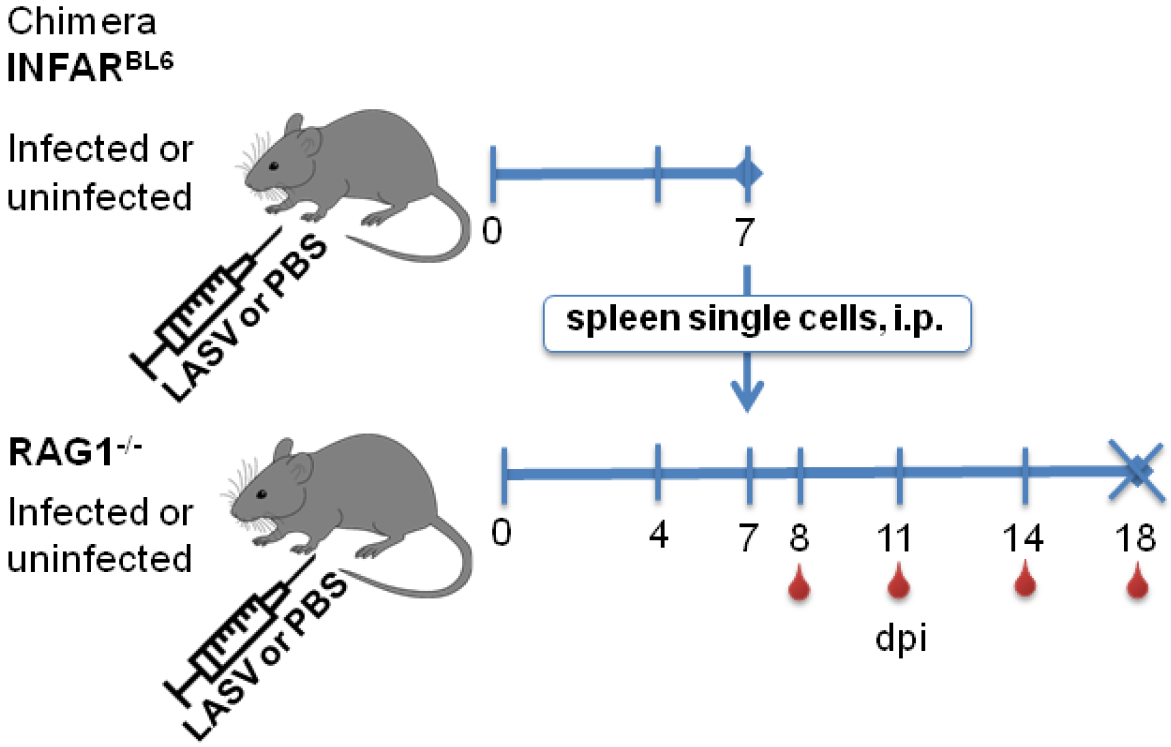

Figure 13 Experimental design of the adoptive transfer into RAG1$^{-/-}$ mice.
IFNAR^{BL6} donor and RAG1$^{-/-}$ recipient mice are inoculated with LASV or PBS at the same day. At 7 dpi donor mice are sacrificed and spleen single cell suspension adoptively transferred into infected or uninfected RAG1$^{-/-}$ mice. RAG1$^{-/-}$ are bled at 8, 11, 14 & 18 dpi to measure T cell repopulation, viremia and serum AST-values. *Recolored mouse graphic from original vector graphic by Gwlz (wikimedia) CC 4.0 BY SA.*

Published experiments [29] argue for a putative CD8 T cell induced immune pathology in LASV infections, as CD8-depleted mice do not show LASV-dependent symptoms or disease progression despite high viral titers. Immune incompetent mice like SCID and RAG1 mice display a similar absence of symptoms as CD8-depleted IFNAR^{BL6} mice. On ground of generating evidence towards the involvement of the hematopoietic immune system in the induction pathologies, RAG1$^{-/-}$ mice, which do not generate cells of the adaptive immune system, received a transfer of 5x10^6 cells of spleen single cell suspension i.p. at seven days post infection (Figure 13). Usage of spleen single cells from synchronized infected donors ensured the transfer of already LASV-primed T cells as well as already LASV-antigen presenting APCs from the IFNAR^{BL6} mice to the recipient mice. As a control, one group of RAG1$^{-/-}$ mice received donor spleen single cell suspension originating naïve C57BL/6 wild type mice (naïve) to test whether priming of T cells and antigenic presentation of APCs was still important at advanced stages of the disease with viremia (7 dpi).

Flow cytometric analysis of blood from receiver RAG1$^{-/-}$ mice was performed 1, 5, 7 and 11 days post transfer to track T cell fate and expansion. One day after transplantation, an influx of CD3 T cells in the blood was measured. The number of CD3 T cells in the blood decreased at the following two sampling time points - 5 dpi and 7 dpi - indicating the T cells either disseminating from the blood into tissue or being partially depleted (Figure 14 A). Eleven days post transplantation (18 dpi) the proportion CD3 T cells in the blood expanded in all groups, except the infected mice, which also received a transplant from LASV-infected immune competent donors (LASV+primed) (Figure 14 A). The transplantation of spleen single cell suspension, which included many different cell types of the innate as well as the adaptive immune system, was not able to induce any immune pathology. Weight, temperature and overall appearance and serum AST levels did not significantly worsen over the course of infection (Figure 14 B&C) even though viremia was high during the course of infection (Figure 14 D) as well as the viral organ burden at time of sacrifice (18 dpi) (Figure 14 E). Even mock-infected mice, which received their cell transfer from infected mice showed detectable viremia and viral organ burden by day 18 post infection (eleven days post transplantation), inadvertently reapproving the sensitivity of immune compromised animal models for the amplification and detection of low amounts of pathogens.

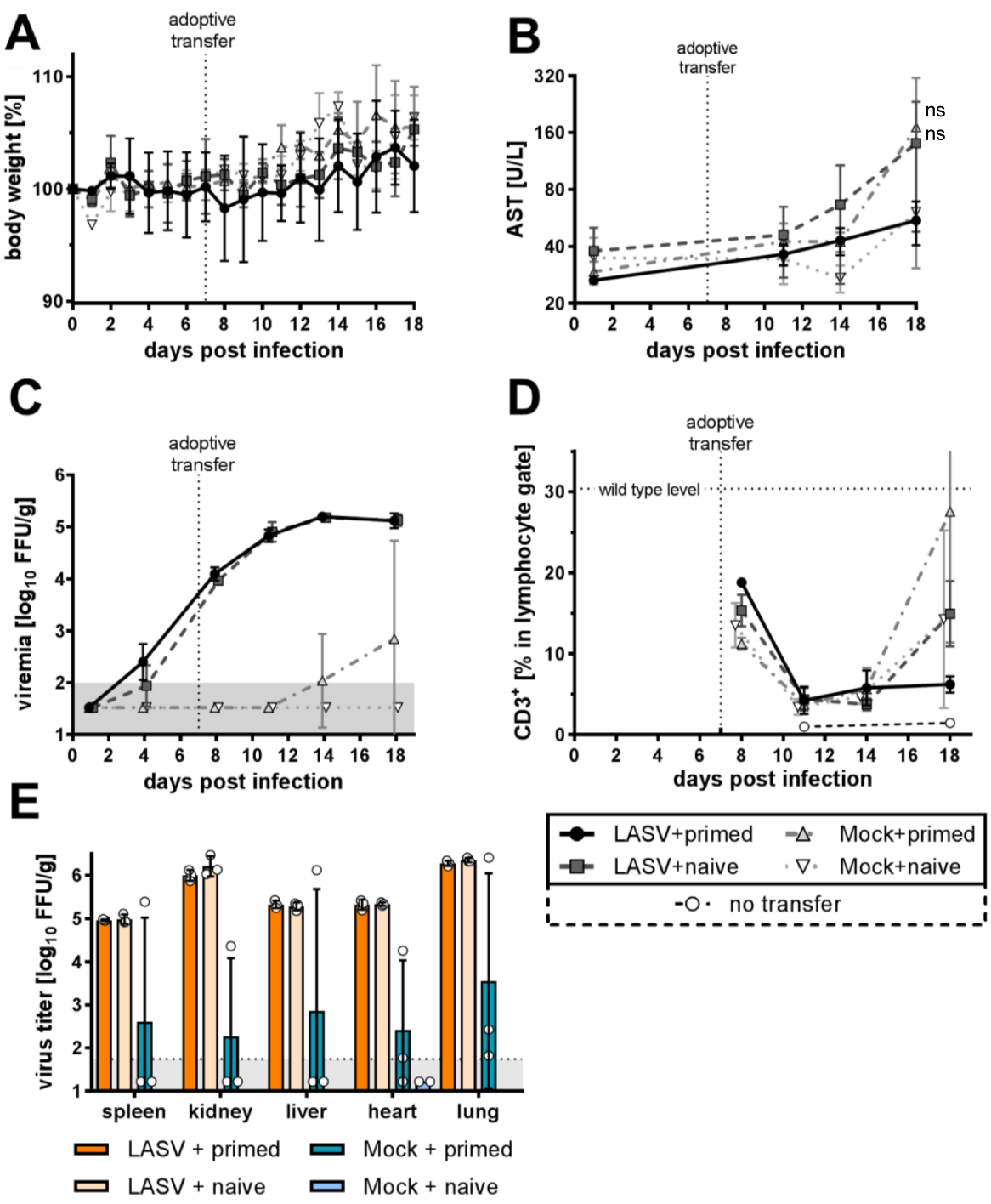

Figure 14 Adoptive transfer of spleen SCS into infected RAG1$^{-/-}$ mice does not induce pathologic infection.
Infected RAG1$^{-/-}$ mice received spleen immune cell transfer from infected IFNAR^{BL6} (primed) or naive wild type donors (naïve) at 7 dpi but failed to exhibit disease symptoms. Weight progression (A) and serum AST concentration (B) do not indicate pathological symptoms despite viremia (C) in LASV infected RAG1$^{-/-}$ mice with primed immune cell transfer (black, solid line) or naïve immune cells (dark grey, dashed line). T cell repopulation occurs only >10 days after transfer in the blood (D), except infected animals with transfer from also infected donors (LASV+ primed: solid line). (E) High LASV organ titers upon sacrifice 18 dpi even in mock-infected animals with primed immune cells (teal). *Data shows mean ±SD n=3; Mann-Whitney test compared to Mock+naive (18 dpi), two-tailed, adjusted p-values with Dunn's correction, $AST_{(18\,dpi)}$ n.s.: p>0.05.*

3.1.5 Adoptive transfer of MACS purified CD3 T cells into RAG1$^{-/-}$ recipients does not induce immune pathology

To specify the transferred cell types and to rule out transfer of insufficient amounts of transferred T cells, 2x10^6 MACS purified CD3 T cells from IFNAR^{BL6} mice were directly transferred i.p. into RAG1$^{-/-}$ mice at 4 dpi. The purified T cells were sourced from animals, which were infected parallel to the RAG1$^{-/-}$ mice with LASV or just mock-infected, four days prior. A period of four days of pre-incubation was chosen, because the time point was situated prior to any observable pathology in the IFNAR^{BL6} model and marks the earliest time point LASV can be detected in the blood of individual animals. This implicates that lymphoid tissues have been sufficiently exposed and encountered the virus antigen by 4 dpi, giving CD8 T cells had ample time (>24 h) for their priming reactions on DCs. As a control, naïve T cells were transplanted to another group to test, whether prior T cell priming in IFNAR^{BL6} was mandatory or sped up T cell reactions in RAG1$^{-/-}$ recipients.

Overall health status, weight, body temperature (not shown) and serum AST levels of the mice stayed within normal ranges during the infection (Figure 15 A & B). Viremia was detectable in all actively infected animals at day seven post infection (3 days post transplantation). Mock-infected mice, which had received transplants from LASV-infected bone-marrow chimeric mice, displayed viremia beginning at day six post transplantation (11 dpi) (Figure 15 C). Flow cytometric analysis of blood showed a slow repopulation of CD3 T cells up to one week after transplantation (11 dpi) with rapid repopulation occurring in the weeks after (16 & 22 dpi) (Figure 15 D). The proportion of activated KLRG1 expressing CD8 T cells (Figure 15 F) and CD4 T cells (Figure 15 G) in spleens at 24 dpi did not differ between the groups displaying the same levels as uninfected mock mice. Only uninfected mock mice with naïvely transplanted T cells displayed a trend of fewer PD-1$^+$ CD8 T cells (Figure 15 F, light blue), implicating that the high viral loads at the time point of sacrifice might have induced T cell exhaustion independent of prior antigen exposure of the T cells in the original donor. Transfer of primed T cells from infected IFNAR^{BL6} into mock-infected animals also resulted in the same activation phenotype of the T cells as seen in the actively LASV-infected groups. Over the course of the experiment a delayed virus replication became imminent in these animals (Figure 15 C Mock+primed: grey triangle), caused by the T cell transfer despite the numerous washing steps during the T cell purification.

Adoptive transfer of CD3 T cells into hosts, which were otherwise devoid of these populations, did not result in a pathologic disease during LASV infection. It remained unresolved whether the LASV antigen abundance or the slow and late repopulation of the CD3 T cells created by the experimental design could have caused a form of anergy or exhaustion in the T cells as indicated by the slight increase in PD-1^{+} CD8 T cells.

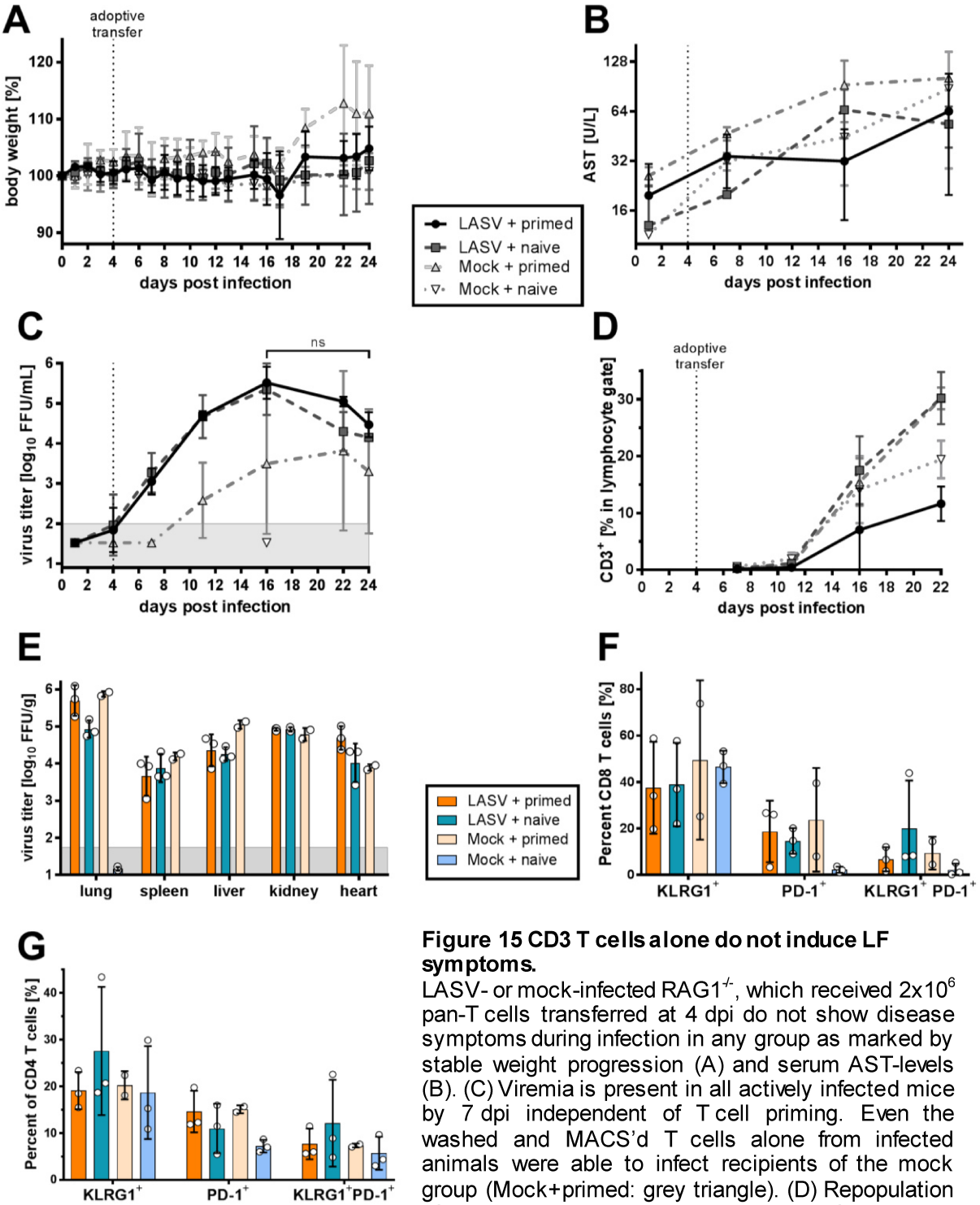

Figure 15 CD3 T cells alone do not induce LF symptoms.
LASV- or mock-infected RAG1$^{-/-}$, which received 2x10^{6} pan-T cells transferred at 4 dpi do not show disease symptoms during infection in any group as marked by stable weight progression (A) and serum AST-levels (B). (C) Viremia is present in all actively infected mice by 7 dpi independent of T cell priming. Even the washed and MACS'd T cells alone from infected animals were able to infect recipients of the mock group (Mock+primed: grey triangle). (D) Repopulation of T cells only occurs >1 week past transfer. (E) High virus titers were consistently detectable in organs upon sacrifice at 24 dpi. (F) CD8 T cells show SLEC phenotype with PD-1 being also upregulated. (G) PD-1 is also observed on CD4 T cells but with less KLRG1 induction. *Data shows mean ±SD (n=3) Friedman test Dunn's multiple comparisons correction: LASV+primed 16 dpi vs 24 dpi p=0.2277; LASV+naïve 16 dpi vs 24 dpi p=0.0537.*

3.1.6 Repopulation of T cells after adoptive transfer might clear low dose infection without induction of immune pathologies

In order for a T cell repopulation to take place before infection, $RAG1^{-/-}$ mice received $2x10^6$ MACS purified CD3 T cells i.p. seven days prior to infection (-7 dpi). The transferred CD3 T cells originated either from naïve $IFNAR^{BL6}$ mice or from reconvalescent $IFNAR^{BL6}$ mice, which survived LASV infection after T-705 treatment and were immunologically protected (as shown through survival of a later rechallenge without any disease symptoms). These T cells are in the following called 'experienced'. Because already low infectious titers of LASV effectively replicated in $RAG1^{-/-}$ mice, the infectious inoculum at 0 dpi was reduced to 100 FFU i.n. to lower the abundance of LASV antigen following the infection and to avoid the generation of anergic or exhausted T cells. Over the course of the infection all animals remained healthy (Figure 16 A). Longitudinal FACS analysis of blood to track T cell repopulation revealed insufficient repopulation in several animals (data not shown, animals excluded from original groups for analyses). The remaining count of animals allowed for analysis on individual basis (Table 2). None of the animals with successful T cell repopulation developed viremia (individuals: A, B & C), while all animals without successful T cell repopulation did (Figure 16 C). Despite no viremia being present, low viral organ burden was found in liver, heart and lung of individual A (experienced T cells) at 21 dpi (Figure 16 B). Organ burden of individuals B, C and D were below the limit of detection. A single individual of the animals without T cell repopulations was titrated to have high LASV organ titers between 10^5 and 10^6 FFU/g (Figure 16 B), similar to $RAG1^{-/-}$ mice of previous experiments.

Table 2 Overview of individual CD3 T cell transferred animals and their parameters. Test subject parameters varied strongly under identical test variables. Animals without successful T cell repopulation are not listed individually.

Individual animal	Origin of T cell transplant	T cell repopulation	Viremia	LASV organ burden	CD8 T cell status
A	experienced survivor	**++**	**-**	**(+)**	blood PD-1 **+++** spleen KLRG1 **+**
B & C	experienced survivor	**+**	**-**	**-**	KLRG1 **+**
D	naïve donor	**+**	**-**	**-**	KLRG1 **++**
Excluded individuals	naïve & exp. donors	**-**	**+**	**+** (based on single individual)	not applicable

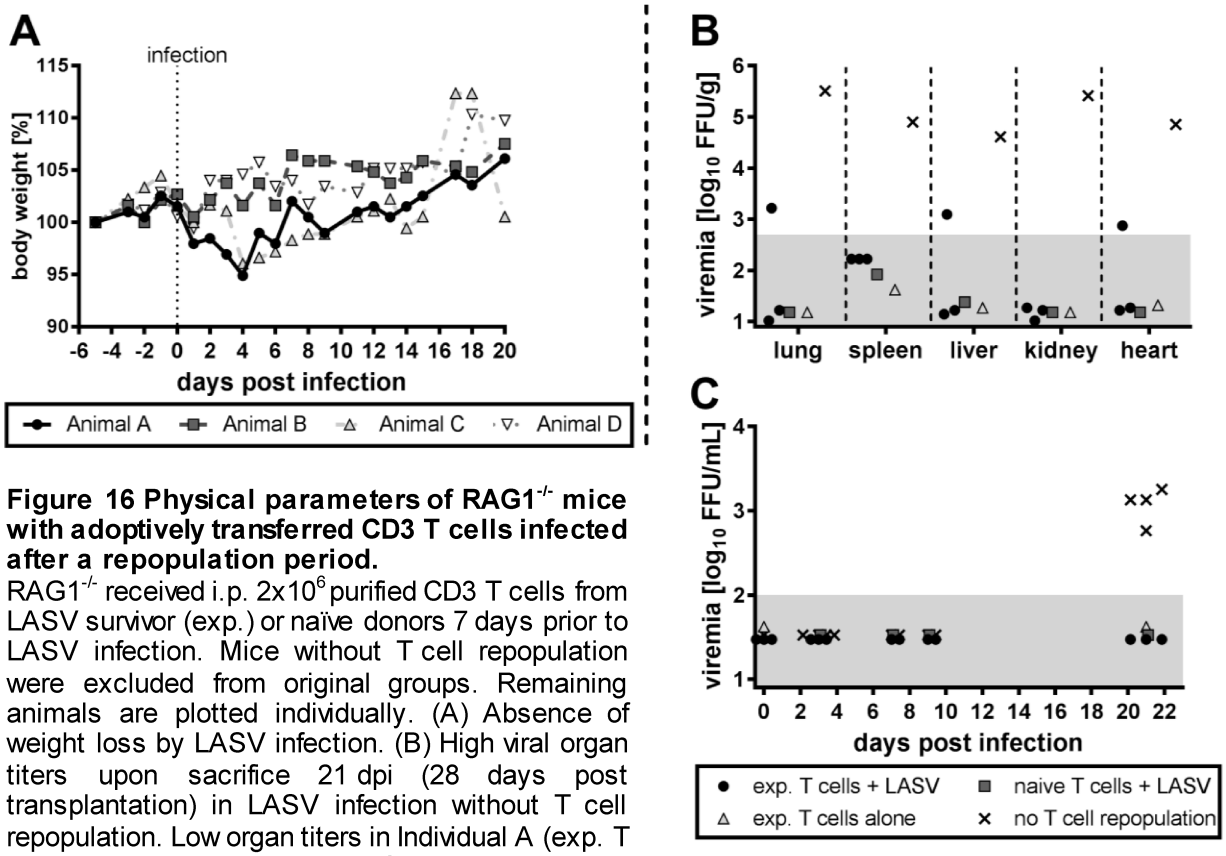

Figure 16 Physical parameters of RAG1$^{-/-}$ mice with adoptively transferred CD3 T cells infected after a repopulation period.
RAG1$^{-/-}$ received i.p. 2x10^6 purified CD3 T cells from LASV survivor (exp.) or naïve donors 7 days prior to LASV infection. Mice without T cell repopulation were excluded from original groups. Remaining animals are plotted individually. (A) Absence of weight loss by LASV infection. (B) High viral organ titers upon sacrifice 21 dpi (28 days post transplantation) in LASV infection without T cell repopulation. Low organ titers in Individual A (exp. T cells) in lung, liver and heart. (C) Viremia was only observed in animals with failed T cell repopulation late in infection. *Data shown as replicates.*

Characterization of the T cells phenotype revealed, that individual D (naïve T cells) displayed a strong CD8 T cell activation expressing KLRG1 on 60.6% of CD8 T cells in the spleen and on 73.0% of circulating CD8 T cells 21 dpi (Figure 17). CD8 T cells of individual A (experienced T cells), which had a low virus burden of the organs, only displayed a KLRG1 expression on 27.6% of circulating CD8 T cells, 21 dpi. Furthermore, 73.7% of circulating CD8 T cells in the blood were positive for PD-1 in individual A, while CD8 T cells in the spleen inexplicably had a normal activation phenotype with 53.3% being KLRG1^{+} and only 4.1% of cells expressing PD-1 at 21 dpi (Figure 17). Within the animals B and C overall less CD8 T cells events were measurable (no detectable virus titers). The circulating CD8 T cells in the blood of individual B and C displayed normal KLRG1 expression at 50.5% and 56.7% and respective 23.9% or 20.6% of CD8 T cell being positive for PD-1 (Supplemental figure S9).

The data might be the first indication, that contrary to the initial experimental hypothesis, T cells are indeed able to clear LASV infections without inducing a pathology within the otherwise adaptive immune incompetent RAG1$^{-/-}$ mouse model. Independent of the origin of the T cells (survivor or naïve donors), upon repopulation, T cells have been able to restrict virus replication in a low dose intranasal infection scenario (individuals B, C & D). On the other hand even in experienced T cells from survivor donors, which most likely also included memory T cells, T cell exhaustion could occur (individual A), although more elaborate experiments are needed in the future to provide ample evidence of the protection and the influence of different T cell subpopulations.

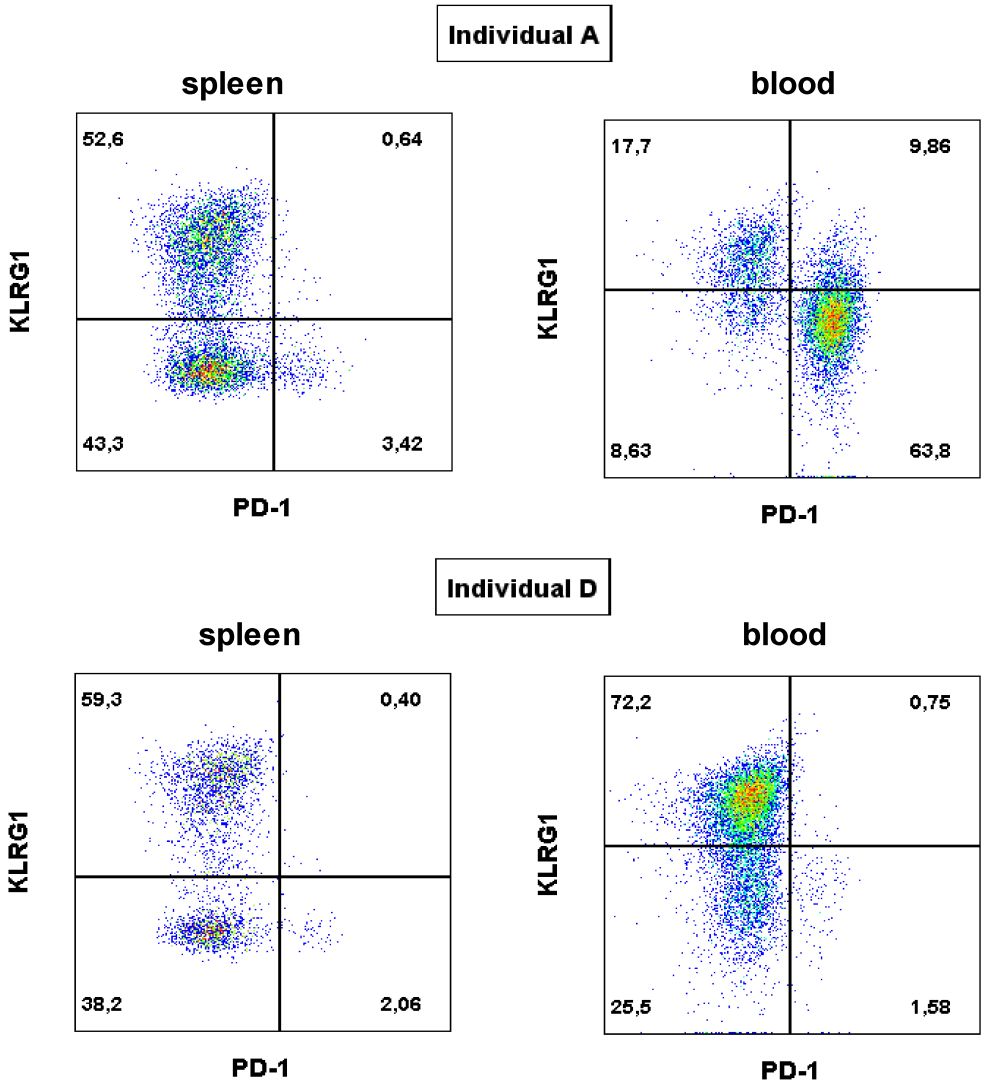

Figure 17 PD-1 T cell exhaustion in the blood of an individual with remaining LASV organ titers. Flow cytometric dot plots of blood (21 dpi) and spleens upon sacrifice (24 dpi). RAG1$^{-/-}$individual 'A' had a transfer of survivor donor T cells and low LASV organ titers upon sacrifice. Individual 'D' received naïve T cells and had no detectable infectious viral titers in blood or organs. Most circulating CD8 T cells fail to activate properly in individual 'A' and express the exhaustion marker PD-1.

3.2 Analysis of myeloid cell populations during LASV infection in the IFNAR^{BL6} mouse model

While focusing on the T cell responses of the IFNAR^{BL6} LF model, it was also important to enhance the knowledge about changes in the compartmentalization of the accompanying myeloid system during LASV infection. Reports have shown cells of the myeloid immune system to be targets of LASV infection.

Testing several antibodies, for the first time reliable staining of LASV-infected myeloid cells was achieved in flow cytometry with an α-LASV-NP antibody, providing a backbone for a time course analysis of infected immune cell populations within the IFNAR^{BL6} bone marrow chimeric disease model for Lassa as well as human samples.

3.2.1 Anti-Lassa anti-NP antibody '2B5' detects LASV-infected cells in vitro during flow cytometric analysis as shown by RNA-fluorescence in situ hybridization (PrimeFlow)

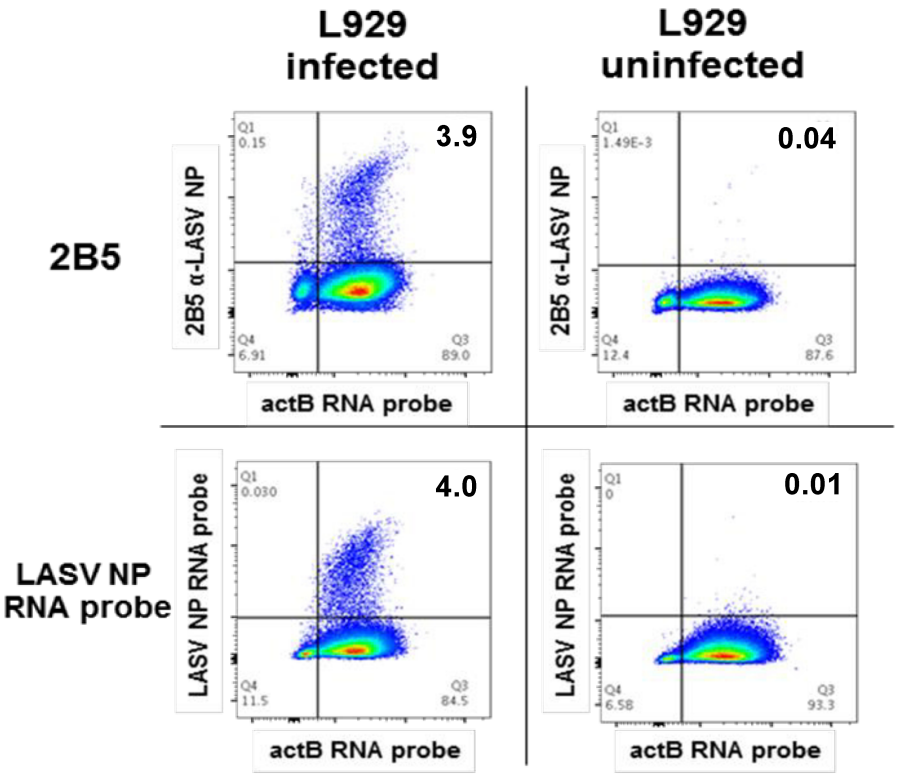

Figure 18 PrimeFlow testing of α-LASV NP antibody '2B5'.
LASV Ba366 infected L929 cells (MOI 0.01) were harvested 4 dpi and intracellular stained with either 2B5 anti-Lassa antibody or with LASV-specific RNA probes and subsequent probe signal amplification. Murine beta-actin (actB) probes were used as positive control of signal amplification in the PrimeFlow assay. Antibody 2B5 shows staining of same specificity as well as sensitivity as the tested LASV-NP RNA-probe.

To identify LASV infected cells flow cytometrically, several anti-LASV antibodies were screened on *ex vivo* mouse samples. The anti-LASV anti-NP antibody '2B5' (kindly provided by Dr. Petra Emmerich) yielded the strongest signals and was additionally tested for specificity in a PrimeFlow RNA hybridization assay on LASV Ba366 infected L929 cells, comparing it to a LASV GA391 NP-specific RNA probe. CF633-coupled 2B5 antibody stained LASV infected cells to the same extend as the LASV-NP RNA hybridization probe (3.97% vs. 3.92% infected cells) (Figure 18). *Ex vivo* the CF633-coupled antibody produced close to no background on spleen single cell suspensions of uninfected mice as well as in mice infected with EBOV Zaire as an unrelated pathogenic virus (Supplemental figure S10). Specificity testing via PrimeFlow was repeated with a CF405S- and Alexa647-coupled 2B5 antibody with similar results. Employment of a LASV-specific antibody staining had several advantages compared to PrimeFlow analysis. PrimeFlow analysis is sensitive to RNA degradation and temperature variability. Also, internal controls for PrimeFlow analysis occupy additional fluorescence channels and PrimeFlow buffers are not compatible with several standard fluorophores. Based on the evidence for sufficient specificity and sensitivity of the 2B5 antibody, it was used in all subsequent experiments.

3.2.2 Intranasal LASV infection leads to reduction of myeloid immune cell presence during late stages of disease due to loss of total lung cell viability

LASV infection in the IFNAR^{BL6} generally leads to high viral titers in the lung with possible pleural effusions in the late stages of the disease. Analyzing the cell viability of lung single cell suspensions by acridine orange and propidium iodide, cell counter measurements revealed a significant reduction of cell viability in the lungs at 10 dpi, which was not observed during MORV infection (Figure 19 A). Calculating absolute numbers of the myeloid compartments for different organs confirmed, that this cell damage coincided with a reduction of the total numbers of viable APCs (MHC II$^+$) during LASV infection (Figure 19 B).A reduction trend from 7 dpi to 9 dpi to 10 dpi could also be seen for non-antigen presenting myeloid cells (CD45.1$^+$ Lin$^-$ Ly6G$^-$ MHC II$^-$), but the effect was not significant compared to mock infected control animals (Figure 19 C). Interestingly, the numbers of Ly6G$^+$ neutrophils in the lung were virtually stable over the time course despite the loss of general cell viability (Figure 19 D). No significant

changes in regard to cell numbers were recorded in the spleen of LASV infected animals (Figure 19 C & D). In MORV infected animals myeloid cell composition in the lung, spleen and blood of did not change between different time points (Supplemental figure S11).

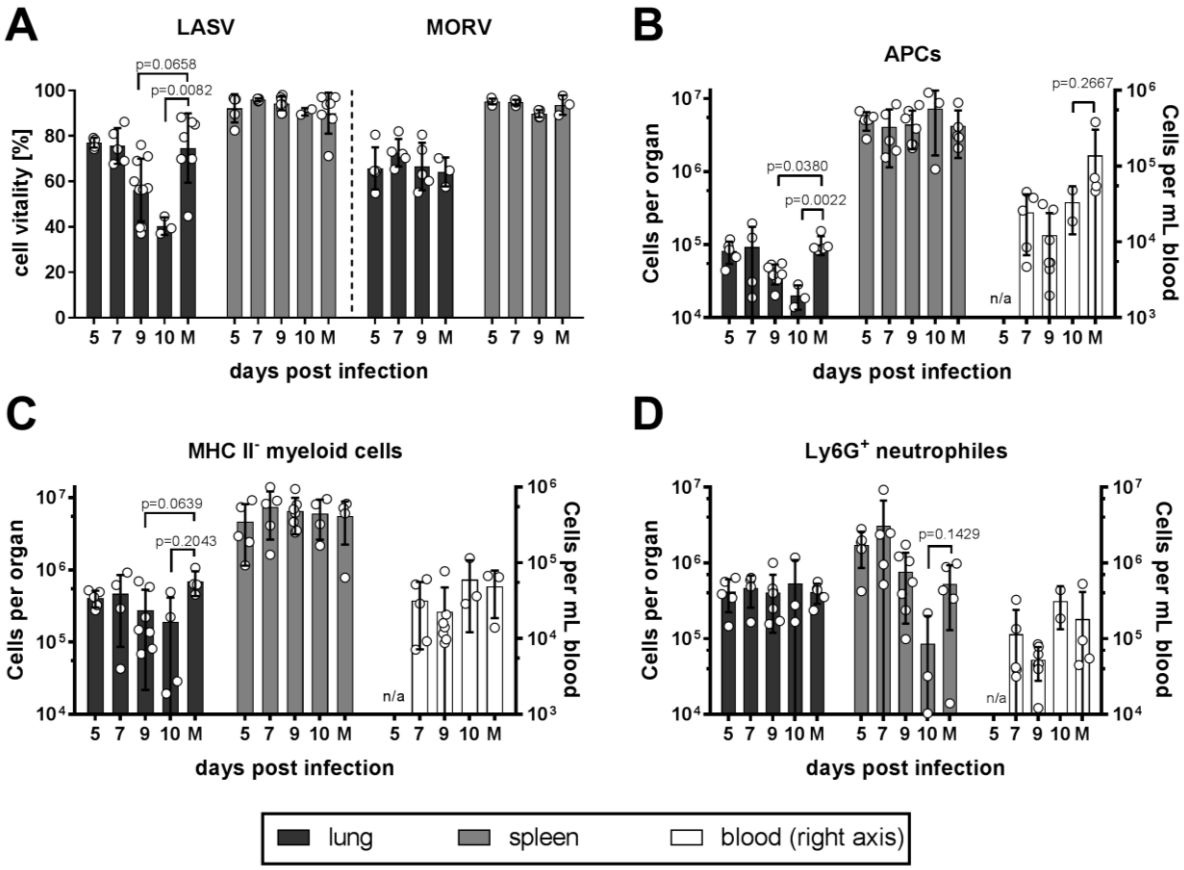

Figure 19 Cell viability reduction in the lung coincides with loss of APCs, but not neutrophil granulocytes.
Mice infected i.n. with LASV, MORV or mock-inoculum (M) were sacrificed at days 5, 7, 9 & 10 dpi. (A) Cell viability of the lung (dark grey) is negatively affected by LASV infection, but not during MORV infection. Extrapolated cell counts in IFNAR^{BL6} lung, spleen (medium grey) and blood (white) of (B) APCs (MHC II^{+}) and (C) non-antigen-presenting myeloid cells (CD45.1^{+} Lin^{-} Ly6G^{-} MHC II^{-}). Significant loss of APCs occurs in the lung at late stages of the disease, but not in spleen and blood. (D) Extrapolated numbers of Ly6G^{+} neutrophil granulocytes in the lung do not change over time despite a general viability reduction. *Data shows mean ±SD and replicates; Kruskal-Wallis test with Dunn's multiple comparison, adjusted p-values.*

3.2.3 Antigen presenting cells stain for LASV-NP during infection

Based on histological and *in vitro* evidence, APCs are considered as important target cells for LASV infections. By employing an intracellular staining for LASV-NP for flow cytometry, approximated *in vivo* kinetics in the IFNAR^{BL6} model could be analyzed.

The flow cytometric analysis with α-LASV-NP '2B5' staining was not able to detect LASV-NP in the analyzed myeloid cells at 5 dpi, except in splenic Ly6C^{hi} monocytes of a single animal at 5 dpi (Figure 20). Reliable detection in myeloid immune cells was achieved only from day seven post infection onward, coinciding with the increase in virus titers seen in previous analyses (Figure 7 D and Figure 8). Analysis of spleen, lung and blood revealed, that a high percentage of cDCs (MHC II$^+$ CD11c$^+$ B220$^-$) stained positive for LASV-NP in the lung, a site of early virus exposition due to the i.n. inoculation of the animals. Similarly, pDCs (MHC II$^+$ CD11c$^+$ B220$^+$) were highly positive for LASV-NP in the late stages of disease, not only in the lung, but also in spleen and blood. Interestingly LASV-NP$^+$ Ly6C^{hi} monocytes (MHC II$^+$ CD11b$^+$) were occurring in the spleen already within days five and seven post infection, while staining became prominent in the lung by day nine post infection. LASV-NP$^+$ Ly6C^{hi} monocytes also occurred only past day nine post infection in the lung, while Ly6C^{lo} remained very low in numbers mostly LASV-NP-negative in all organs during the infection (with the exception of one animal at 9 dpi). Separate from the high portion of pDCs staining for LASV-NP, as already mentioned, also alveolar macrophages (alv. MΦ) (SiglecF$^+$ CD11c$^+$ Ly6G$^-$) in lungs, as well as F4/80$^+$ macrophages show LASV-NP staining albeit to higher percentages in the blood than in the spleens. Ly6C^{hi} monocytes and alveolar macrophages readily stained for LASV-NP in the lung, monocytes and F4/80$^+$ macrophages in the spleen, however, only to a lesser extent. The positive LASV-NP$^+$ status of F4/80$^+$ macrophages in the blood correlated with the viremia of the animals. Furthermore, Ly6G$^+$ neutrophils (Figure 20) and lineage-marker-positive lymphocytes (not shown) displayed no staining of LASV-NP above the mock infected background levels. Despite DCs being often described as early target of LASV in primate infections and of human cell lines, only later time points of infection readily showed those immune cell types staining positively LASV-NP within our mouse model. Nevertheless this experiment also proved the principle, that α-LASV-NP antibody staining can be employed on in flow cytometric analysis on blood, which was a prerequisite for our propositioned human studies in Nigeria.

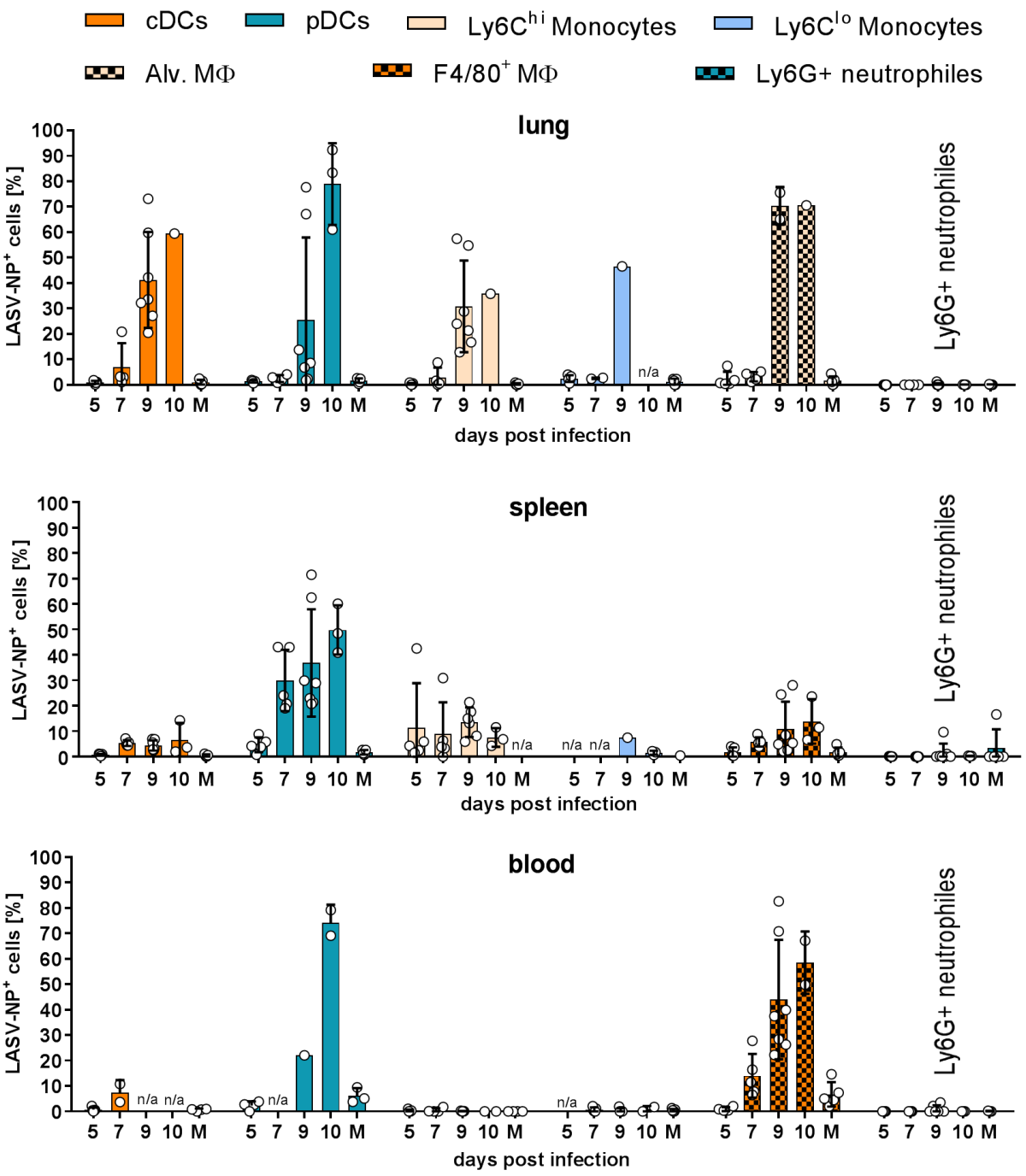

Figure 20 LASV-NP status within different myeloid immune cell populations determined by flow cytometry.
Single cell suspensions of lung, spleen and blood from LASV- and mock-infected (M) IFNAR^{BL6} mice were intracellular stained with '2B5' α-LASV-NP antibody 5, 7, 9 & 10 dpi. Myeloid compartments of lung, spleen and blood were analyzed. Cell populations <80 events were excluded from further analysis. *Data shows mean ±SD and replicates*.

3.3 On-site flow cytometry on patient samples in Nigeria

In vivo animal data of experimental models always represents model data and needs to be assed against the observations in humans to test the model validity and to discriminate possible model artifacts. As part of a LF patient cohort study in the Lassa fever ward at the Irrua Specialist Teaching Hospital during the Nigerian LF outbreak in 2018 we therefore carried out stainings on thymocyte and myeloid blood compartments of human patients. Restricted by material availability, infrastructure and personal safety it was possible to generate limited longitudinal cell analyses by first purifying and inactivating blood samples in a biosafety-glovebox to be then later measured on a portable table-top flow cytometer. This enabled measurements with restricted small antibody panels on freshly isolated myeloid and T cells directly on site. Human infections with LASV usually occur without special notable incidences, which complicates defined tracing of infection time points. The longitudinal patient data sets were attempted to be synchronized dependent on different parameters like self-reported onset of symptoms and AST serum concentrations, which were insufficient in providing a synchronization baseline. Synchronization based on quantitative RT-PCR data also failed due to incomplete data sets. To position the longitudinal samples in a temporal time frame, samples were normalized on the day of the patient's first study sample collection. For data analysis patients were retrospectively categorized into mild and severe cases dependent whether their AST serum concentrations reached more than 200 U/L in the first study sample (Figure 22). Fatal cases were categorized as severe cases, because the low number of LASV-associated fatalities did not warrant sub-categorization for statistical purposes. Both mild and severe LF patient groups did not significantly differ in regards to the self-reported days pasted since onset of symptoms at the day the first study sample was collected (Figure 21), hence indicating a similar time frame until admission at the hospital regardless of the disease severity, making the groups longitudinally comparable. Purified cell counts from blood, time restirctions and resources usually only allowed for measurements of two panels at each time point split between different myeloid and T cell panels. Different analytical panels were run on different patients, reusing the same panels on later samples of the patient to achieve longitudinal data sets.

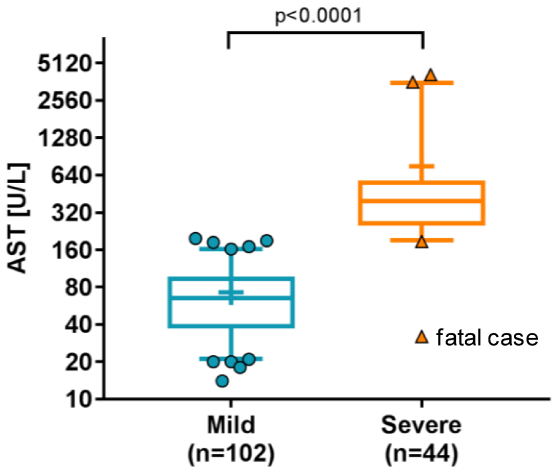

Figure 22 AST values of mild (teal) and severe (orange) patient groups at the time point of first study sample collection. *Data displayed as mean (cross) with median (horizontal line), 25-75% percentile (box), 5-95% percentile (whiskers) and outliers (circles & triangles) Mann-Whitney rank test, two-tailed.*

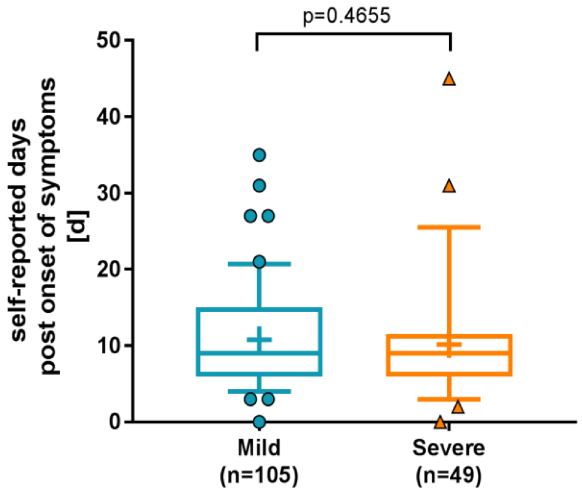

Figure 21 Comparison of self-reported day of onset. Elapsed days since self-reported onset of symptoms at the time point of first study sample collection compared between mild (teal) and severe (orange). LF cases were compared. *Data displayed as mean (cross) with median (horizontal line), 25-75% percentile (box), 5-95% percentile (whiskers) and outliers (circles & triangles) Mann-Whitney rank test, two-tailed.*

3.3.1 Human CD8 T cells of LASV patients become activated but are inhibited in severe LF cases

To assess the validity of previously observed upregulation of effector cell markers on cytotoxic T cells as well as inhibitory molecules like PD-1 and CLTA-4 in the LF small animal disease model, blood samples of LF patients were analyzed on-site in Irrua, Nigeria.

Staining the cytotoxic T cells of LF patients for the activation markers HLA-DR and CD86 presented T cells of an activated phenotype during flow cytometric analyses. Concentrations of $CD86^+$ CD8 T cells showed a trend of gradual decrease over the sampling time frame (Figure 23 A); nevertheless severe cases might have displayed elevated concentrations of CD86-positive cytotoxic T cells to begin with. HLA-DR expression on the other hand did not greatly differ between mild and severe cases of LF. The proportion of HLA-DR-positive CD8 T cells fluctuated in both groups (Figure 23 B), which could also be observed for T cells expressing the activation marker KLRG1 (Figure 23 C). Likewise no activation-linked reduction of $CCR7^+$ CD8 T cells connected to the severity of the disease was observed (Supplemental figure S12). Moreover, large portions HLA-DR expressing CD8 T cells of severe LF patients additionally to also expressed CTLA-4, possibly indicating an inhibitory regulation on these cells (Figure

23 D). T cell inhibition was not only indicated by CTLA-4 expression on CD8 T cells (Figure 24 A), but also by CD8 T cells displaying PD-1 (Figure 24 B) in the blood of patients with severe LF, some of which even expressed both inhibitory markers (Figure 24 C). Exhaustion of T cells marked by these inhibitory factors might thus be involved the severity of the disease. A similar upregulation of inhibitory markers on CD8 T cells was also observed in the previously characterized bone marrow chimeric mouse model for LF (see 3.1.2), but future studies on the human immune responses to LASV infections are needed to define similarities and differences to the disease models more clearly.

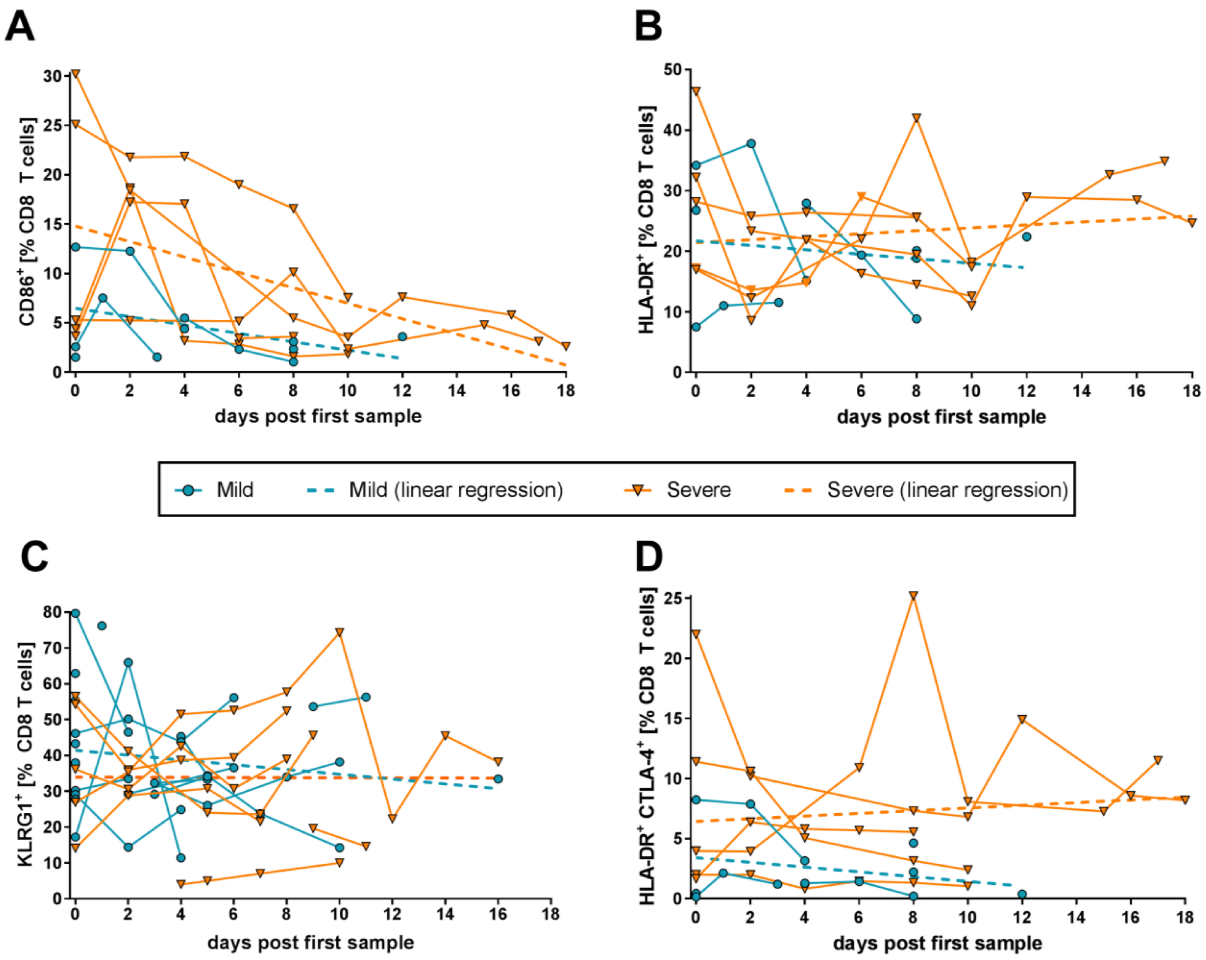

Figure 23 Activation markers expressed on CD8 T cells CD86, HLA-DR, KLRG1 during LF. T cells of patients with mild (teal) and severe (orange) LF progression were flow cytometrically analyzed over the course of infection. The concentration of CD8 T cells positive for the activation markers (A) CD86, (B) HLA-DR and (C) KLRG1 are plotted with longitudinal data points of each individual patient connected by a line. (D) Additionally expression of the inhibitory marker CTLA-4 is displayed within the HLA-DR$^+$ CD8 T cell population. Data displayed as single patient replicates with lines connecting samples of each individual. For visual clarity linear regressions (dashed lines) of the subgroup's means are displayed and not as descriptive models. Cross-sectional analysis of day 0 is displayed in Supplemental figure S13.

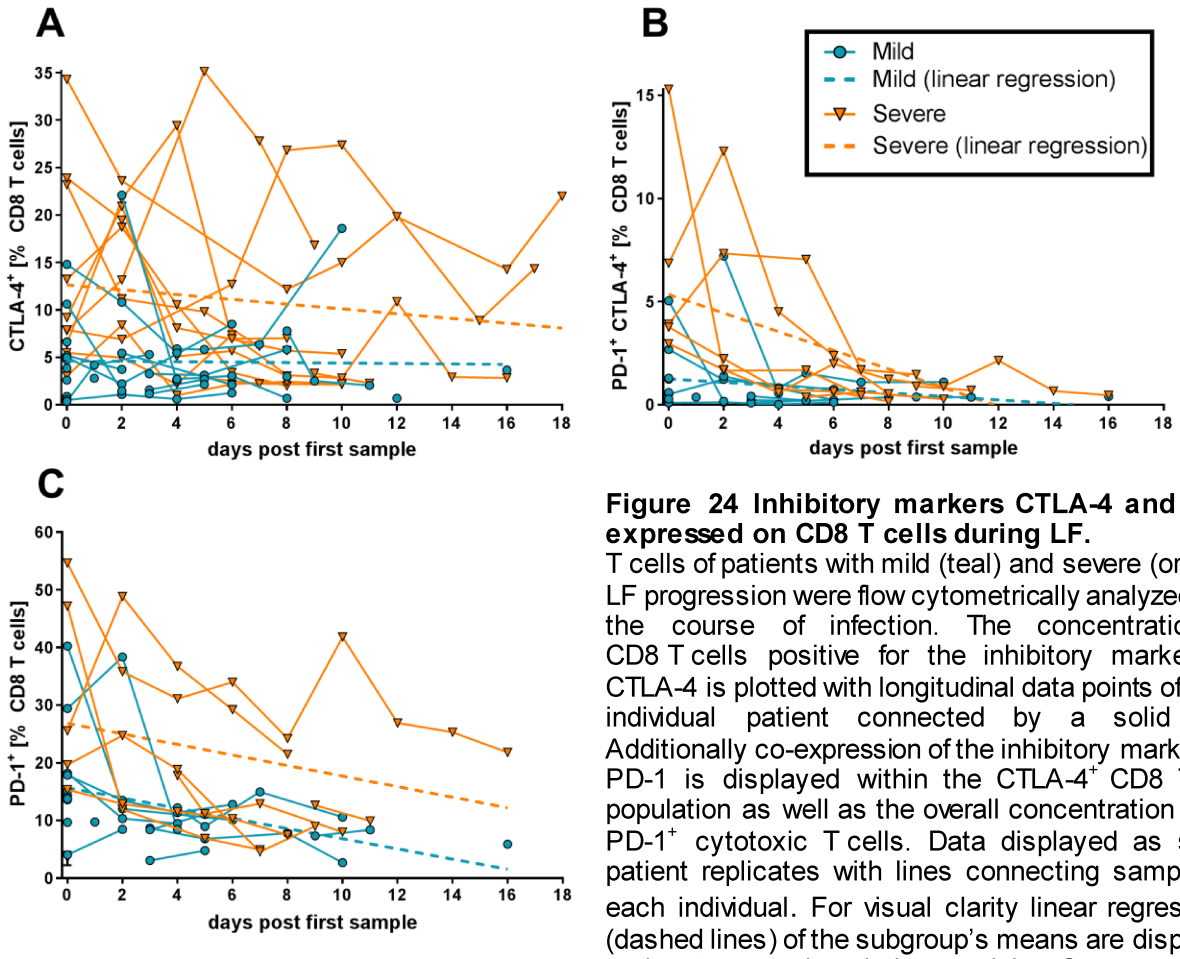

Figure 24 Inhibitory markers CTLA-4 and PD-1 expressed on CD8 T cells during LF.
T cells of patients with mild (teal) and severe (orange) LF progression were flow cytometrically analyzed over the course of infection. The concentration of CD8 T cells positive for the inhibitory marker (A) CTLA-4 is plotted with longitudinal data points of each individual patient connected by a solid line. Additionally co-expression of the inhibitory marker (B) PD-1 is displayed within the CTLA-4$^+$ CD8 T cell population as well as the overall concentration of (C) PD-1$^+$ cytotoxic T cells. Data displayed as single patient replicates with lines connecting samples of each individual. For visual clarity linear regressions (dashed lines) of the subgroup's means are displayed and not as descriptive models. Cross-sectional analysis of day 0 is displayed in Supplemental figure S14.

3.3.2 Human plasmacytoid DCs stain for α-LASV-NP during LF

Antigen presenting cells are an important interface of the innate and adaptive immune system. With previous studies pointing towards DCs as early targets of LASV infections and the infection-associated inhibitions of cellular responses [143], it was important to contextualize dendritic cell attributes within the course of LF due to strong interconnected influences of DCs on T cells [144] and vice versa. Hence, possible changes in the compartmentalization of professional APCs and correlations to the severity of the clinical progression of LF were analyzed. FACS analysis, on-site in Nigeria, allowed for the identification of classical DCs (cDC: CD11c$^+$, CD141∨CD370$^+$, SSC^{low}) and plasmacytoid DCs (pDC: CD141∨CD370$^+$, CD303∨CD304$^+$, CD123$^+$) and their infection status without staining artifacts due to cryopreservation. Nigerian patients with severe or mild LF did only display minor biological differences in the frequency of circulating cDCs or pDCs (Figure 25 A&B). While in general pDC- and cDC-frequencies

of patients with mild disease progression seemed higher than in severe cases, the relative biological differences still were less than two-fold. The majority of the patients with mild LF displayed similar pDC and cDC frequencies to the severe LF group; only a few individuals in the mild LF group were marked with far higher cell frequencies. At late time points of infections pDCs and cDCs frequencies trended towards base levels seen in healthy individuals (hollow circles). In effect the relative nature of this measurement leaves questions open if the changes are due to early dendritic cell depletion and subsequent repopulation in late reconvalescent stages of the disease or if other not-analyzed cell compartments were just contracting. The analysis of the LASV-NP status of dendritic cells unfortunately remained not fully conclusive. To assure a numerical confidence of the parameter derived from flow cytometric analysis, cell populations below 80 events were excluded from further subanalyzes, thereby greatly reducing the size of analyzed data sets. Percentages of pDCs and cDCs ranged from 0-12% of the cells staining positive for LASV-NP. At large a trend with higher infection rates in pDCs of severe LF cases compared to mild LF patients could have occurred, but in both groups LASV-NP$^+$ cells also diminished over time (Figure 25 C). Similar assumptions regarding an infection rate decrease over time can be made for cDCs of severe LF cases. Mild cases seemed to still harbor more LASV-NP$^+$ cDCs at late time points of the disease (Figure 25 D); however these assumptions can also be attributed to chance, because the later time points of the analysis only encompassed 1-3 measurements.

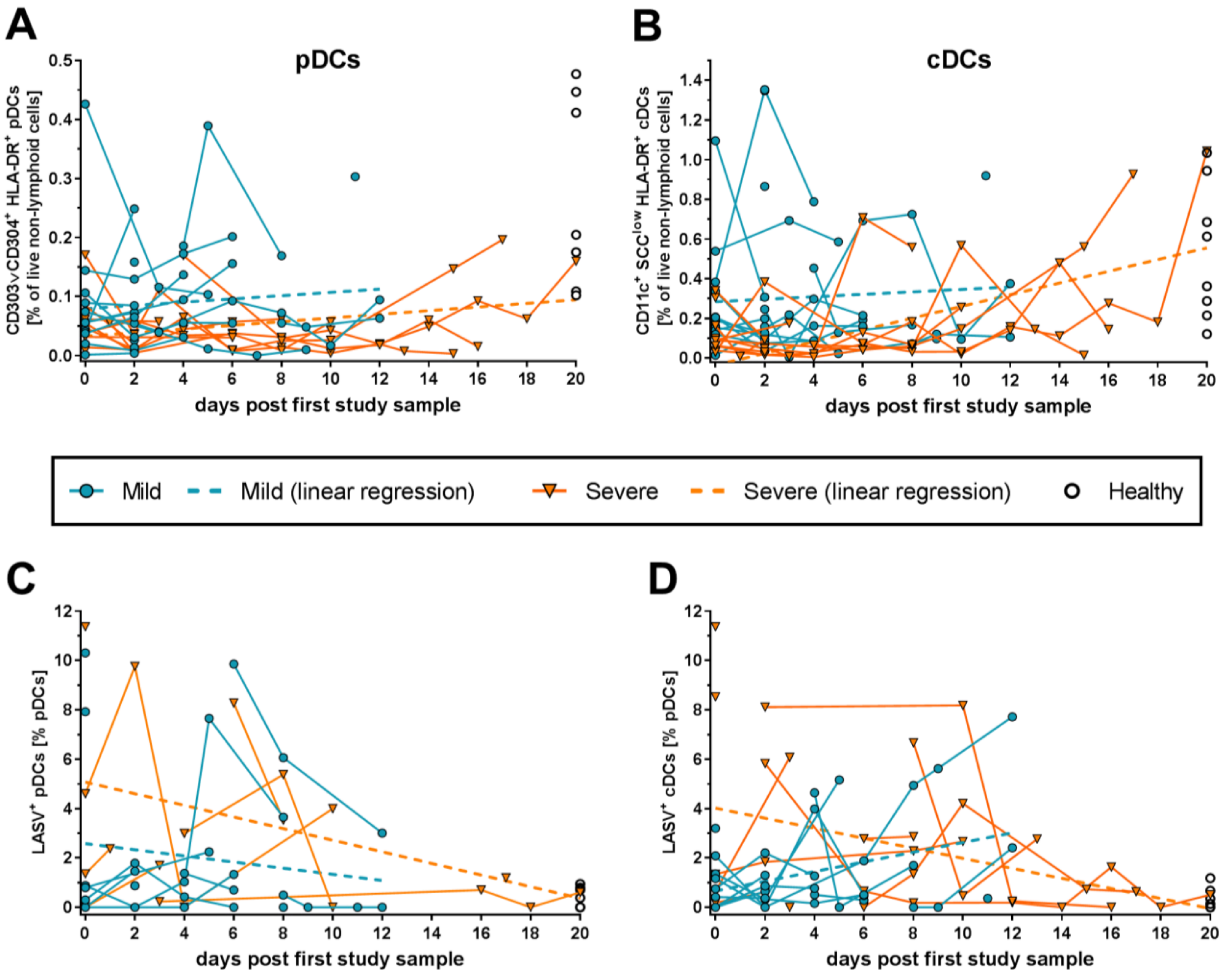

Figure 25 Monitoring of circulating pDCs and cDCs and their LASV infection status during LF. APCs from blood of patients with mild (teal) and severe (orange) LF progression were flow cytometrically analyzed over the course of infection. The proportion of (A) pDCs (CD141vCD370$^+$ CD303vCD304$^+$ CD123$^+$ HLA-DR$^+$) and (B) cDCs (CD1c$^+$ CD11c$^+$, CD141vCD370$^+$ SSC^{low}) within living Lin$^-$ cells (CD3$^-$, CD19$^-$, CD56$^-$) is plotted. Percentages pDCs (C) and cDCs (D) positive for LASV-NP of patients with mild and severe LF decrease over the course of infection. Data sets of individual patients are connected by a solid line. For visual clarity linear regressions (dashed lines) of the subgroup's means are displayed and not asdescriptive models. Data points of healthy staff members inserted as point of reference (hollow circle) Cell populations <80 events were excluded from further subanalysis. Cross-sectional analysis of pDC and cDC fractions in the first study sample is displayed in Supplemental figure S15.

3.3.3 Monocyte concentrations did not show stark differences between mild and severe LF cases

Not dissimilar to the analyzes of patient blood for DCs, samples stained for CD14 and CD16 monocyte populations also did not reveal stark differences in monocyte concentrations between severe and mild LF cases (Figure 26 A&B), which also held true for $CD14^+$ $CD1c^+$ $CD11c^+$ DCs co-analyzed within this antibody panel (Figure 26 C). Even though cells seemed to show a short transient increase of LASV-NP^+ cells around one week after admission to the hospital (Supplemental figure S16), the data has to be interpreted carefully, because the α-LASV-NP was too unreliable within the employed panel's design due to contamination of the LASV-NP^+ populations with unspecific stained rogue granulocytes and mast cells, which could not be completely gated out. Taken together if major biological differences in dendritic cell and monocyte populations between mild and severe cases of LF exist, these should rather be limited to their phenotype as no indication of differences in their frequencies within the blood of patients could be identified in this study.

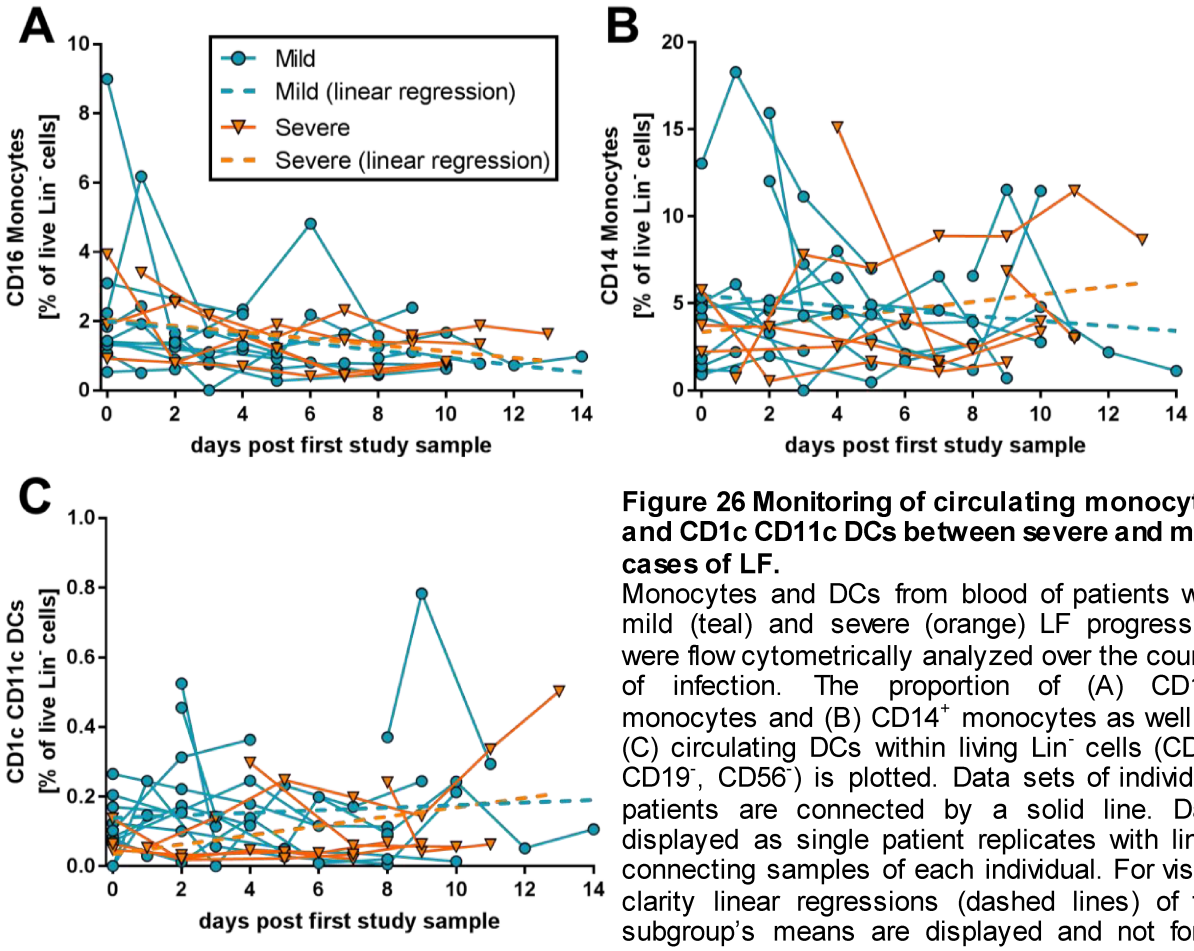

Figure 26 Monitoring of circulating monocytes and CD1c CD11c DCs between severe and mild cases of LF.
Monocytes and DCs from blood of patients with mild (teal) and severe (orange) LF progression were flow cytometrically analyzed over the course of infection. The proportion of (A) $CD16^+$ monocytes and (B) $CD14^+$ monocytes as well as (C) circulating DCs within living Lin^- cells ($CD3^-$, $CD19^-$, $CD56^-$) is plotted. Data sets of individual patients are connected by a solid line. Data displayed as single patient replicates with lines connecting samples of each individual. For visual clarity linear regressions (dashed lines) of the subgroup's means are displayed and not for a predictive modeling. Cross-sectional analysis of day 0 is displayed in Supplemental figure S17.

3.4 Findings

This thesis set out to evaluate the involvement of the immune system with a special focus on cytotoxic T cells during the infection with LASV. Study of the IFNAR^{BL6} mouse model for Lassa fever, revealed that strong CD8 T cell activation occurred in the late and severe stages of the disease with increased expression of the inhibitory cell markers CTLA-4 and PD-1 at the same time. This reaction did not seem to stem from a general unspecific reaction of the CD8 T cells as shown by studying reactions of LASV-unspecific transgenic OT-I T cells in the IFNAR^{BL6} model. However, LASV-specific staining with peptide-loaded tetramers failed to be implemented shrouding the true extent of the LASV-specific T cell responses further into mystery.

Transplantation of immune cells and magnetically sorted T cells in RAG1$^{-/-}$ mice showed, that late implementation of an adaptive immune system during LASV infection could neither clear the infection nor induce immune pathology, ruling out immune pathology solely based on CD8 T cells as the cause of LASV disease [29]. During this study it was possible to prospectively indicate, that implementation of an adaptive immune system in the immune incompetent RAG1$^{-/-}$ mice prior to low dose i.n. infection with LASV was able to clear LASV infection without induction of any symptomatology.

With the use of α-LASV-NP '2B5' antibody, tested and validated during this thesis, it was for the first time possible to identify LASV antigen-positive myeloid cells via flow cytometry during the course of infection. The staining identified phagocytic cells like cDCs, pDCs, alveolar macrophages and monocytes in the lung staining positively for LASV-NP coinciding with rising viral titers. Interestingly, distanced from the first infection site in the respiratory tract analyzed spleens and blood samples stained positively for LASV-NP specifically in pDCs and F4/80^{+} macrophages, which could point towards a possible role of the cells in the dissemination of the virus.

Translating the knowledge acquired from the model system to the human situation on samples of Lassa fever patients in Nigeria, unfortunately resulted in inexplicit vague data sets based on study size, equipment and human variability. Between mild and severe LF cases no indication of differences in the population of antigen-presenting cells could be distinguished in the blood. The collected human data might point towards immunological differences between mild and severe LF cases confined to cytotoxic T cell early activation and a following expression of the inhibitory markers CTLA-4 and PD-1, but further more elaborate research on samples of LF patients is needed to verify these interpretations.

4. Discussion

Lassa virus, the agent causing Lassa fever in humans, is endemic and widespread in West African countries.

Due to its clinical lethality rate of up to 65% [12] and restriction to BSL4 laboratories, knowledge and research on pathological mechanisms of the disease are still limited.

Advances in the generation of suitable small animal models [29, 145, 146] and the resurging importance of the disease by special recognition of the WHO in the last decade [6] enabled the generation of new insights into parts of the pathology and immune reactions to LF [28, 147], nevertheless a definite cause of death in LASV infections remains unknown.

A goal of this thesis was to shed additional light on the unknown immunological reactions in a small animal disease model for LASV infections and to gather information on the immune reaction of human LF cases from Nigeria.

4.1 The IFNAR^{BL6} Lassa fever disease model

The *in vivo* studies performed in this study were based on the previously established IFNAR^{BL6} chimeric mouse model [29]. Previous attempts to model LF disease in mice were based on i.p. and i.v. inoculations with the virus circumventing natural defense barriers and immune system responses by those invasive exposures. Within this thesis LASV-susceptible IFNAR^{BL6} mice were inoculated intranasally not only providing a more natural infection route via the mucosae of the respiratory and possibly digestive tract due to involuntary swallowing, but also increased the safety of the experimenter by absence of sharp cannulas.

The mucosae of the respiratory tract are highly important barriers and sentinel outposts for the immune system. Respiratory epithelial cells and mucosal resident antigen-presenting cells constantly encounter antigens and pathogens here for the first time, evoking and instilling subsequent immune reactions [148]. Mucosal tissue of the respiratory tract is especially adapted to resist viral infections by secreting host-defense molecules and initiating innate immune reactions e.g. by rapid induction and reactions to interferon-λ upon viral infection. Interferon-λ signaling is part of the innate immune response and has been shown to greatly inhibit viral replication in the respiratory tract for influenza virus [149]. Respiratory tracts additionally enable a special form of lymphocyte priming by induction of bronchus-associated lymphoid tissue (BALT) as a

secondary lymphoid organ upon infections; a subform of the mucosa-associated lymphoid tissue (MALT), which plays a crucial role in the immune response to viral infections [150].

Infecting animals via the intranasal route, as established in this thesis, resulted in slightly slower disease progression, identical expression of symptoms and virus titers within one order of magnitude as previously published work via i.p. infection in the IFNAR^{BL6} model [29].

Considering the special adaption of the mucosal infection route to pathogens as well as the mechanistically higher probability of virus particle transmission via inhaled aerosols or smear infections to the oral or nasal mucosa in non-artificial circumstances, distinguishes the i.n. infection route as a more realistic model in reflecting LASV entry into the host. Therefore, future research on previously mentioned interferon-λ and MALT reactions might provide key knowledge of early immunological reactions present during LASV infection.

4.2 Involvement of CD8 T cells in the pathology of murine LASV infection

Past studies performed in mouse models for LF [29, 145] indicated a strong involvement of CD8^{+} immune cells in murine disease models, because α-CD8 antibody treatment resulted in strongly diminished symptoms including absence of a vascular leakage syndrome during LASV infection despite high viral titers. Immune-pathological effects of CD8 T cells have been reported for several viral infection like influenza [151] and LCMV [152] and by memory CD8 T cells also for dengue virus infection [153]. Despite evidence pointing towards a CD8 T cell-mediated immune pathology in the IFNAR^{BL6} and HHD mouse models for LF, adoptive transfer experiments performed in this thesis could not provide positive proof for an immune-mediated pathology induction. T cells transplanted from infected mice into infected T cell-deficient RAG1$^{-/-}$ mice did not induce pathology despite high viral titers being present. Only a limited portion of the transferred T cells developed a SLEC phenotype and additionally PD-1 expression was encountered.

Transferred T cells only had an effect on LASV infection when given sufficient time for repopulation in the new host, being transferred one week prior to infection. This resulted in viral clearance in RAG1$^{-/-}$ mice during low dose i.n. infection. Viral clearance was only observed, when T cell repopulation was successful, while individuals without

successfully established T cell populations developed viral titers. Transferred T cells could therefore have been responsible for viral clearance without the induction of any gross symptoms. In a RAG1$^{-/-}$ mouse, which received T cells from a donor that previously survived LASV infection, exhaustion markers were observed on CD8 T cells, likely resulting in the measured persisting low viral burden despite the presence of T cells. This could point towards the intricate interactions between different subtypes transplanted T cells. The heterogeneous make-up of the transferred T cells included apart from CD8 T cells and CD4 helper cells with high likelihood also several types of regulatory T cells. While important in immune regulation of autoreactive cells, immune inhibition by regulatory T cells and inhibitory CD8 T cells can also be detrimental to viral clearance as shown for influenza [154] and LCMV [155], which could have profound influences on the outcome of LF and would require additional research.

The observations noted for the murine model of LF during this study shifts the hypothesis of a sole T cell-dependent immune pathology during LASV infection to more complex and largely still undefined mechanisms. By design, antibody-mediated depletions of CD8 of previous studies will also have had off-target effects on murine IL12-producing CD8^{+} DCs. These cross-presenting antiviral DCs could hence also be convoluted into the malignant reaction of the immune system against the host. Flatz and colleagues [145] previously scenarized a putative mode by which interactions of infected macrophages together with T cells could induce significant detrimental cytokine releases. Such a mode could be applied as fittingly to cross-presenting CD8^{+} DC populations. On the other hand, experiments on diphtheria toxin treated IFNAR$^{CD11c\text{-}DTR}$ mice by Oestereich and colleagues did show no significant influence of CD11c^{+} cell depletion on the course of the LASV infection. However, ablation of CD11c^{+} cells in the CD11c-DTR model not only targets DCs, but can also target macrophages, activated cytotoxic thymocytes and alveolar macrophages, while sparing some CD11c^{intermediate} populations like monocytes-derived DCs and CD11c^{int} pDCs [156]. It remains thereby questionable, which immune cell populations are crucial for the absence of pathology absence during described CD8^{+} immune cell ablations of previous studies. While CD8 T cells seem to play a role in the pathology of LF, they cannot be considered the sole perpetrators.

Given the information from the results at hand, different scenarios can be postulated (Figure 27). Within the IFNAR^{BL6} disease model T cells might induce an overstimulation of cytokine producing macrophages and dendritic cells [157, 158]; as hypothesized by

previous publications [23, 145] (Figure 27 A). Release and accumulation of high levels of inflammatory cytokines (here represented by TNFα and IFNγ) from APCs could result in damaging tissue reactions similar to what can be observed during severe inflammatory response syndrome or sepsis. LASV-infected dendritic cells and macrophages fail to activate on their own [143] leading to high titers and no symptoms (Figure 27 B), which could also entail the absence of a pathology as seen in $RAG1^{-/-}$ mice or CD8-depleted $IFNAR^{BL6}$ chimeras or HHD mice. When transferring T cells into infected $RAG1^{-/-}$ mice, the present antigenic burden encountered by the comparatively low amount of T cells seemed to induce inhibitory markers on the T cells resembling a T cell exhaustion (Figure 27 C). Incapable of facilitating stimulation to the APCs, no viral clearance and pathogenesis occurs. The only effective response of transferred T cells encountered in this study occurred when low amounts of repopulated T cells were present in $RAG1^{-/-}$ mice (Figure 27 D). Under these circumstances a balanced T cell reaction with subsequent viral clearance and without pathogenesis was induced, but further studies have to be undertaken to verify these possible modes.

The general immune system-reliant induction of the gross LASV-infection pathology is also reemphasized by results of preliminary *in vivo* studies with FDA-approved immune suppressors during LASV infection. Sirolimus (rapamycin), a mTOR inhibitor, causing cell cycle arrest in the G1-phase of T cells [159], significantly prolonged survival in the $IFNAR^{BL6}$ model system by seven days with survival rate of 50% at 21 dpi (endpoint) instead of 100% lethality already at 9 dpi (personal communication, Lisa Oestereich, May 2nd, 2019). The prolonged survival as well as strongly reduced symptomatology despite high ever-present LASV viremia underscores the bivalent nature of immune reactions. In the same wake, similar results were also achieved with cyclophosphamide-treatment, an NFAT inhibitor (personal communication, Lisa Oestereich, May 2nd, 2019). CD8 T cell characterizations conducted as part of this thesis have shown that within $IFNAR^{BL6}$ mice CD8 T cells switch to a highly activated phenotype in the time frame of 7 dpi to 9 dpi with simultaneous upregulation of the inhibitory factors PD-1 and CTLA-4. CTLA-4 and PD-1 have been described in many cases as indicators and actors of T cell exhaustion during chronic viral infections [113, 117] and during immune reactions to cancer cells [110, 119]. It remains to be argued if the observed inhibition in acute infections is a natural counter-reaction to the highly activated T cell phenotype observed in the murine LASV infection model, to reduce untargeted overreactions of effector cells, or if the monitored upregulation of inhibitory factors on $CD8^+$ T cells restricts

beneficial immune reactions and clearance of the virus. Blocking of the respective inhibitory receptors via antagonistic antibodies [117] during the infection or at the late time points coinciding with the shift to highly activated T cell phenotypes could provide important answers to this question and is an exciting perspective for future research.

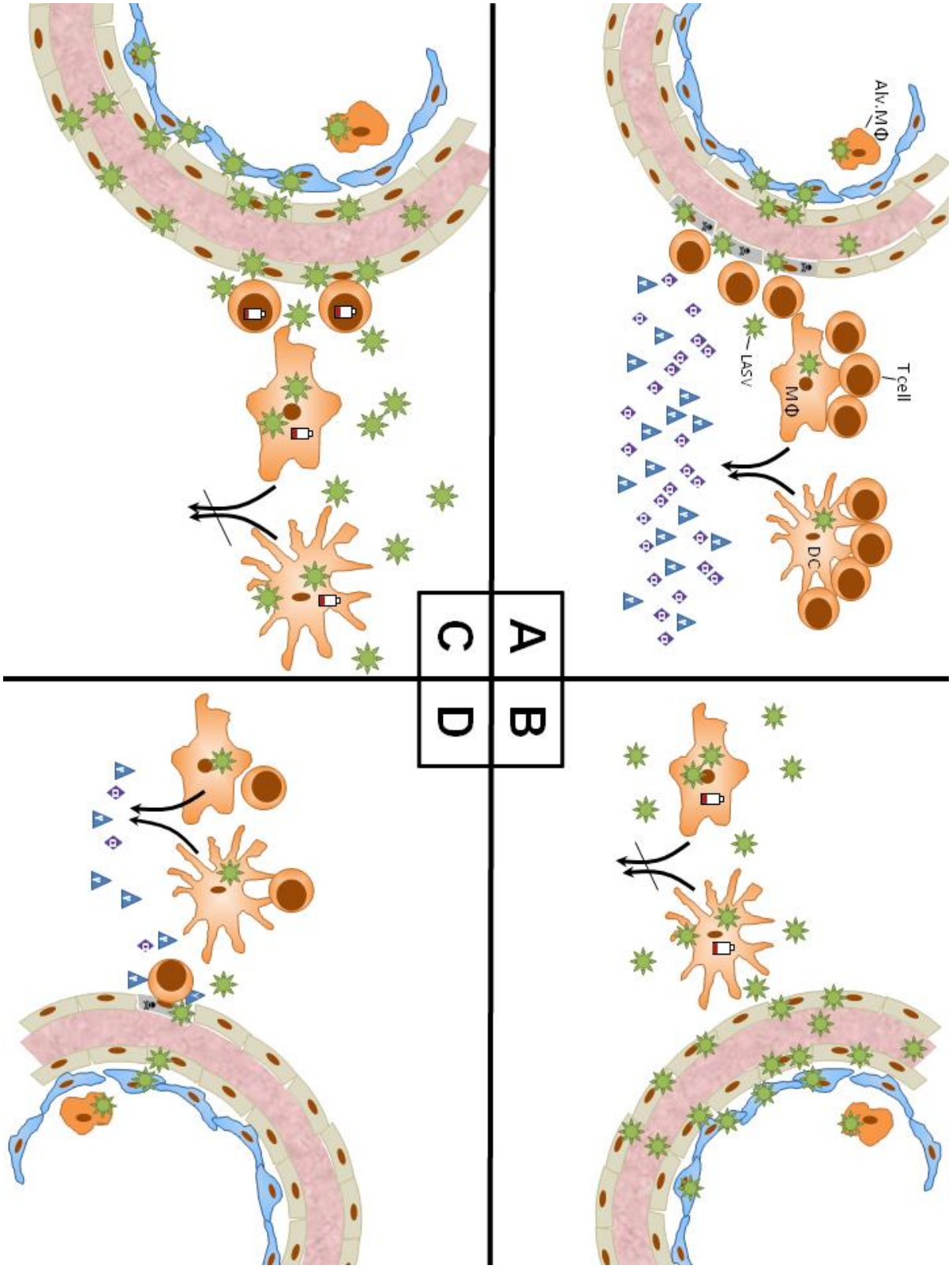

Figure 27 Putative modes of LASV infection outcomes in IFNAR^{BL6} and different RAG1$^{-/-}$ adoptive T cell transfer situations.
Intranasal inoculation of mice with LASV leads to infection of alveolar macrophages (alv. MΦ) epithelial, endothelial cells and finally also other APCs. (A) Infected APCs release high amounts of inflammatory cytokines (purple rhomb: TNFα, blue triangle: IFNγ) due to overwhelming T cell co-stimulation resulting in tissue damage and pathogenesis. (B) In absence of T cells like in RAG1$^{-/-}$ or under T cell ablation, APCs remain inactive, LASV freely replicates and no pathogenesis occurs. (C) Transfer of T cells into infected mice leads to exhaustion of the T cells due to antigenic overabundance leaving APCs still inactive and LASV free to replicate alike scenario 'B'. (D) Low co-stimulation of APCs through low concentration of T cells results in a balanced immune response and viral clearance without induction of pathogenesis.

4.3 Flow cytometric staining of LASV-proteins

Flow cytometry is a powerful, yet finicky, tool of modern immunology. Not every antibody working in histological settings also works in short-timed measurements of single cell suspensions. Reports of immune cells as early replication sites of arenaviruses exist [160, 161], but *in vivo* evidence depicting this circumstance has been restricted to histological stainings of advanced infection stages [145, 162].

Antibody based detection of LCMV-GP in flow cytometry is readily used in *in vitro* analyses e.g. with GP-overexpressing cells line [163] or recombinant viruses *in vivo* [164]. But the GP-expression of natural infection was too inadequate for our flow cytometric setups. The high NP-expression in arenaviral infections, however, allows for sufficient detection *in vivo* [165, 166], but requires intracellular staining procedures. Establishing a staining procedure for LASV, several antibodies targeting both antigens were tested during this thesis with only 2B5 proven effective enough for the application. Another nanobody (not shown), kindly provided by Dr. Florian Krammer from the Icahn School of Medicine at Mount Sinai (New York), also achieved good staining results but inexplicably completely lost its function after prolonged storage at 4 °C, deeming it too unreliable for time-intensive BSL4 experiments and fieldwork in Nigeria.

The antibody 2B5 showed highly specific staining of *in vitro* infected murine fibroblasts; identical to identification via RNA-hybridization probe amplification during PrimeFlow assays. The tested nanobody, however, had not been compatible with the PrimeFlow staining protocols.

Despite the *in vitro* tests for specificity, unspecific staining of uninfected granulocytes did occur *in vivo*, although CD16 and CD32 were blocked prior to staining. Subsequently, mock-infected controls were essential at every sacrifice time point.

It is unknown if the unspecific staining in uninfected animals did stem from antibody capture via Fcγ-receptors, but enzymatically fragmenting the 2B5 antibody down to Fab- or $F(ab')_2$ fragments could provide a remedy for the problem. Still the smaller size of the Fab- or $F(ab')_2$ fragments might also introduce new problems regarding the fluorophore-labeling efficiencies.

Because the flow cytometric results for α-LASV-NP staining were not microscopically verified in this study, cells were generally described only as LASV-NP-positive instead of LASV-infected. It remains unknown to which extent the analyzed cells were productively LASV-infected cells or if positive signals could have been partly caused by

phagocytic processes of e.g. LASV-NP laden cell debris. Future usage of 2B5-antibody, hence, should be accompanied by microscopic analyses.

The infection time point series of infected myeloid cells within this thesis did provide low numbers of infected immune cells compared to the viral titers seen at each time point. The receptor for arenaviral entry, α-dystroglycan, is ubiquitous in several tissues [167]. Even though APCs are considered early target cells of LASV infection with their high expression of α-dystroglycan [168], the bulk of early infected cells facilitating virus production might rather be of non-hematopoietic origin due to their sheer amount. In this study putative infected myeloid cells could only be detected by day five post infection. Previous studies in HHD-mice could also only show intracellular LASV in Iba-1^{+} monocytes by confocal microscopy by day eight post infection, while immune histochemical detection in macrophages of cynomoglus macaques has been restricted to seven days post infection earliest [162]. Thus, myeloid cells might only have a lesser role in virus replication than often stated in literature [124, 143]. Though, final results on the microscopic LASV detection in myeloid cells within the IFNAR^{BL6} disease model are still pending.

4.4 Role of myeloid cells in LASV infection

Interactions of infected APCs with the adaptive immune system have been hypothesized to play an important role in the developments of symptoms *in vivo* [145] In this study, a tropism of LASV for the infection of hematopoietic alveolar macrophages as well as pDCs could be indicated. Due to the radiation injury of mice in the generation of the IFNAR^{BL6} model, analyzed alveolar macrophages were repopulated from myeloid precursor cells expressing CD45 instead of their CD45-negative natural phenotype by fetal origin in non-irradiated hosts [169, 170].

LASV-NP signals were present in F4/80^{+} macrophages and pDC of the spleen, which was also observed in the blood. This fits into a model of dendritic cells and other APCs as vectors of virus dissemination *in vivo* as also speculated for LCMV and EBOV infections [125, 171].

Unlike in reports of LCMV infection [172, 173], in the LASV infection model, presented here, a loss of APCs could be observed only in the lung during LASV infection, together with a general decline in viable cell numbers in the lungs of infected animals, which was most likely caused by overall lung tissue damage. Likewise, MORV in myeloid cells had

not been detected (not shown), despite cross-reactivity of the antibody. This further underscores previous *in vitro* results showing MORV incapable of productively infecting murine APCs, which might play a role in its apathogenicity.

4.5 Immune reactions in human cases of Lassa fever

Despite the provided research efforts on the immunology during LASV infections in model systems, immunological studies on LF in humans in contrast are scarce. Great efforts were undertaken researching the human disease shortly after its discovery in the second half of the 20th century [2, 18, 25, 45, 64], while molecular immunology was still in its infancy. These studies even nowadays provide important groundwork for the virology and the study of general pathology of LASV infection. Most modern immunological findings describing the infection with LASV originate either from single case studies [174], patients evacuated to first-world nations [31, 147], few serological studies [135] or are derived from studies in NHP [28, 162]. Published information describes early robust immune reactions as an important survival correlate [175]. However, it remains unclear, if the recapitulation of the LF symptoms observed in small animal models and its absence during inhibition of the adaptive immune system is mechanistically identical to the human situation. Hence, we set out to acquire immune relevant data of human cases in Nigeria within the scope of our resources, comparing mild course of the disease with the courses of severe and fatal cases.

In the examined time frames T cells of LF patients did not reveal any significant upregulation of the activation markers, HLA-DR or KLRG1. CD86, while often being thought of as an activation molecule on APCs to facilitate CD28 ligation and signaling to T cells; it is also expressed transiently on CD8 T cells after stimulation [176-178]. At early time points of the infection, blood samples displayed CD86^{+} T cells declining over the course of the infection. Severe cases even seemed to display higher proportions of CD86^{+} T cells at these early time points; however, the overall data density for FACS analyses including this marker is too low for statistical analysis and needs additional observation in the future. Other activation markers like CD69, CD38 and the proliferation marker, Ki-67, might also prove fruitful in future research efforts on the activation of human CD8^{+} T cells in LASV infection, as they were already employed in other studies [147].

During the measurements, the inhibitory cell markers, CTLA-4 and PD-1, were also revealed to be elevated in severe cases of the disease. In contrast to the lethal *in vivo* mouse model these cell markers did not escalate in their expression over the course of the disease in humans but instead displayed a trend of slow decline.

CTLA-4 and PD-1 are topics of lively discussion in immune responses to cancers and during chronic viral infections due to their strong immune inhibitory properties. However, in acute infection and inflammation their role as marker molecules is debatable. In circumstances of acute infection CD8 T cells expressing high levels of CTLA-4 and PD-1 have been shown to still elicit strong effector functions [177, 179-181]. In the end, inhibitory T cell markers generally correlate with high antigenic burden (viremia/parasitemia) as also seen in patients and *in vivo* during this study, but the determination of effect and cause in this relation still needs to be clarified.

4.6 Scientific Contribution

In this thesis I was able to show, that CD8 T cell responses in the IFNAR^{BL6} chimeric mouse model of Lassa fever show a deregulation of high activation (CD44, KLRG1) and inhibition markers (CTLA-4, PD-1) in the moribund stages of infection correlating with symptom severity and subsequent death. Utilization of OT-I mixed bone-marrow chimeras additionally provided evidence that the strong T cell activation during LASV infection was not caused through bystander activation of unspecific T cells. By adoptively transferring CD3 T cells into RAG1$^{-/-}$ mice, I was also able to indicate, that while important in the pathology of LASV infection, in this model T cells are not solely responsible for the induction of the pathology. The conducted T cell transfers even point towards a viral clearance through CD3 T cells without the induction of any pathology.

For the first time, flow cytometrical identification of LASV-infected immune cells *in vivo* confirmed prior observations of infected immune cells only manifesting by day seven post infection. While LASV-NP could be detected in dendritic cells during the infection, the contribution of DCs to virus replication needs reconsideration due to the low numbers of cells found in the analyzed tissues, marking immune cells rather vehicles of viral dissemination than places of large scale viral replication.

Analyses of human patient samples from Nigeria directly on-site indicate a correlation of Lassa fever severity with increased expression of CTLA-4 and PD-1 on CD8 T cells. Differences in activation marker expression and in the innate immune cell composition

could not be observed when comparing severe to mild LF cases, furthermore, leaving the pathological mechanisms during LF in humans still unknown.

5. Supplementary information

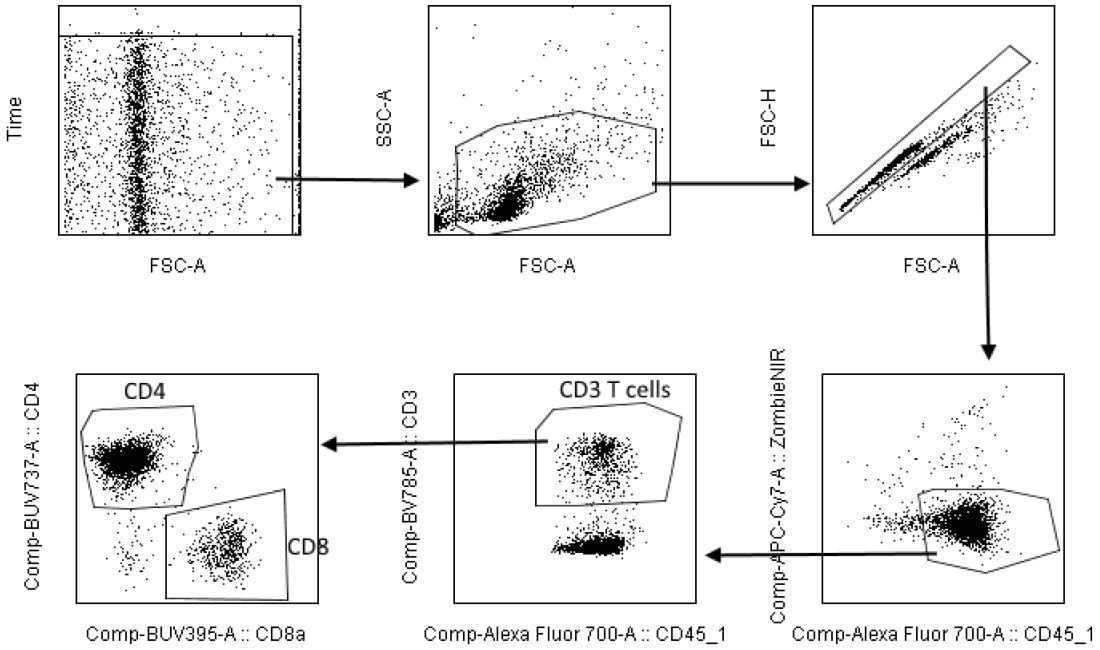

Supplemental figure S1 Gating scheme for chimeric mouse T cells.
Basic gating strategy employed to gate for CD4 and CD8 T cells in bone marrow chimeric mice.

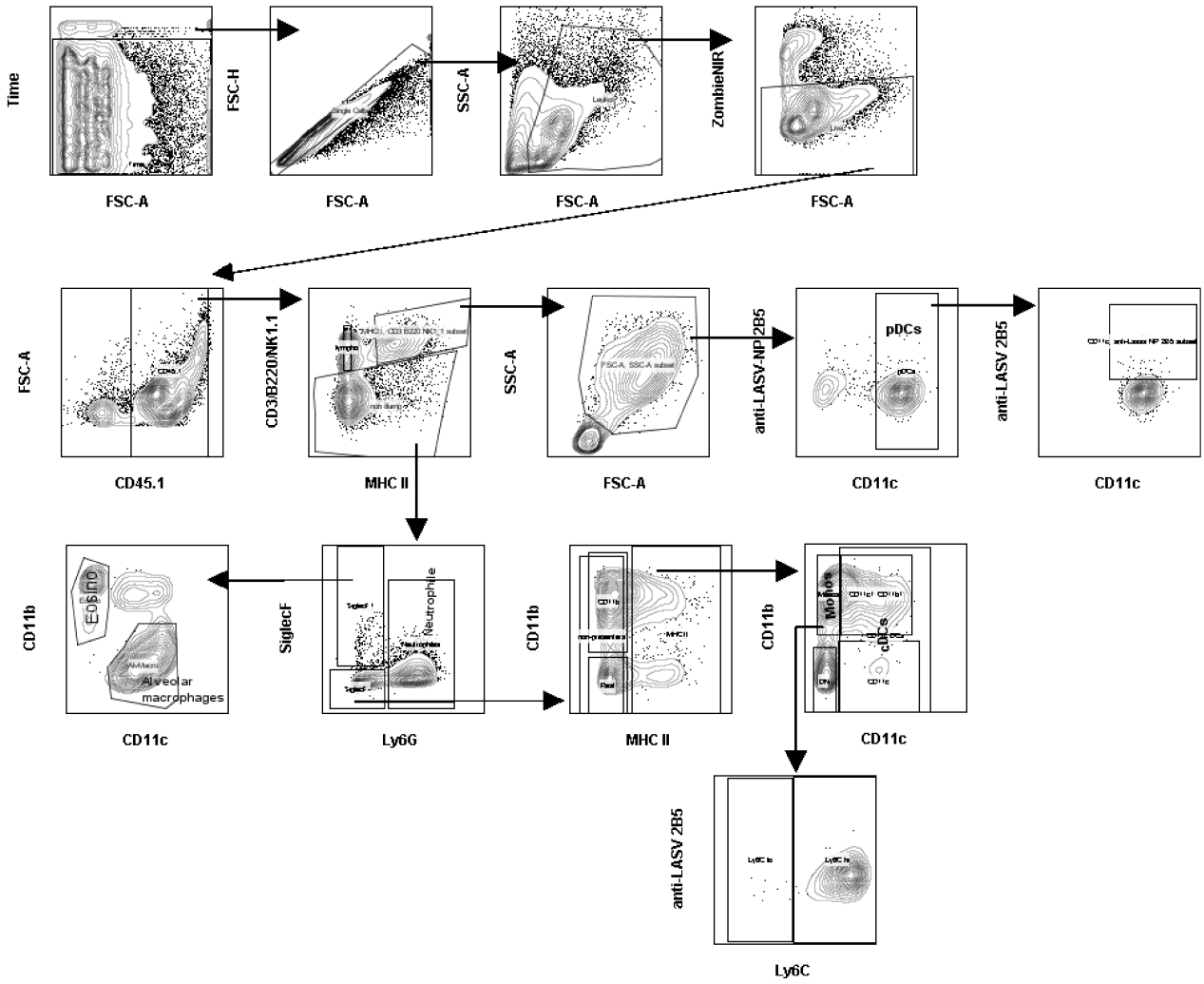

Supplemental figure S2 Gating scheme for murine myeloid cells of the lung.
Basic gating strategy employed to gate for myeloid cell populations and subpopulations in lungs of bone marrow chimeric mice.

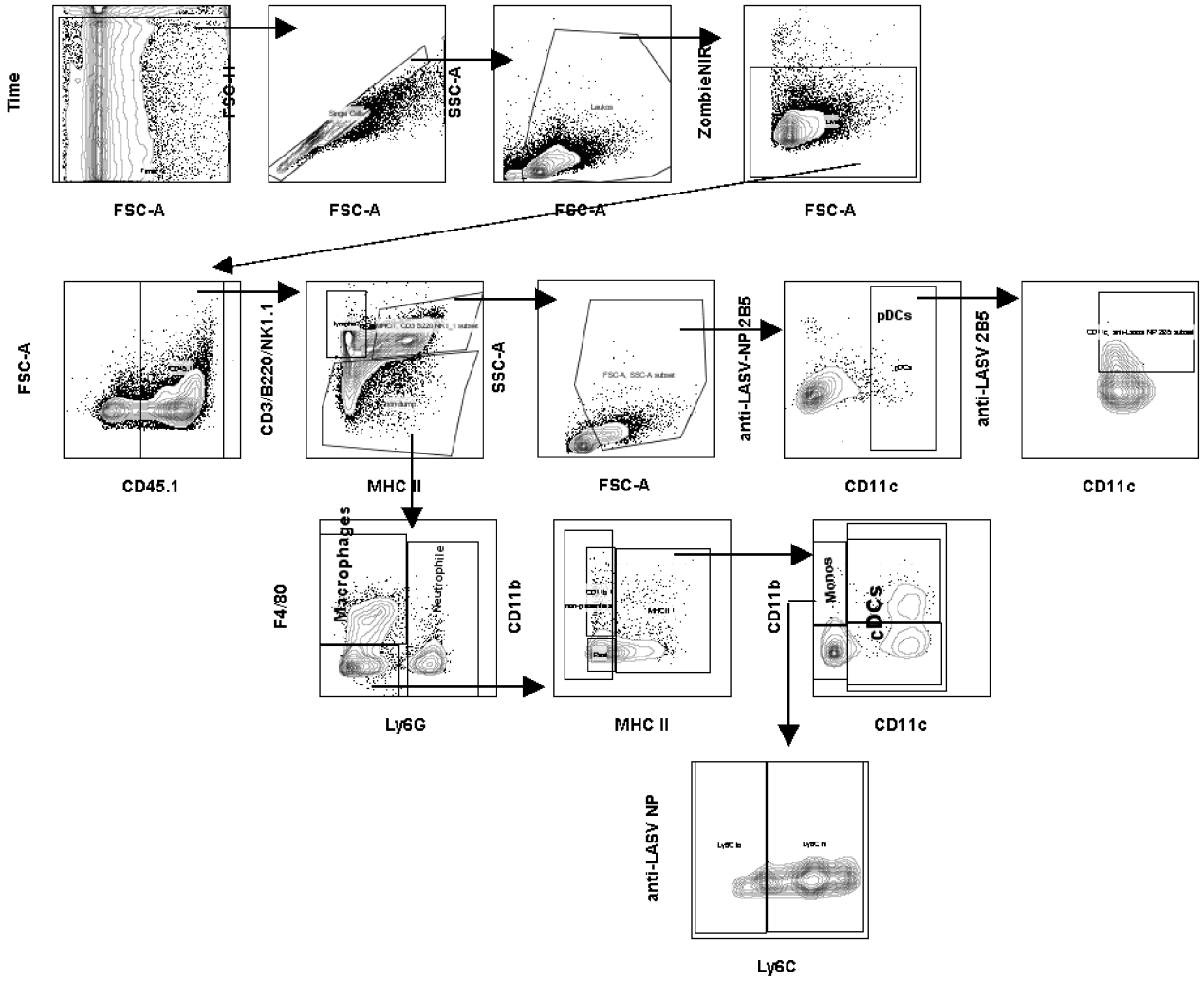

Supplemental figure S3 Gating scheme for murine myeloid cells of spleen and blood.
Basic gating strategy employed to gate for myeloid cell populations and subpopulations in spleens and blood of bone marrow chimeric mice.

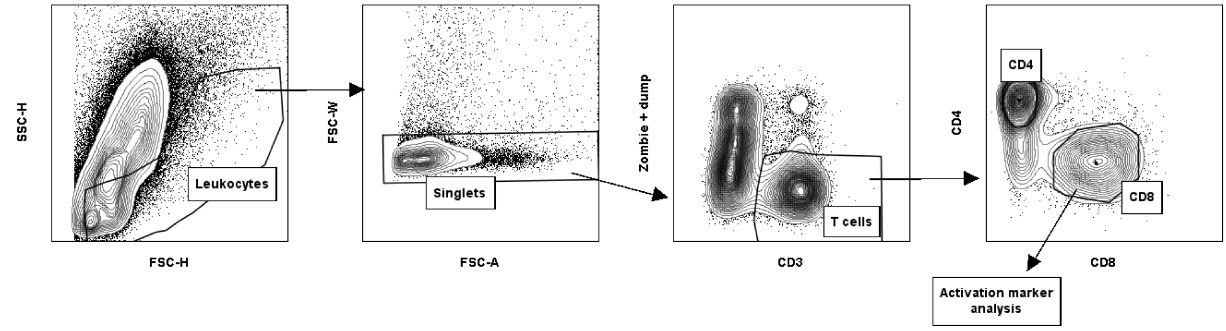

Supplemental figure S4 On-site gating scheme of human T cells from blood.
Basic gating strategy employed to gate T cell populations in the blood of LF patients in Nigeria using a Guava 12 flow cytometer.

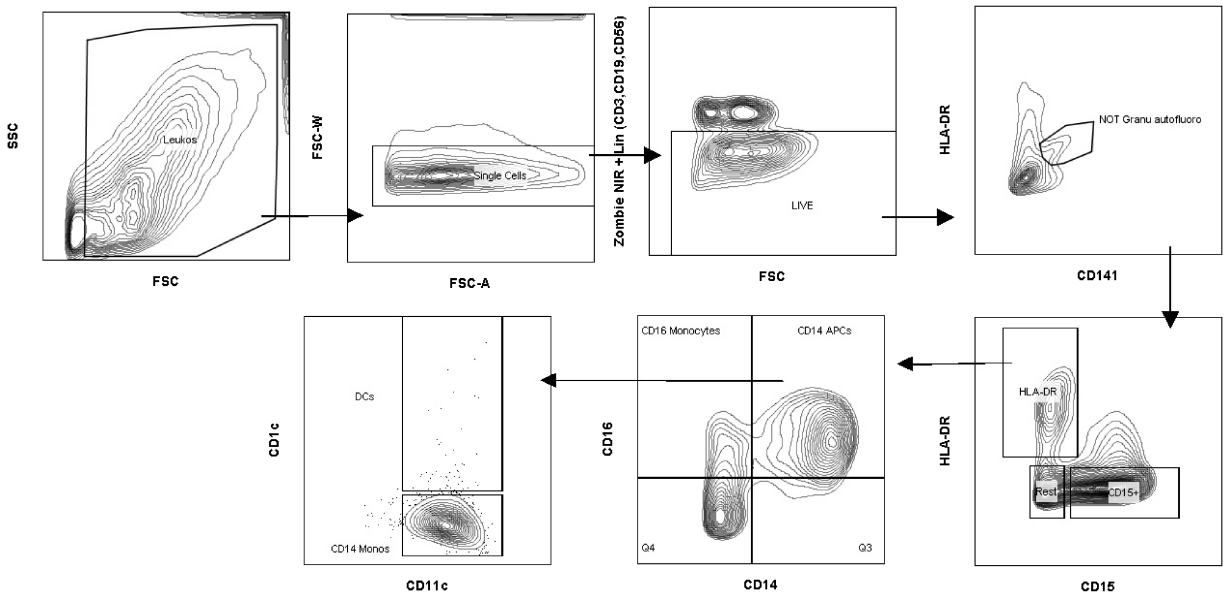

Supplemental figure S5 Gating scheme of human patient blood myeloid cells on-site.
Basic gating strategy employed to gate for monocytic cell populations in the blood of LF patients in Nigeria using a Guava 12 flow cytometer.

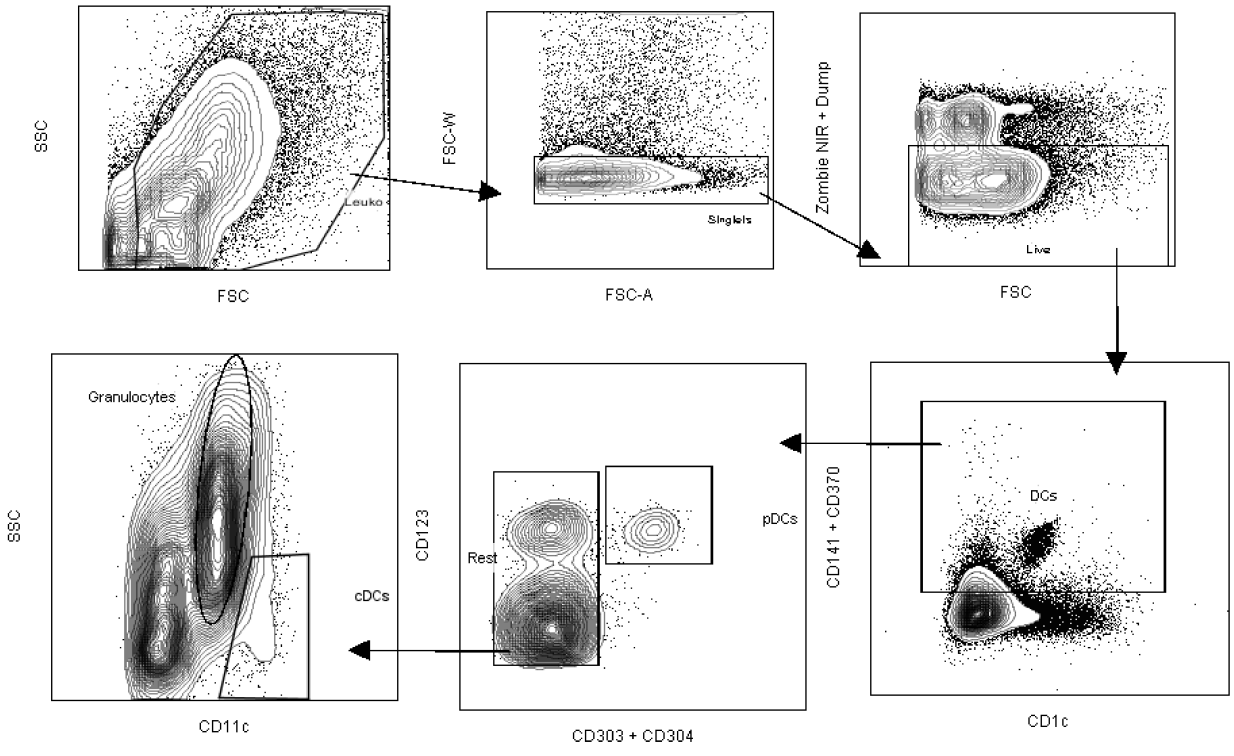

Supplemental figure S6 Gating scheme of human patient blood dendritic cells on-site.
Basic gating strategy employed to gate for dendritic cell populations in the blood of LF patients in Nigeria using a Guava 12 flow cytometer.

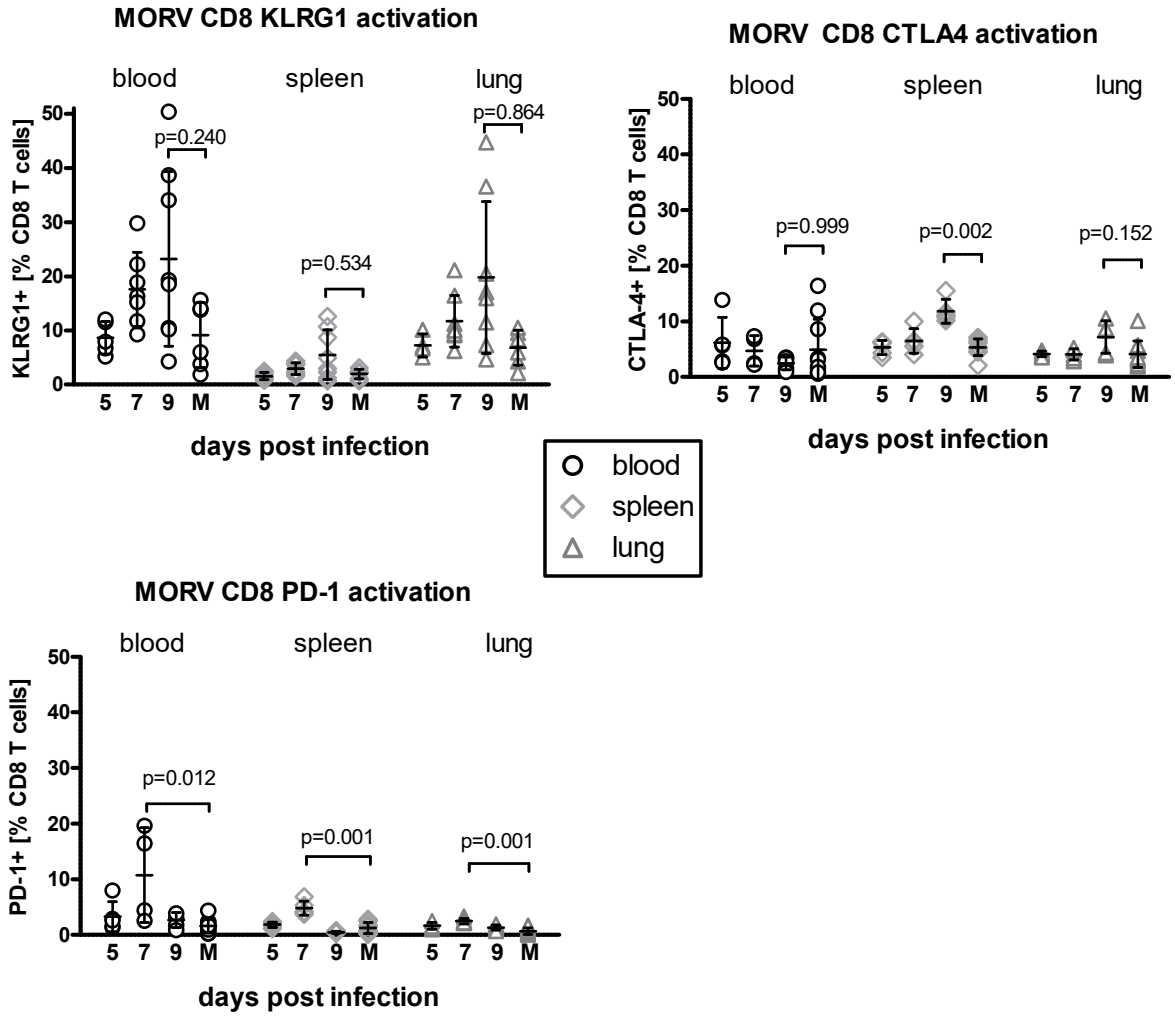

Supplemental figure S7 T cell reactions to MORV over the course of the infection.
Mice infected i.n. with LASV or mock-inoculum (M) were sacrificed at days 5, 7 & 9 dpi. KLRG1, CTLA-4 and PD-1 (teal) phenotypes of CD8 T lymphocytes in the blood, spleen and lung were determined flow cytometrically. While CTL become activated (KLRG1) over the course of the infection, the inhibitory markers CTLA-4 and PD-1 remain only low expressed. *Mann-Whitney-test, two-tailed, adjusted p-values with Dunn's correction. Data shows mean ±SD (+replicates).*

A

Cubic Regression Curve Fit

	LASV	LASV + OT-I T cells	LASV OT-I triple BM chimera	Global (shared)
Comparison of Fits				
Null hypothesis				3 parameters same for all data sets
Alternative hypothesis				3 parameters different for each data set
P value				0,0058
Conclusion (alpha = 0.05)				Reject null hypothesis
Preferred model				3 parameters different for each data set
F (DFn, DFd)				3,099 (6, 329)
3 parameters different for each data set				
Best-fit values				
B0	= 100	= 100	= 100	
B1	-0,6726	-0,1728	0,4629	
B2	0,2411	0,03921	-0,107	
B3	-0,03996	-0,02693	-0,01322	
95% CI (profile likelihood)				
B1	-1,41 to 0,06439	-1,71 to 1,364	-0,5081 to 1,434	
B2	0,001572 to 0,4807	-0,4453 to 0,5237	-0,409 to 0,195	
B3	-0,0584 to -0,02152	-0,0635 to 0,009634	-0,03563 to 0,009186	
Goodness of Fit				
Degrees of Freedom	170	48	111	
R square	0,7435	0,8218	0,7376	
Absolute Sum of Squares	1385	449,1	1050	
Sy.x	2,854	3,059	3,076	
Constraints				
B0	B0 = 100	B0 = 100	B0 = 100	
3 parameters same for all data sets				
Best-fit values				
B0	= 100	= 100	= 100	
B1	-0,1643	-0,1643	-0,1643	-0,1643
B2	0,07321	0,07321	0,07321	0,07321
B3	-0,02734	-0,02734	-0,02734	-0,02734
95% CI (profile likelihood)				
B1	-0,7182 to 0,3895	-0,7182 to 0,3895	-0,7182 to 0,3895	-0,7182 to 0,3895
B2	-0,1031 to 0,2495	-0,1031 to 0,2495	-0,1031 to 0,2495	-0,1031 to 0,2495
B3	-0,04069 to -0,014	-0,04069 to -0,014	-0,04069 to -0,014	-0,04069 to -0,014
Goodness of Fit				
Degrees of Freedom				335
R square	0,7406	0,7871	0,7226	0,7481
Absolute Sum of Squares	1400	536,5	1110	3047

B

Regression curve derived datasets

dpi	IFNAR^{BL6} LASV	LASV + OT-I T cells	LASV OT-I triple BM chimera
0,000	100,000	100,000	100,000
1,001	99,528	99,839	100,343
2,002	99,299	99,595	100,392
3,003	99,072	99,105	100,067
4,004	98,608	98,208	99,290
5,005	97,664	96,740	97,979
6,006	96,001	94,541	96,057
7,007	93,379	91,448	93,442
8,008	89,556	87,299	90,056
9,009	84,293	81,931	85,819
10,000	77,427	75,259	80,708

C

2-way ANOVA multiple comparison Compare column means (main column effect)

Number of families	1
Number of comparisons per family	3
Alpha	0,05

Tukey's multiple comparisons test	Mean Diff.	95,00% CI of dif	Significant?	Summary	Adjusted P Value
LASV vs. LASV + OT-I T cells	0,9873	0,03531 to 1,93	Yes	*	0,0413
LASV vs. LASV OT-I triple BM chimera	-0,8479	-1,8 to 0,1041	No	ns	0,0864
LASV + OT-I T cells vs. LASV OT-I triple BM chimera	-1,835	-2,787 to -0,883	Yes	***	0,0003

Supplemental table S1 Cubic regression curve modeling and XY-data points of weight loss during LASV infection of IFNAR$^{BL6+OT-I}$ and IFNAR^{BL6} with adoptively transferred OT-I T cells and IFNAR^{BL6}.

Measurements between groups were not available for the same days for, a cubic regression curves (A) were fitted onto the datasets. ANOVA analysis was performed on datasets generate by the cubic regression curves (B), significant differences were seen for IFNAR^{BL6} with adoptively transferred OT-I T cells, weight loss occured about half a day earlier.

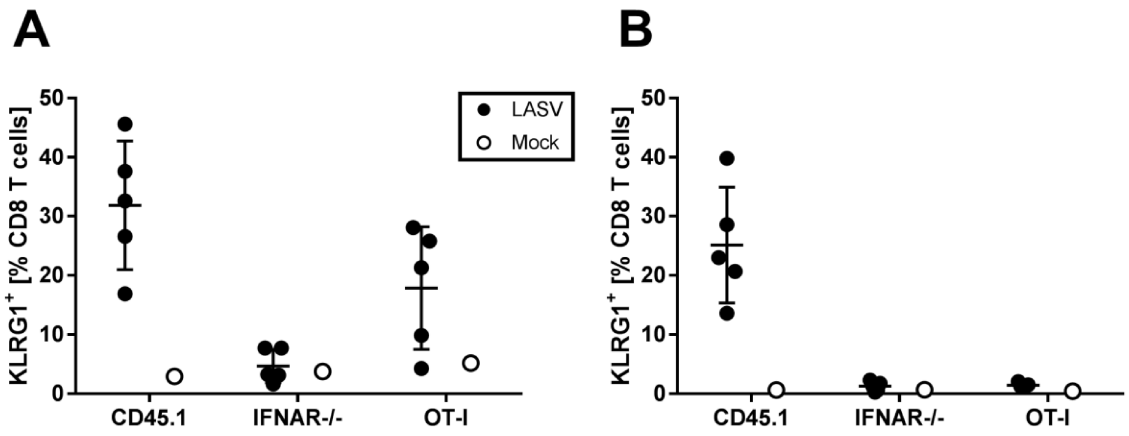

Supplemental figure S8 KLRG1 expression of IFNAR^{BL6} with adoptively transferred OT-I T cells on the CTL in the blood and spleen.
IFNAR^{BL6} were infected with 1000 FFU LASV i.n.one day after receiving an adoptive transfer of OT-I cell i.v. . Fractions KLRG1-positive CD8 T cells in (A) the blood and (B) the spleen at 9 dpi are displayed categorized by genotype of the T cell. *Data shows mean ±SD (+replicates).*

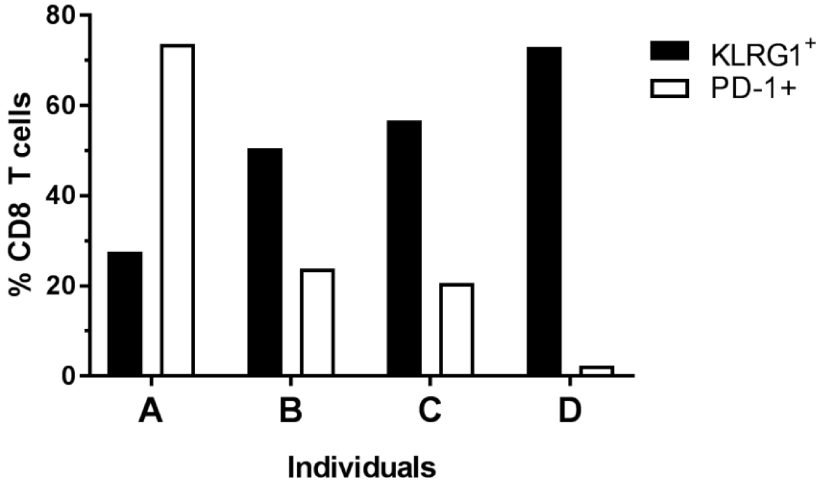

Supplemental figure S9 KLRG1 and PD-1 expression on the T cells in the blood of RAG1$^{-/-}$ with T cell transfer prior to LASV infection.
RAG1$^{-/-}$ mice were infected with 100 FFU LASV i.n.seven day after receiving an adoptive transfer of MACS purified CD3 T cells i.p. . Fractions KLRG1^{+} and PD-1^{+}CD8 T cells in (A) the blood and (B) the spleen at 21 dpi are displayed, divided as individual animals. For description of the individual animals referre to Table 1.

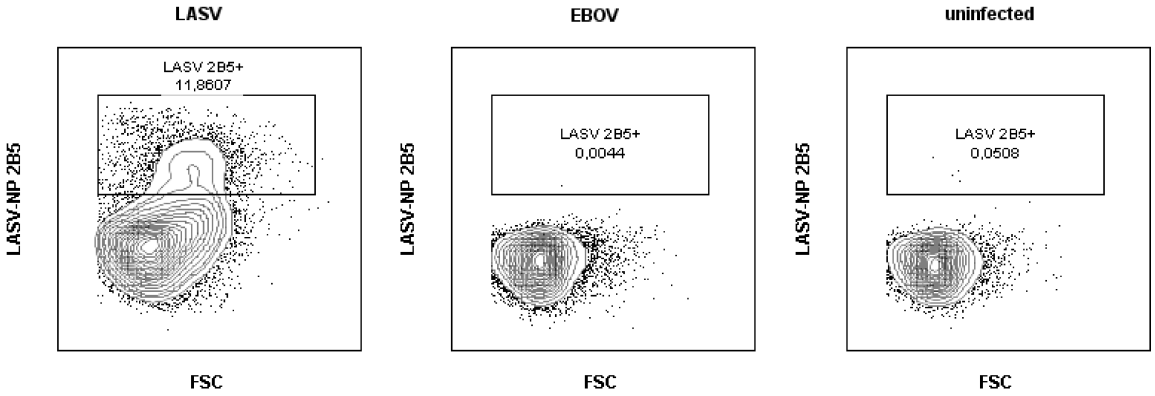

Supplemental figure S10 Specificity of anti-LASV-NP '2B5' *in vivo.*
Spleens of mice infected with either with i.n. 1000 FFU LASV Ba366, EBOV Zaire or mock inoculum were analyzed on day eight post infection. Intracellular staining of 2B5 showed no cross-reactivity to cells of EBOV or mock infected animals.

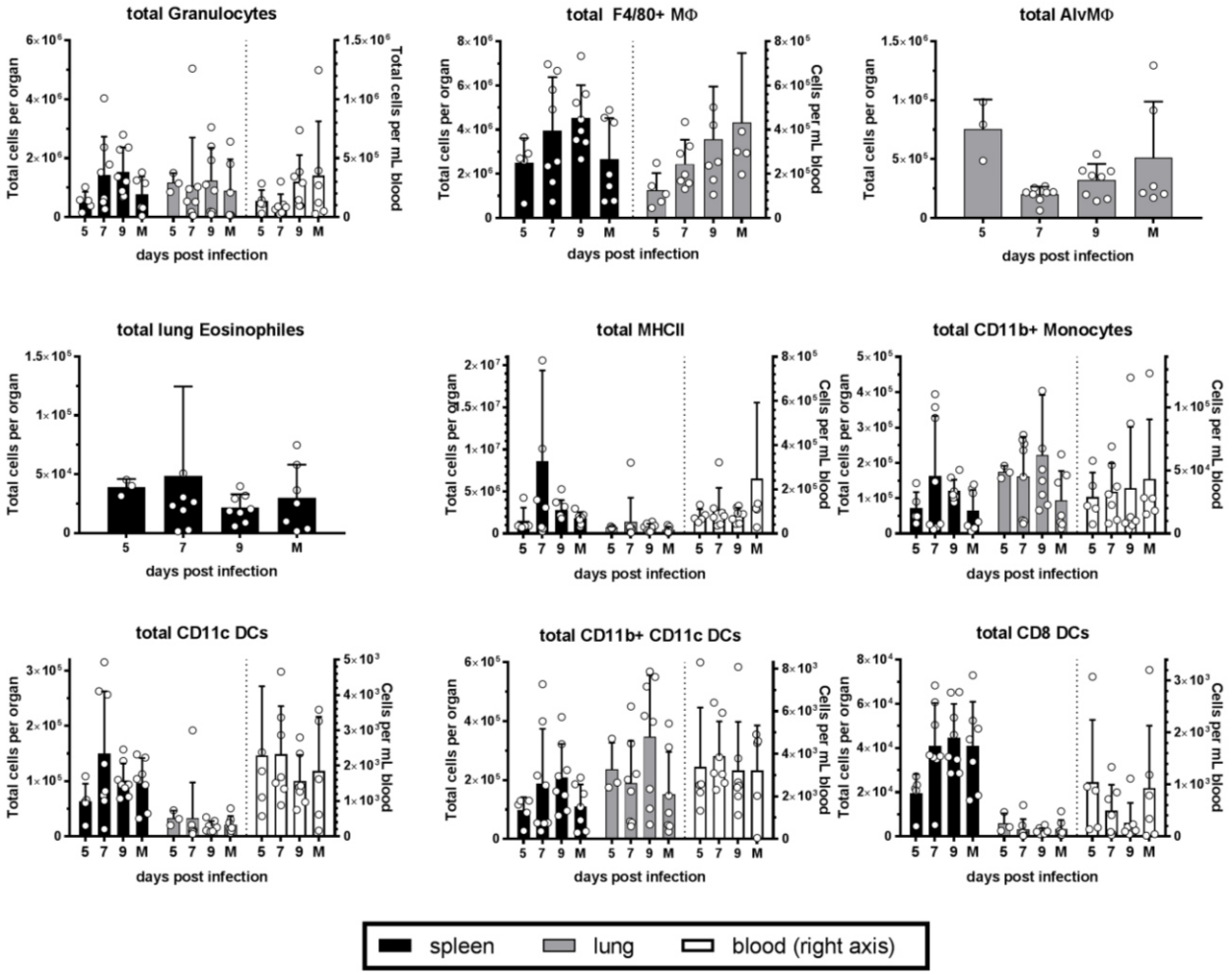

Supplemental figure S11 Myeloid cell population in MORV infected IFNAR^{BL6}.
IFNAR^{BL6} mice were infected with 1000 FFU MORV i.n. or PBS (M) and sacrificed at 5, 7 and 9 dpi. Total cell numbers per organ or per milliliter blood (right axis) are displayed. The lung tissue does not present loss of myeloid cells at late time points of the infection as seen during LASV infection. *Data shows mean ±SD (+replicates).*

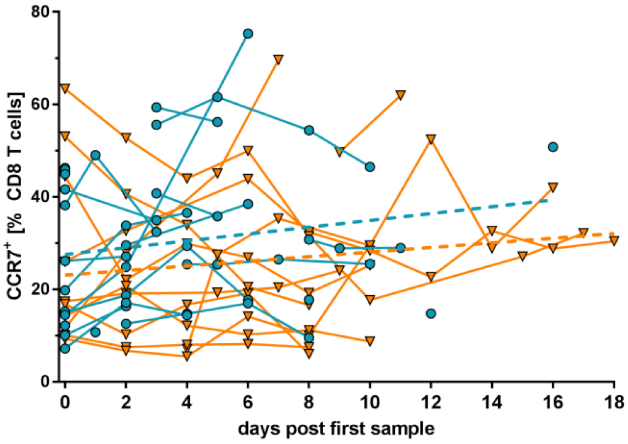

Supplemental figure S12 No CCR7+ CD8 T cell reduction in human patients.
T cells from blood of LF patients in Nigeria was analyzed longitudinally. No marked differences in the downregulation of CCR7 as a sign of T cell activation is observed on CD8 T cell of mild (teal) and severe (orange) cases over the course of infection. Data sets of individual patients are connected by a solid line. For visual clarity linear regressions (dashed lines) of the subgroup's means are displayed and not for a predictive modeling.

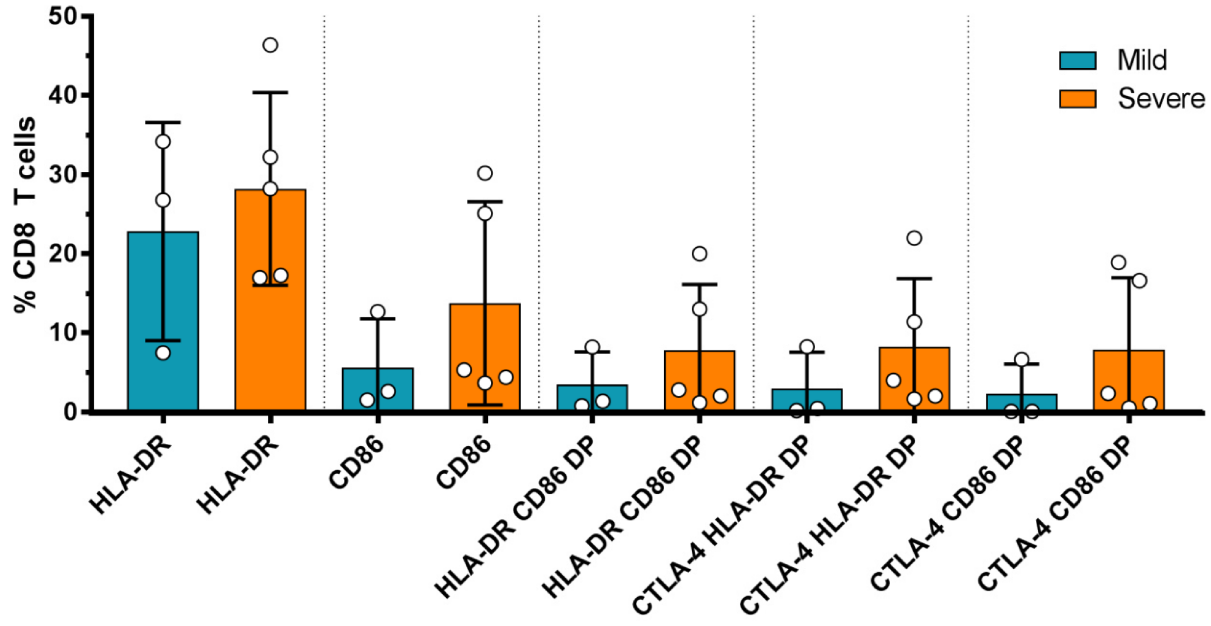

Supplemental figure S13 Cross-sectional display of activation markers on T cells of patients in the first study samples.
Plotting of CD8 T cells positive for either HLA-DR, CD86 or double positive (DP) cells. This is a subanalysis of the first study sample from the longitudinal analysis of patients seen in Figure 23. *Data shows mean ±SD (+replicates).*

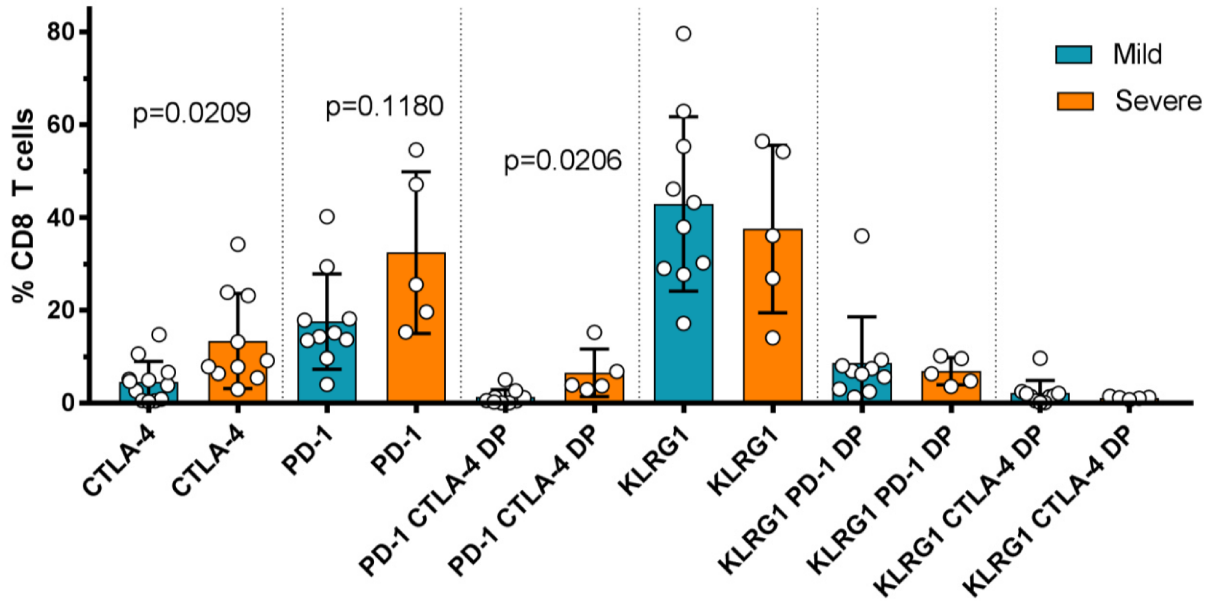

Supplemental figure S14 Cross-sectional display of inhibitiory markers on T cells of patients in the first study samples.
Plotting of CD8 T cells positive for either CTLA-4, PD-1, KLRG1 or double positive (DP) cells. This is a subanalysis of the first study sample from the longitudinal analysis of patients seen in Figure 24. *Data shows mean ±SD (+replicates). Mann-Whitney-test, two-tailed, adjusted p-values with Dunn's correction.*

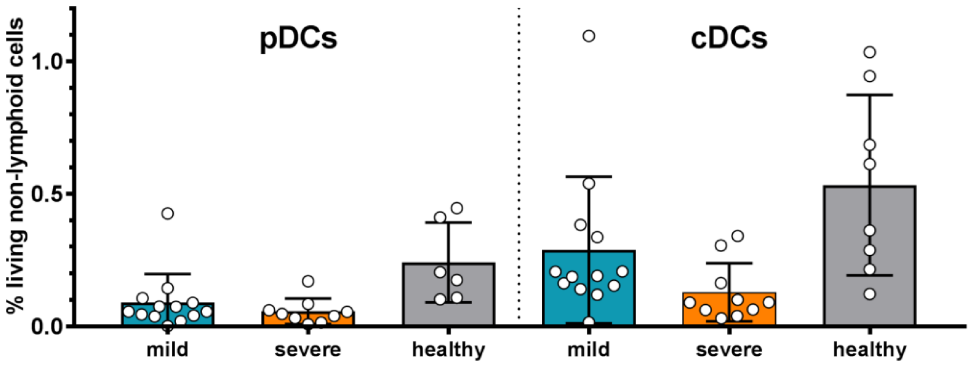

Supplemental figure S15 Cross-sectional plotting of pDCs and cDCs fractions in the first study samples.
Plotting of pDC and cDC fractions in the first study sample of mild and severe cases as well as healthy controls. This is a subanalysis of the first study sample from the longitudinal analysis of patients seen in Figure 25. *Data shows mean ±SD (+replicates).*

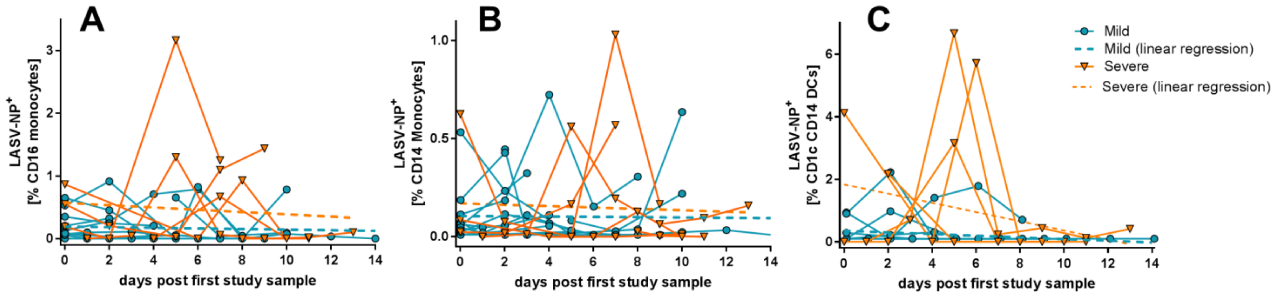

Supplemental figure S16 Longitudinal plotting of LASV-NP staining in CD16 monocytes, CD14 monocytes and CD14 CD1c CD11c DCs.
Results are to be considered with caution as autofluorescent unspecific LASV-NP stained granulocytes could not be completely gated out of the analysis, resulting in strong fluctuations.

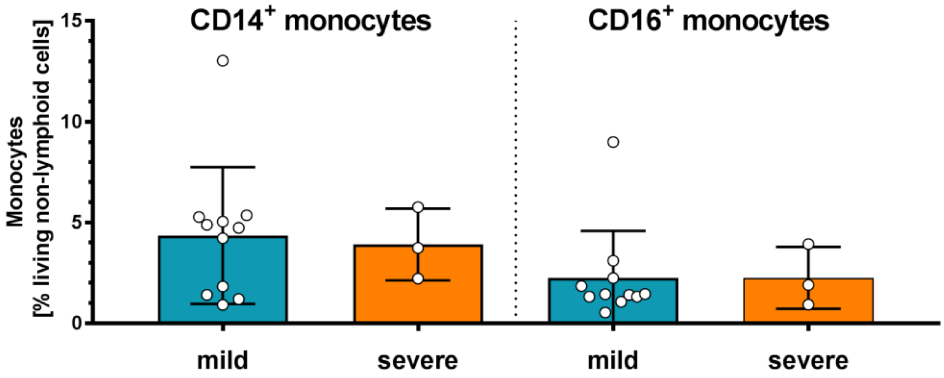

Supplemental figure S17 Cross-sectional display of monocyte populations of patients in the first study samples.
Plotting of CD14-positive and CD16-positive monocyte fractions in the first study sample of mild and severe cases. This is a subanalysis from the longitudinal analysis of patients seen in Figure 26. *Data shows mean ±SD (+replicates).*

6. Abstract/Zusammenfassung

6.1 Abstract

Lassa fever (LF) is a widespread viral infectious disease in West Africa that is estimated to infect up to 300,000 people per year. LF is caused by the *Lassa mammarenavirus* (LASV), which occurs naturally in the Natal-multimammate mouse (*Mastomys natalensis*), and belongs to the virus family *Arenaviridae*. LF is a viral hemorrhagic fever in severity comparable to ebola, dengue or yellow fever. While serological studies indicate that the majority of infections are mild or asymptomatic, LF can reach a lethality rate of up to 65% in nosocomial outbreaks. The discovery of LASV dates back almost 50 years, but still there is no approved vaccination or specific therapy against this disease. Due to its potential lethality and the potential use as a biological weapon, LASV is categorized as a Biological Safety Level 4 agent. The necessary laboratory prerequisites as well as the lack of suitable small animal models have for a long time thwarted the research on pathophysiology and immunology of the LF.

Using a small animal model previously newly established by Dr. Lisa Oestereich, it could be shown in this thesis that the pathology in the IFNAR^{BL6} chimeric mice is associated with a dysregulated activation of the CD8 T cell response. Besides a strong expression of activation markers such as KLRG1 and CD44 on CD8 T cells, an increased expression of the inhibitory cell markers CTLA-4 and PD-1 in the highly acute phase of the disease could also be detected. Moreover, OT-I T cells in a mixed bone marrow model showed that the dysregulation is not due to a general activation of non-specific CD8 T cells. A similar expression of activation markers on CD8 T cells in humans could, however,not be confirmed in this study. The investigations undertaken on-site in a LASV-endemic area in Nigeria showed increased incidences of CTLA-4- and PD-1-positive CD8 T cells in linked to severe progressions of LF.

T-cell transfer experiments in RAG1$^{-/-}$ mice additionally indicated that the pathology observed during LASV infection is not solely T cell-dependent, as assumed from previous T cell depletion studies. Contrary to earlier assumptions, there was even evidence of successful control of viral infection by T cells without induction of any macroscopic symptoms.

Furthermore, establishment of a labeled antibody against LASV-NP for the first time enabled the identification of LASV-infected immune cells in the course of the disease by means of flow cytometry from *in vivo* samples. In this way, a tropism of LASV for

antigen-presenting cells (APC) could be shown within the animal model, detected only from the seventh day after infection onward. Previous postulations from *in vitro* studies on APCs as early targets of infection by LASV can therefore no longer be fully maintained.

The results of this work provide important insights into the immunology of LASV disease, allow a more profound characterization of the IFNAR^{BL6} mouse model for LASV infections, and point out possible target markers for future immunomodulatory studies in order to control Lassa fever pathology.

6.2 Zusammenfassung

Das Lassa-Fieber (LF) ist eine in West-Afrika weitverbreitete virale Infektionskrankheit mit der sich schätzungsweise bis zu 300.000 Menschen im Jahr anstecken. Ausgelöst wird LF durch das natürlich in Natal-Vielzitzenmäusen (*Mastomys natalensis*) vorkommende *Lassa mammarenavirus* (LASV) aus der Familie der *Arenaviridae*. LF zählt zu den viralen hämorrhagischen Fiebern vergleichbar mit Ebola-, Dengue- oder Gelbfieber. Während serologische Studien andeuten, dass ein Großteil der Infektionen mit LASV mild oder asymptomatisch verlaufen, so kann LF in nosokomialen Ausbrüchen auch eine Lethalitätsrate von bis zu 65% erreichen. Obwohl die Entdeckung des LASV fast 50 Jahre zurückreicht, existieren keine zugelassene Impfung oder spezifische Therapien gegen diese Erkrankung. Aufgrund seiner Gefährlichkeit und der potentiellen Nutzung von LASV als biologisches Kampfmittel, ist das LASV unter der biologischen Sicherheitsstufe 4 kategorisiert. Die entsprechend benötigten labortechnische Voraussetzung als auch das Fehlen geeigneter Kleintiermodelle haben lange Zeit die Forschung der Pathophysiologie und Immunologie des LF stark eingeschränkt.

Basierend auf der Nutzung eines vorangegangen durch Dr. Lisa Oestereich etablierten, neuen Kleintiermodelles, konnte im Verlauf der diesigen Niederschrift zur Promotion gezeigt werden, dass die Pathologie im Tiermodell mit einer dysregulierten Aktivierung der CD8-T-Zellantwort eingehergeht. Neben einer starken Expression von Aktivierungsmarkern wie KLRG1 und CD44 auf CD8-T-Zellen konnte ebenso eine erhöhte Expression der inhibierenden Zellmarker CTLA-4 und PD-1 in der hochakuten

Phase der Krankheit im Tiermodell erfasst werden. Dabei konnte mit Hilfe von OT-I T-Zellen gezeigt werden, dass die Dysregulation nicht auf eine generelle Aktivierung unspezifischer CD8-T-Zellen zurückgeht. Gleichartige Aktivierungen der CD8-T-Zellen im Menschen konnten im Rahmen dieser Arbeit nicht bestätigt werden. Die unternommenen Untersuchungen zeigten jedoch ein verstärktes Auftreten von CTLA-4- und PD-1-positiven CD8-T-Zellen im Zusammenhang mit schwerwiegenderen Verläufen von Patienten aus Nigeria, die am LF erkrankt waren.
Zusätzlich konnte mit T-Zell-Transfer-Experimente in $RAG1^{-/-}$-Mäusen gezeigt werden, dass beobachtete Pathologien während der LASV-Infektion nicht alleinig auf T-Zellen zurückzuführen sind wie aus früheren T-Zell-Depletionsstudien angenommen. Gegenteilig zu den früheren Annahmen gab es sogar Indizien einer erfolgreichen Bekämpfung der viralen Infektion durch die T-Zellen ohne eine Induktion jeglicher makroskopischer Symptomatik.
Ein im Rahmen dieser Arbeit etablierter Antikörper erlaubte zudem erstmalig die Identifikation von LASV-infizierten Zellen des Immunsystems aus *in-vivo*-Proben im Verlauf der Krankheit mittels Durchflusszytometrie. Auf diese Weise konnte innerhalb des Tiermodells ein viraler Tropismus für antigenpräsentierende Zellen (APZ) ab dem siebten Tag nach Infektion gezeigt werden. Frühere Postulierungen aus *in vitro*-Studien zu APZ als frühe Infektionsherde von LASV können folglich nicht mehr uneingeschränkt gehalten werden.

Die Ergebnisse dieser Arbeit bieten wichtige Einblicke in die Immunologie der LASV-Erkrankung, erlauben eine tiefgehendere Charakterisierung des vielseitig anwendbaren $IFNAR^{BL6}$-Mausmodells und zeigen mögliche Zielmarker für zukünftige immun-modulatorische Studien zur Eindämmung der Lassafieberpathologie auf.

7. References

[1] McCormick JB, Webb PA, Krebs JW, Johnson KM, Smith ES. A Prospective Study of the Epidemiology and Ecology of Lassa Fever. The Journal of Infectious Diseases. 1987;155:437-44.

[2] Frame JD, Baldwin JM, Jr., Gocke DJ, Troup JM. Lassa fever, a new virus disease of man from West Africa. I. Clinical description and pathological findings. Am J Trop Med Hyg. 1970;19:670-6.

[3] Dzotsi EK, Ohene SA, Asiedu-Bekoe F, Amankwa J, Sarkodie B, Adjabeng M, et al. The first cases of Lassa fever in Ghana. Ghana medical journal. 2012;46:166-70.

[4] Sogoba N, Rosenke K, Adjemian J, Diawara SI, Maiga O, Keita M, et al. Lassa Virus Seroprevalence in Sibirilia Commune, Bougouni District, Southern Mali. Emerg Infect Dis. 2016;22:657-63.

[5] Patassi AA, Landoh DE, Mebiny-Essoh Tchalla A, Halatoko WA, Assane H, Saka B, et al. Emergence of Lassa Fever Disease in Northern Togo: Report of Two Cases in Oti District in 2016. Case Reports in Infectious Diseases. 2017;2017:5.

[6] WHO. 2018 Annual review of diseases prioritized under the Research and Development Blueprint. https://www.who.int/emergencies/diseases/2018prioritization-report.pdf2018.

[7] Fichet-Calvet E, Lecompte E, Koivogui L, Soropogui B, Doré A, Kourouma F, et al. Fluctuation of Abundance and Lassa Virus Prevalence in Mastomys natalensis in Guinea, West Africa. Vector-Borne and Zoonotic Diseases. 2007;7:119-28.

[8] Stephenson EH, Larson EW, Dominik JW. Effect of environmental factors on aerosol-induced lassa virus infection. Journal of Medical Virology. 1984;14:295-303.

[9] Emmerich P, Thome-Bolduan C, Drosten C, Gunther S, Ban E, Sawinsky I, et al. Reverse ELISA for IgG and IgM antibodies to detect Lassa virus infections in Africa. J Clin Virol. 2006;37:277-81.

[10] Kerneis S, Koivogui L, Magassouba N, Koulemou K, Lewis R, Aplogan A, et al. Prevalence and risk factors of Lassa seropositivity in inhabitants of the forest region of Guinea: a cross-sectional study. PLoS Negl Trop Dis. 2009;3:e548.

[11] Gibb R, Moses LM, Redding DW, Jones KE. Understanding the cryptic nature of Lassa fever in West Africa. Pathog Glob Health. 2017;111:276-88.

[12] Fisher-Hoch SP, Tomori O, Nasidi A, Perez-Oronoz GI, Fakile Y, Hutwagner L, et al. Review of cases of nosocomial Lassa fever in Nigeria: the high price of poor medical practice. BMJ (Clinical research ed). 1995;311:857-9.

[13] Fiore AE, Uyeki TM, Broder K, Finelli L, Euler GL, Singleton JA, et al. Prevention and Control of Influenza with Vaccines. CDC MMWR. 2010;59:1-62.

[14] Kafetzopoulou LE, Pullan ST, Lemey P, Suchard MA, Ehichioya DU, Pahlmann M, et al. Metagenomic sequencing at the epicenter of the Nigeria 2018 Lassa fever outbreak. Science. 2019;363:74-7.

[15] Olayemi A, Cadar D, Magassouba NF, Obadare A, Kourouma F, Oyeyiola A, et al. New Hosts of The Lassa Virus. Scientific Reports. 2016;6:25280.

[16] Fichet-Calvet E, Rogers DJ. Risk Maps of Lassa Fever in West Africa. PLOS Neglected Tropical Diseases. 2009;3:e388.

[17] Gryseels S, Baird SJ, Borremans B, Makundi R, Leirs H, Gouy de Bellocq J. When Viruses Don't Go Viral: The Importance of Host Phylogeographic Structure in the Spatial Spread of Arenaviruses. PLoS Pathog. 2017;13:e1006073.

[18] Walker DH, Wulff H, Lange JV, Murphy FA. Comparative pathology of Lassa virus infection in monkeys, guinea-pigs, and Mastomys natalensis. Bulletin of the World Health Organization. 1975;52:523-34.

[19] Monath TP. Lassa fever: review of epidemiology and epizootiology. Bulletin of the World Health Organization. 1975;52:577-92.

[20] Meulen JT, Lukashevich I, Sidibe K, Inapogui A, Marx M, Dorlemann A, et al. Hunting of Peridomestic Rodents and Consumption of Their Meat as Possible Risk Factors for Rodent-to-Human Transmission of Lassa Virus in the Republic of Guinea. The American Journal of Tropical Medicine and Hygiene. 1996;55:661-6.

[21] Raabe VN, Mehta AK, Ribner BS, Lyon GM, Varkey JB, Raabe VN, et al. Favipiravir and Ribavirin Treatment of Epidemiologically Linked Cases of Lassa Fever. Clinical Infectious Diseases. 2017;65:855-9.

[22] Andersen Kristian G, Shapiro BJ, Matranga Christian B, Sealfon R, Lin Aaron E, Moses Lina M, et al. Clinical Sequencing Uncovers Origins and Evolution of Lassa Virus. Cell. 2015;162:738-50.

[23] Günther S, Lenz O. Lassa virus. Crit Rev Clin Lab Sci. 2004;41:339-90.

[24] Cummins D, McCormick JB, Bennett D, Samba JA, Farrar B, Machin SJ, et al. Acute Sensorineural Deafness in Lassa Fever. JAMA. 1990;264:2093-6.

[25] Fisher-Hoch SP, McCormick JB, Sasso D, Craven RB. Hematologic dysfunction in Lassa fever. Journal of Medical Virology. 1988;26:127-35.

[26] Geisbert TW. Predicting outcome and improving treatment for Lassa fever. The Lancet Infectious Diseases. 2018;18:594-5.

[27] Yun NE, Ronca S, Tamura A, Koma T, Seregin AV, Dineley KT, et al. Animal Model of Sensorineural Hearing Loss Associated with Lassa Virus Infection. Journal of Virology. 2016;90:2920-7.

[28] Cashman KA, Wilkinson ER, Zeng X, Cardile AP, Facemire PR, Bell TM, et al. Immune-Mediated Systemic Vasculitis as the Proposed Cause of Sudden-Onset Sensorineural Hearing Loss following Lassa Virus Exposure in Cynomolgus Macaques. MBio. 2018;9:e01896-18.

[29] Oestereich L, Lüdtke A, Ruibal P, Pallasch E, Kerber R, Rieger T, et al. Chimeric Mice with Competent Hematopoietic Immunity Reproduce Key Features of Severe Lassa Fever. PLOS Pathogens. 2016;12:e1005656.

[30] Ignatyev G, Steinkasserer A, Streltsova M, Atrasheuskaya A, Agafonov A, Lubitz W. Experimental study on the possibility of treatment of some hemorrhagic fevers. Journal of Biotechnology. 2000;83:67-76.

[31] Schmitz H, Köhler B, Laue T, Drosten C, Veldkamp PJ, Günther S, et al. Monitoring of clinical and laboratory data in two cases of imported Lassa fever. Microbes and Infection. 2002;4:43-50.

[32] Wulff H, Lange JV, Webb PA. Interrelationships Among Arenaviruses Measured by Indirect Immunofluorescence. Intervirology. 1978;9:344-50.

[33] Hufert FT, Lüdke W, Schmitz A. Epitope mapping of the Lassa virus nucleoprotein using monoclonal anti-nucleocapsid antibodies. Arch Virol. 1989;106:201-12.

[34] Smith ES, King IJ, McCormick JB, Johnson KM, Elliott LH, Webb PA. Clinical Virology of Lassa Fever in Hospitalized Patients. The Journal of Infectious Diseases. 1987;155:456-64.

[35] Panning M, Emmerich P, Olschläger S, Bojenko S, Koivogui L, Marx A, et al. Laboratory diagnosis of Lassa fever, liberia. Emerging infectious diseases. 2010;16:1041-3.

[36] McCormick JB, King IJ, Webb PA, Scribner CL, Craven RB, Johnson KM, et al. Lassa fever. Effective therapy with ribavirin. The New England journal of medicine. 1986;314:20-6.

[37] Wang P, Liu Y, Zhang G, Wang S, Guo J, Cao J, et al. Screening and Identification of Lassa Virus Entry Inhibitors from an FDA-Approved Drug Library. J Virol. 2018;92:e00954-18.

[38] Oestereich L, Rieger T, Lüdtke A, Ruibal P, Wurr S, Pallasch E, et al. Efficacy of Favipiravir Alone and in Combination With Ribavirin in a Lethal, Immunocompetent Mouse Model of Lassa Fever. The Journal of infectious diseases. 2016;213:934-8.

[39] Rosenke K, Feldmann H, Westover JB, Hanley PW, Martellaro C, Feldmann F, et al. Use of Favipiravir to Treat Lassa Virus Infection in Macaques. Emerging Infectious Disease journal. 2018;24:1696.

[40] Mire CE, Cross RW, Geisbert JB, Borisevich V, Agans KN, Deer DJ, et al. Human-monoclonal-antibody therapy protects nonhuman primates against advanced Lassa fever. Nature Medicine. 2017;23:1146.

[41] Mateo M, Reynard S, Baillet N, Carnec X, Fizet A, Jourdain M, et al. One-shot immunization using a Measles/Lassa vaccine fully protects cynomolgus monkeys against Lassa fever. International Journal of Infectious Diseases. 2019;79:6.

[42] Zapata JC, Poonia B, Bryant J, Davis H, Ateh E, George L, et al. An attenuated Lassa vaccine in SIV-infected rhesus macaques does not persist or cause arenavirus disease but does elicit Lassa virus-specific immunity. Virology Journal. 2013;10:52.

[43] Carrion R, Patterson JL, Johnson C, Gonzales M, Moreira CR, Ticer A, et al. A ML29 reassortant virus protects guinea pigs against a distantly related Nigerian strain of Lassa virus and can provide sterilizing immunity. Vaccine. 2007;25:4093-102.

[44] Bond N, Schieffelin JS, Moses LM, Bennett AJ, Bausch DG. A Historical Look at the First Reported Cases of Lassa Fever: IgG Antibodies 40 Years After Acute Infection. The American Journal of Tropical Medicine and Hygiene. 2013;88:241-4.

[45] Buckley SM, Casals J. Lassa Fever, a New Virus Disease of Man from West Africa. The American Journal of Tropical Medicine and Hygiene. 1970;19:680-91.

[46] Speir RW, Wood O, Liebhaber H, Buckley SM. Lassa Fever, a New Virus Disease of Man from West Africa. The American Journal of Tropical Medicine and Hygiene. 1970;19:692-4.

[47] Kerber R, Reindl S, Romanowski V, Gomez RM, Ogbaini-Emovon E, Gunther S, et al. Research efforts to control highly pathogenic arenaviruses: a summary of the progress and gaps. J Clin Virol. 2015;64:120-7.

[48] Lukashevich IS, Djavani M, Shapiro K, Sanchez A, Ravkov E, Nichol ST, et al. The Lassa fever virus L gene: nucleotide sequence, comparison, and precipitation of a predicted 250 kDa protein with monospecific antiserum. Journal of General Virology. 1997;78:547-51.

[49] Vieth S, Torda AE, Asper M, Schmitz H, Günther S. Sequence analysis of L RNA of Lassa virus. Virology. 2004;318:153-68.

[50] Lehmann M, Pahlmann M, Jérôme H, Busch C, Lelke M, Günther S. Role of the C terminus of Lassa virus L protein in viral mRNA synthesis. Journal of virology. 2014;88:8713-7.

[51] Morin B, Coutard B, Lelke M, Ferron F, Kerber R, Jamal S, et al. The N-Terminal Domain of the Arenavirus L Protein Is an RNA Endonuclease Essential in mRNA Transcription. PLOS Pathogens. 2010;6:e1001038.

[52] Fuller-Pace FV, Southern PJ. Detection of virus-specific RNA-dependent RNA polymerase activity in extracts from cells infected with lymphocytic choriomeningitis virus: in vitro synthesis of full-length viral RNA species. Journal of Virology. 1989;63:1938-44.

[53] Hastie KM, King LB, Zandonatti MA, Saphire EO. Structural Basis for the dsRNA Specificity of the Lassa Virus NP Exonuclease. PLOS ONE. 2012;7:e44211.

[54] Hass M, Golnitz U, Muller S, Becker-Ziaja B, Gunther S. Replicon system for Lassa virus. J Virol. 2004;78:13793-803.

[55] Lenz O, ter Meulen J, Klenk HD, Seidah NG, Garten W. The Lassa virus glycoprotein precursor GP-C is proteolytically processed by subtilase SKI-1/S1P. Proc Natl Acad Sci U S A. 2001;98:12701-5.

[56] Xing J, Ly H, Liang Y. The Z Proteins of Pathogenic but Not Nonpathogenic Arenaviruses Inhibit RIG-i-Like Receptor-Dependent Interferon Production. Journal of Virology. 2015;89:2944-55.

[57] Maes P, Alkhovsky SV, Bao Y, Beer M, Birkhead M, Briese T, et al. Taxonomy of the family Arenaviridae and the order Bunyavirales: update 2018. Arch Virol. 2018;163:2295-310.

[58] Fehling SK, Lennartz F, Strecker T. Multifunctional Nature of the Arenavirus RING Finger Protein Z. Viruses. 2012;4:2973.

[59] Balasuriya UBR, Bird B. Chapter 23 - Arenaviridae. In: MacLachlan NJ, Dubovi EJ, editors. Fenner's Veterinary Virology (Fifth Edition). Boston: Academic Press; 2017. p. 425-34.

[60] Brouillette RB, Phillips EK, Patel R, Mahauad-Fernandez W, Moller-Tank S, Rogers KJ, et al. TIM-1 Mediates Dystroglycan-Independent Entry of Lassa Virus. Journal of Virology. 2018;92:e00093-18.

[61] Cohen-Dvashi H, Israeli H, Shani O, Katz A, Diskin R. Role of LAMP1 Binding and pH Sensing by the Spike Complex of Lassa Virus. Journal of Virology. 2016;90:10329-38.

[62] Strecker T, Eichler R, Meulen Jt, Weissenhorn W, Dieter Klenk H, Garten W, et al. Lassa Virus Z Protein Is a Matrix Protein Sufficient for the Release of Virus-Like Particles. Journal of Virology. 2003;77:10700-5.

[63] Urata S, Noda T, Kawaoka Y, Yokosawa H, Yasuda J. Cellular Factors Required for Lassa Virus Budding. Journal of Virology. 2006;80:4191-5.

[64] Peters CJ, Lin C-T, Anderson GW, Jr., Morrill JC, Jahrling PB. Pathogenesis of Viral Hemorrhagic Fevers: Rift Valley Fever and Lassa Fever Contrasted. Reviews of Infectious Diseases. 1989;11:S743-S9.

[65] Urata S, Yasuda J. Molecular Mechanism of Arenavirus Assembly and Budding. Viruses. 2012;4:2049.

[66] Brinkmann V, Reichard U, Goosmann C, Fauler B, Uhlemann Y, Weiss DS, et al. Neutrophil Extracellular Traps Kill Bacteria. Science. 2004;303:1532-5.

[67] Chow OA, von Köckritz-Blickwede M, Bright AT, Hensler ME, Zinkernagel AS, Cogen AL, et al. Statins enhance formation of phagocyte extracellular traps. Cell host & microbe. 2010;8:445-54.

[68] Alberts B, Johnson A, Lewis J, Raff M, Roberts K, Walter P. The Generation of Antibody Diversity. Molecular Biology of the Cell. New York: Garland Science; 2002.

[69] Vivier E, Raulet DH, Moretta A, Caligiuri MA, Zitvogel L, Lanier LL, et al. Innate or Adaptive Immunity? The Example of Natural Killer Cells. Science. 2011;331:44-9.

[70] Sun JC, Beilke JN, Lanier LL. Adaptive immune features of natural killer cells. Nature. 2009;457:557-61.

[71] Schoenberger SP, Toes REM, van der Voort EIH, Offringa R, Melief CJM. T-cell help for cytotoxic T lymphocytes is mediated by CD40–CD40L interactions. Nature. 1998;393:480-3.

[72] Murphy KM, Weaver C, Mowat A, Berg L, Chaplin D, Janeway CA, et al. Janeway's immunobiology. 8th ed: Garland Science; 2012.

[73] Spörri R, Reis e Sousa C. Inflammatory mediators are insufficient for full dendritic cell activation and promote expansion of CD4+ T cell populations lacking helper function. Nature Immunology. 2005;6:163.

[74] Cohen S, Shachar I. Cytokines as regulators of proliferation and survival of healthy and malignant peripheral B cells. Cytokine. 2012;60:13-22.

[75] Fitzgerald ME, Rawling DC, Vela A, Pyle AM. An evolving arsenal: viral RNA detection by RIG-I-like receptors. Current Opinion in Microbiology. 2014;20:76-81.

[76] Kang D-c, Gopalkrishnan RV, Wu Q, Jankowsky E, Pyle AM, Fisher PB. mda-5: An interferon-inducible putative RNA helicase with double-stranded RNA-dependent ATPase

activity and melanoma growth-suppressive properties. Proceedings of the National Academy of Sciences of the United States of America. 2002;99:637-42.

[77] Verhelst J, Hulpiau P, Saelens X. Mx proteins: antiviral gatekeepers that restrain the uninvited. Microbiol Mol Biol Rev. 2013;77:551-66.

[78] Stetson DB, Medzhitov R. Type I Interferons in Host Defense. Immunity. 2006;25:373-81.

[79] Cheng BY, Ortiz-Riano E, de la Torre JC, Martinez-Sobrido L. Arenavirus Genome Rearrangement for the Development of Live Attenuated Vaccines. J Virol. 2015;89:7373-84.

[80] Zuzarte-Luis V, Berciano MT, Lafarga M, Hurlé JM. Caspase redundancy and release of mitochondrial apoptotic factors characterize interdigital apoptosis. Apoptosis. 2006;11:701-15.

[81] von Boehmer H. Positive selection of lymphocytes. Cell. 1994;76:219-28.

[82] Nossal GJV. Negative selection of lymphocytes. Cell. 1994;76:229-39.

[83] Besch R, Poeck H, Hohenauer T, Senft D, Häcker G, Berking C, et al. Proapoptotic signaling induced by RIG-I and MDA-5 results in type I interferon–independent apoptosis in human melanoma cells. The Journal of Clinical Investigation. 2009;119:2399-411.

[84] Lam E, Kato N, Lawton M. Programmed cell death, mitochondria and the plant hypersensitive response. Nature. 2001;411:848.

[85] Fuertes Marraco SA, Scott CL, Bouillet P, Ives A, Masina S, Vremec D, et al. Type I Interferon Drives Dendritic Cell Apoptosis via Multiple BH3-Only Proteins following Activation by PolyIC In Vivo. PLOS ONE. 2011;6:e20189.

[86] Vivier E, Nunès JA, Vély F. Natural Killer Cell Signaling Pathways. Science. 2004;306:1517-9.

[87] Nagata S. Fas Ligand-Induced Apoptosis. Annual Review of Genetics. 1999;33:29-55.

[88] Veugelers K, Motyka B, Goping IS, Shostak I, Sawchuk T, Bleackley RC. Granule-mediated killing by granzyme B and perforin requires a mannose 6-phosphate receptor and is augmented by cell surface heparan sulfate. Molecular biology of the cell. 2006;17:623-33.

[89] Nikolich-Žugich J, Slifka MK, Messaoudi I. The many important facets of T-cell repertoire diversity. Nature Reviews Immunology. 2004;4:123.

[90] Laydon Daniel J, Bangham Charles RM, Asquith B. Estimating T-cell repertoire diversity: limitations of classical estimators and a new approach. Philosophical Transactions of the Royal Society B: Biological Sciences. 2015;370:20140291.

[91] Deftos ML, Huang E, Ojala EW, Forbush KA, Bevan MJ. Notch1 Signaling Promotes the Maturation of CD4 and CD8 SP Thymocytes. Immunity. 2000;13:73-84.

[92] Hu X, Herrero C, Li W-P, Antoniv TT, Falck-Pedersen E, Koch AE, et al. Sensitization of IFN-γ Jak-STAT signaling during macrophage activation. Nature Immunology. 2002;3:859.

[93] Ahmed KA, Wang L, Munegowda MA, Mulligan SJ, Gordon JR, Griebel P, et al. Direct in vivo evidence of CD4+ T cell requirement for CTL response and memory via pMHC-I targeting and CD40L signaling. Journal of Leukocyte Biology. 2012;92:289-300.

[94] Delamarre L, Holcombe H, Mellman I. Presentation of exogenous antigens on major histocompatibility complex (MHC) class I and MHC class II molecules is differentially regulated during dendritic cell maturation. The Journal of experimental medicine. 2003;198:111-22.

[95] Castellino F, Huang AY, Altan-Bonnet G, Stoll S, Scheinecker C, Germain RN. Chemokines enhance immunity by guiding naive CD8+ T cells to sites of CD4+ T cell–dendritic cell interaction. Nature. 2006;440:890.

[96] Tham EL, Shrikant P, Mescher MF. Activation-Induced Nonresponsiveness: A Th-Dependent Regulatory Checkpoint in the CTL Response. The Journal of Immunology. 2002;168:1190-7.

[97] Gérard A, Khan O, Beemiller P, Oswald E, Hu J, Matloubian M, et al. Secondary T cell–T cell synaptic interactions drive the differentiation of protective CD8+ T cells. Nature Immunology. 2013;14:356.

[98] Li S, Gowans EJ, Chougnet C, Plebanski M, Dittmer U. Natural Regulatory T Cells and Persistent Viral Infection. Journal of Virology. 2008;82:21-30.

[99] Coffin KM, Liu J, Warren TK, Blancett CD, Kuehl KA, Nichols DK, et al. Persistent Marburg Virus Infection in the Testes of Nonhuman Primate Survivors. Cell Host & Microbe. 2018;24:405-16.e3.

[100] Sabbagh P, Karkhah A, Nouri HR, Javanian M, Ebrahimpour S. The significance role of regulatory T cells in the persistence of infections by intracellular bacteria. Infection, genetics and evolution : journal of molecular epidemiology and evolutionary genetics in infectious diseases. 2018;62:270-4.

[101] Youngblood B, Hale JS, Kissick HT, Ahn E, Xu X, Wieland A, et al. Effector CD8 T cells dedifferentiate into long-lived memory cells. Nature. 2017;552:404.

[102] Pollizzi KN, Sun I-H, Patel CH, Lo Y-C, Oh M-H, Waickman AT, et al. Asymmetric inheritance of mTORC1 kinase activity during division dictates CD8+ T cell differentiation. Nature Immunology. 2016;17:704.

[103] Kim EH, Sullivan JA, Plisch EH, Tejera MM, Jatzek A, Choi KY, et al. Signal integration by Akt regulates CD8 T cell effector and memory differentiation. Journal of immunology (Baltimore, Md : 1950). 2012;188:4305-14.

[104] Badovinac VP, Porter BB, Harty JT. Programmed contraction of CD8(+) T cells after infection. Nat Immunol. 2002;3:619-26.

[105] Rosshart S, Hofmann M, Schweier O, Pfaff A-K, Yoshimoto K, Takeuchi T, et al. Interaction of KLRG1 with E-cadherin: New functional and structural insights. European Journal of Immunology. 2008;38:3354-64.

[106] Henson SM, Akbar AN. KLRG1--more than a marker for T cell senescence. Age (Dordr). 2009;31:285-91.

[107] Gründemann C, Schwartzkopff S, Koschella M, Schweier O, Peters C, Voehringer D, et al. The NK receptor KLRG1 is dispensable for virus-induced NK and CD8+ T-cell differentiation and function in vivo. European Journal of Immunology. 2010;40:1303-14.

[108] Joshi NS, Cui W, Chandele A, Lee HK, Urso DR, Hagman J, et al. Inflammation Directs Memory Precursor and Short-Lived Effector CD8+ T Cell Fates via the Graded Expression of T-bet Transcription Factor. Immunity. 2007;27:281-95.

[109] Blair HA, Deeks ED. Abatacept: A Review in Rheumatoid Arthritis. Drugs. 2017;77:1221-33.

[110] Camacho LH. CTLA-4 blockade with ipilimumab: biology, safety, efficacy, and future considerations. Cancer medicine. 2015;4:661-72.

[111] Alegre ML, Noel PJ, Eisfelder BJ, Chuang E, Clark MR, Reiner SL, et al. Regulation of surface and intracellular expression of CTLA4 on mouse T cells. The Journal of Immunology. 1996;157:4762-70.

[112] Tivol EA, Borriello F, Schweitzer AN, Lynch WP, Bluestone JA, Sharpe AH. Loss of CTLA-4 leads to massive lymphoproliferation and fatal multiorgan tissue destruction, revealing a critical negative regulatory role of CTLA-4. Immunity. 1995;3:541-7.

[113] Wherry EJ, Ha S-J, Kaech SM, Haining WN, Sarkar S, Kalia V, et al. Molecular Signature of $CD8^+$ T Cell Exhaustion during Chronic Viral Infection. Immunity. 2007;27:670-84.

[114] Lindsten T, Lee KP, Harris ES, Petryniak B, Craighead N, Reynolds PJ, et al. Characterization of CTLA-4 structure and expression on human T cells. The Journal of Immunology. 1993;151:3489.

[115] Perkins D, Wang Z, Donovan C, He H, Mark D, Guan G, et al. Regulation of CTLA-4 expression during T cell activation. The Journal of Immunology. 1996;156:4154.

[116] Ahn E, Araki K, Hashimoto M, Li W, Riley JL, Cheung J, et al. Role of PD-1 during effector CD8 T cell differentiation. Proceedings of the National Academy of Sciences. 2018;115:4749-54.

[117] Barber DL, Wherry EJ, Masopust D, Zhu B, Allison JP, Sharpe AH, et al. Restoring function in exhausted CD8 T cells during chronic viral infection. Nature. 2005;439:682.

[118] Reck M, Rodríguez-Abreu D, Robinson AG, Hui R, Csőszi T, Fülöp A, et al. Pembrolizumab versus Chemotherapy for PD-L1–Positive Non–Small-Cell Lung Cancer. New England Journal of Medicine. 2016;375:1823-33.

[119] Krieg C, Nowicka M, Guglietta S, Schindler S, Hartmann FJ, Weber LM, et al. High-dimensional single-cell analysis predicts response to anti-PD-1 immunotherapy. Nature Medicine. 2018;24:144.

[120] Mills CD, Ley K. M1 and M2 macrophages: the chicken and the egg of immunity. J Innate Immun. 2014;6:716-26.

[121] Collin M, Bigley V. Human dendritic cell subsets: an update. Immunology. 2018;154:3-20.

[122] Patente TA, Pinho MP, Oliveira AA, Evangelista GCM, Bergami-Santos PC, Barbuto JAM. Human Dendritic Cells: Their Heterogeneity and Clinical Application Potential in Cancer Immunotherapy. Front Immunol. 2018;9:3176.

[123] Reizis B, Bunin A, Ghosh HS, Lewis KL, Sisirak V. Plasmacytoid dendritic cells: recent progress and open questions. Annu Rev Immunol. 2011;29:163-83.

[124] Mahanty S, Hutchinson K, Agarwal S, Mcrae M, Rollin PE, Pulendran B. Cutting Edge: Impairment of Dendritic Cells and Adaptive Immunity by Ebola and Lassa Viruses. The Journal of Immunology. 2003;170:2797-801.

[125] Lüdtke A, Ruibal P, Wozniak DM, Pallasch E, Wurr S, Bockholt S, et al. Ebola virus infection kinetics in chimeric mice reveal a key role of T cells as barriers for virus dissemination. Scientific Reports. 2017;7:43776.

[126] Edelson Brian T, Bradstreet Tara R, Hildner K, Carrero Javier A, Frederick Katherine E, Kc W, et al. CD8α+ Dendritic Cells Are an Obligate Cellular Entry Point for Productive Infection by Listeria monocytogenes. Immunity. 2011;35:236-48.

[127] Pythoud C, Rodrigo WWSI, Pasqual G, Rothenberger S, Martínez-Sobrido L, de la Torre JC, et al. Arenavirus Nucleoprotein Targets Interferon Regulatory Factor-Activating Kinase IKKε. Journal of Virology. 2012;86:7728-38.

[128] Rodrigo WWSI, Ortiz-Riaño E, Pythoud C, Kunz S, de la Torre JC, Martínez-Sobrido L. Arenavirus Nucleoproteins Prevent Activation of Nuclear Factor Kappa B. Journal of Virology. 2012;86:8185-97.

[129] Miethke T, Duschek K, Wahl C, And KH, Wagner H. Pathogenesis of the toxic shock syndrome: T cell mediated lethal shock caused by the superantigen TSST-1. European Journal of Immunology. 1993;23:1494-500.

[130] Kemp SF, Lockey RF. Anaphylaxis: A review of causes and mechanisms. Journal of Allergy and Clinical Immunology. 2002;110:341-8.

[131] Teijaro JR, Walsh KB, Rice S, Rosen H, Oldstone MBA. Mapping the innate signaling cascade essential for cytokine storm during influenza virus infection. Proceedings of the National Academy of Sciences. 2014;111:3799-804.

[132] WHO. Avian Influenza A (H5N1) Infection in Humans. New England Journal of Medicine. 2005;353:1374-85.

[133] Srikiatkhachorn A, Mathew A, Rothman AL. Immune-mediated cytokine storm and its role in severe dengue. Seminars in immunopathology. 2017;39:563-74.

[134] Kerber R, Krumkamp R, Korva M, Rieger T, Wurr S, Duraffour S, et al. Kinetics of Soluble Mediators of the Host Response in Ebola Virus Disease. The Journal of Infectious Diseases. 2018;218:S496-S503.

[135] Branco LM, Grove JN, Boisen ML, Shaffer JG, Goba A, Fullah M, et al. Emerging trends in Lassa fever: redefining the role of immunoglobulin M and inflammation in diagnosing acute infection. Virology Journal. 2011;8:478.

[136] Robert C, Schachter J, Long GV, Arance A, Grob JJ, Mortier L, et al. Pembrolizumab versus Ipilimumab in Advanced Melanoma. New England Journal of Medicine. 2015;372:2521-32.

[137] Comi G, Radaelli M, Soelberg Sørensen P. Evolving concepts in the treatment of relapsing multiple sclerosis. The Lancet. 2017;389:1347-56.

[138] Chang JT, Wherry EJ, Goldrath AW. Molecular regulation of effector and memory T cell differentiation. Nat Immunol. 2014;15:1104-15.

[139] Steinberg P, Fischer T, Kiulies S, Biefang K, Platt K-L, Oesch F, et al. Drug Metabolizing Capacity of Cryopreserved Human, Rat, and Mouse Liver Parenchymal Cells in Suspension. Drug Metabolism and Disposition. 1999;27:1415.

[140] Terry C, Dhawan A, Mitry RR, Lehec SC, Hughes RD. Optimization of the cryopreservation and thawing protocol for human hepatocytes for use in cell transplantation. Liver Transpl. 2010;16:229-37.

[141] Honge BL, Petersen MS, Olesen R, Moller BK, Erikstrup C. Optimizing recovery of frozen human peripheral blood mononuclear cells for flow cytometry. PLoS One. 2017;12:e0187440.

[142] Ruibal P, Oestereich L, Ludtke A, Becker-Ziaja B, Wozniak DM, Kerber R, et al. Unique human immune signature of Ebola virus disease in Guinea. Nature. 2016;533:100-4.

[143] Baize S, Kaplon J, Faure C, Pannetier D, Georges-Courbot MC, Deubel V. Lassa virus infection of human dendritic cells and macrophages is productive but fails to activate cells. Journal of Immunology. 2004;172:2861-9.

[144] Gessani S, Conti L, Del Corno M, Belardelli F. Type I interferons as regulators of human antigen presenting cell functions. Toxins (Basel). 2014;6:1696-723.

[145] Flatz L, Rieger T, Merkler D, Bergthaler A, Regen T, Schedensack M, et al. T Cell-Dependence of Lassa Fever Pathogenesis. PLOS Pathogens. 2010;6:e1000836.

[146] Yun NE, Seregin AV, Walker DH, Popov VL, Walker AG, Smith JN, et al. Mice lacking functional STAT1 are highly susceptible to lethal infection with Lassa virus. J Virol. 2013;87:10908-11.

[147] McElroy AK, Akondy RS, Harmon JR, Ellebedy AH, Cannon D, Klena JD, et al. A Case of Human Lassa Virus Infection With Robust Acute T-Cell Activation and Long-Term Virus-Specific T-Cell Responses. J Infect Dis. 2017;215:1862-72.

[148] Whitsett JA, Alenghat T. Respiratory epithelial cells orchestrate pulmonary innate immunity. Nature Immunology. 2014;16:27.

[149] Klinkhammer J, Schnepf D, Ye L, Schwaderlapp M, Gad HH, Hartmann R, et al. IFN-lambda prevents influenza virus spread from the upper airways to the lungs and limits virus transmission. Elife. 2018;7.

[150] Halle S, Dujardin HC, Bakocevic N, Fleige H, Danzer H, Willenzon S, et al. Induced bronchus-associated lymphoid tissue serves as a general priming site for T cells and is maintained by dendritic cells. J Exp Med. 2009;206:2593-601.

[151] Duan S, Thomas PG. Balancing Immune Protection and Immune Pathology by CD8(+) T-Cell Responses to Influenza Infection. Front Immunol. 2016;7:25.

[152] Fung-Leung WP, Kundig TM, Zinkernagel RM, Mak TW. Immune response against lymphocytic choriomeningitis virus infection in mice without CD8 expression. J Exp Med. 1991;174:1425-9.

[153] Mongkolsapaya J, Dejnirattisai W, Xu X-n, Vasanawathana S, Tangthawornchaikul N, Chairunsri A, et al. Original antigenic sin and apoptosis in the pathogenesis of dengue hemorrhagic fever. Nature Medicine. 2003;9:921-7.

[154] Haeryfar SMM, DiPaolo RJ, Tscharke DC, Bennink JR, Yewdell JW. Regulatory T Cells Suppress CD8+ T Cell Responses Induced by Direct Priming and Cross-Priming and Moderate Immunodominance Disparities. The Journal of Immunology. 2005;174:3344-51.

[155] Holderried TA, Lang PA, Kim HJ, Cantor H. Genetic disruption of CD8+ Treg activity enhances the immune response to viral infection. Proc Natl Acad Sci U S A. 2013;110:21089-94.

[156] Bar-On L, Jung S. Defining In Vivo Dendritic Cell Functions Using CD11c-DTR Transgenic Mice. In: Naik SH, editor. Dendritic Cell Protocols. Totowa, NJ: Humana Press; 2010. p. 429-42.

[157] Schümann J, Wolf D, Pahl A, Brune K, Papadopoulos T, van Rooijen N, et al. Importance of Kupffer Cells for T-Cell-Dependent Liver Injury in Mice. The American Journal of Pathology. 2000;157:1671-83.

[158] Feldmann H, Bugany H, Mahner F, Klenk HD, Drenckhahn D, Schnittler HJ. Filovirus-induced endothelial leakage triggered by infected monocytes/macrophages. Journal of Virology. 1996;70:2208-14.

[159] Abraham RT, Wiederrecht GJ. IMMUNOPHARMACOLOGY OF RAPAMYCIN. Annual Review of Immunology. 1996;14:483-510.

[160] Baize S, Pannetier D, Faure C, Marianneau P, Marendat I, Georges-Courbot M-C, et al. Role of interferons in the control of Lassa virus replication in human dendritic cells and macrophages. Microbes and Infection. 2006;8:1194-202.

[161] Macal M, Lewis GM, Kunz S, Flavell R, Harker JA, Zuniga EI. Plasmacytoid dendritic cells are productively infected and activated through TLR-7 early after arenavirus infection. Cell Host Microbe. 2012;11:617-30.

[162] Hensley LE, Smith MA, Geisbert JB, Fritz EA, Daddario-DiCaprio KM, Larsen T, et al. Pathogenesis of lassa fever in cynomolgus macaques. Virology Journal. 2011;8:205.

[163] Sommerstein R, Flatz L, Remy MM, Malinge P, Magistrelli G, Fischer N, et al. Arenavirus Glycan Shield Promotes Neutralizing Antibody Evasion and Protracted Infection. PLoS Pathog. 2015;11:e1005276.

[164] Lee AM, Cruite J, Welch MJ, Sullivan B, Oldstone MB. Pathogenesis of Lassa fever virus infection: I. Susceptibility of mice to recombinant Lassa Gp/LCMV chimeric virus. Virology. 2013;442:114-21.

[165] Sullivan BM, Emonet SF, Welch MJ, Lee AM, Campbell KP, de la Torre JC, et al. Point mutation in the glycoprotein of lymphocytic choriomeningitis virus is necessary for receptor binding, dendritic cell infection, and long-term persistence. Proc Natl Acad Sci U S A. 2011;108:2969-74.

[166] Korns Johnson D, Homann D. Accelerated and improved quantification of lymphocytic choriomeningitis virus (LCMV) titers by flow cytometry. PLoS One. 2012;7:e37337.

[167] Durbeej M, Henry MD, Ferletta M, Campbell KP, Ekblom P. Distribution of Dystroglycan in Normal Adult Mouse Tissues. Journal of Histochemistry & Cytochemistry. 1998;46:449-57.

[168] Sevilla N, Kunz S, Holz A, Lewicki H, Homann D, Yamada H, et al. Immunosuppression and resultant viral persistence by specific viral targeting of dendritic cells. J Exp Med. 2000;192:1249-60.

[169] Guilliams M, De Kleer I, Henri S, Post S, Vanhoutte L, De Prijck S, et al. Alveolar macrophages develop from fetal monocytes that differentiate into long-lived cells in the first week of life via GM-CSF. The Journal of Experimental Medicine. 2013;210:1977-92.

[170] Gibbings SL, Goyal R, Desch AN, Leach SM, Prabagar M, Atif SM, et al. Transcriptome analysis highlights the conserved difference between embryonic and postnatal-derived alveolar macrophages. Blood. 2015;126:1357-66.

[171] Matloubian M, Kolhekar SR, Somasundaram T, Ahmed R. Molecular determinants of macrophage tropism and viral persistence: importance of single amino acid changes in the polymerase and glycoprotein of lymphocytic choriomeningitis virus. Journal of Virology. 1993;67:7340-9.

[172] Borrow P, Evans CF, Oldstone MB. Virus-induced immunosuppression: immune system-mediated destruction of virus-infected dendritic cells results in generalized immune suppression. Journal of Virology. 1995;69:1059-70.

[173] Zinkernagel RM, Planz O, Ehl S, Battegay M, Odermatt B, Klenerman P, et al. General and specific immunosuppression caused by antiviral T-cell responses. Immunological Reviews. 1999;168:305-15.

[174] Branco LM, Boisen ML, Andersen KG, Grove JN, Moses LM, Muncy IJ, et al. Lassa hemorrhagic fever in a late term pregnancy from northern sierra leone with a positive maternal outcome: case report. Virology Journal. 2011;8:404.

[175] Baize S, Marianneau P, Loth P, Reynard S, Journeaux A, Chevallier M, et al. Early and strong immune responses are associated with control of viral replication and recovery in lassa virus-infected cynomolgus monkeys. J Virol. 2009;83:5890-903.

[176] Paine A, Kirchner H, Immenschuh S, Oelke M, Blasczyk R, Eiz-Vesper B. IL-2 upregulates CD86 expression on human CD4(+) and CD8(+) T cells. J Immunol. 2012;188:1620-9.

[177] Radziewicz H, Ibegbu CC, Hon H, Bedard N, Bruneau J, Workowski KA, et al. Transient CD86 expression on hepatitis C virus-specific CD8+ T cells in acute infection is linked to sufficient IL-2 signaling. J Immunol. 2010;184:2410-22.

[178] Azuma M, Ito D, Yagita H, Okumura K, Phillips JH, Lanier LL, et al. B70 antigen is a second ligand for CTLA-4 and CD28. Nature. 1993;366:76-9.

[179] Johnson S, Bergthaler A, Graw F, Flatz L, Bonilla WV, Siegrist CA, et al. Protective efficacy of individual CD8+ T cell specificities in chronic viral infection. J Immunol. 2015;194:1755-62.

[180] Urbani S, Amadei B, Tola D, Massari M, Schivazappa S, Missale G, et al. PD-1 expression in acute hepatitis C virus (HCV) infection is associated with HCV-specific CD8 exhaustion. J Virol. 2006;80:11398-403.

[181] Hafalla JC, Claser C, Couper KN, Grau GE, Renia L, de Souza JB, et al. The CTLA-4 and PD-1/PD-L1 inhibitory pathways independently regulate host resistance to Plasmodium-induced acute immune pathology. PLoS Pathog. 2012;8:e1002504.

Diese Version der Dissertationsschrift enthält im Vergleich zur Prüfungsversion orthographische, grammatikalische und syntaktische Überarbeitungen zur Verbesserung des Leseflusses und Verständnisses. Zusätzliche Literaturnachweise wurden zugefügt. Ergebnisse, Grafiken und Aussagen bleiben unverändert. Die ausführliche Danksagung wurde zum Schutz der informationellen Selbstbestimmung vor der Veröffentlichung entfernt.

This work is licensed under the Creative Commons Attribution-ShareAlike 4.0 International License.
To view a copy of this license, visit http://creativecommons.org/licenses/by-sa/4.

Publication list David Maximilian Wozniak

2020

The Utility of Human Immune System Mice for High-Containment Viral Hemorrhagic Fever Research
Wozniak, D.M.; Lavender, K.J.; Prescott, J.; Spengler, J.R. *Vaccines* 2020, *8*(1), 98; https://doi.org/10.3390/vaccines8010098

2019

Metagenomic sequencing at the epicenter of the Nigeria 2018 Lassa fever outbreak.
Kafetzopoulou LE, Pullan ST, Lemey P, Suchard MA, Ehichioya DU, Pahlmann M, Thielebein A, Hinzmann J, Oestereich L, **Wozniak DM**, Efthymiadis K, Schachten D, Koenig F, Matjeschk J, Lorenzen S, Lumley S, Ighodalo Y, Adomeh DI, Olokor T, Omomoh E, Omiunu R, Agbukor J, Ebo B, Aiyepada J, Ebhodaghe P, Osiemi B, Ehikhametalor S, Akhilomen P, Airende M, Esumeh R, Muoebonam E, Giwa R, Ekanem A, Igenegbale G, Odigie G, Okonofua G, Enigbe R, Oyakhilome J, Yerumoh EO, Odia I, Aire C, Okonofua M, Atafo R, Tobin E, Asogun D, Akpede N, Okokhere PO, Rafiu MO, Iraoyah KO, Iruolagbe CO, Akhideno P, Erameh C, Akpede G, Isibor E, Naidoo D, Hewson R, Hiscox JA, Vipond R, Carroll MW, Ihekweazu C, Formenty P, Okogbenin S, Ogbaini-Emovon E, Günther S, Duraffour S. Science. 2019 Jan 4;363(6422):74-77. doi:10.1126/science.aau9343.

2017

Different features of Vδ2 T and NK cells in fatal and non-fatal human Ebola infections. Cimini E, Viola D, Cabeza-Cabrerizo M, Romanelli A, Tumino N, Sacchi A, Bordoni V, Casetti R, Turchi F, Martini F, Bore JA, Koundouno FR, Duraffour S, Michel J, Holm T, Zekeng EG, Cowley L, Garcia Dorival I, Doerrbecker J, Hetzelt N, Baum JHJ, Portmann J, Wölfel R, Gabriel M, Miranda O, Díaz G, Díaz JE, Fleites YA, Piñeiro CA, Castro CM, Koivogui L, Magassouba N, Diallo B, Ruibal P, Oestereich L**, Wozniak DM**, Lüdtke A, Becker-Ziaja B, Capobianchi MR, Ippolito G, Carroll MW, Günther S, Di Caro A, Muñoz-Fontela C, Agrati C. PLoS Negl Trop Dis. 2017 May 30;11(5):e0005645.

Ebola virus infection kinetics in chimeric mice reveal a key role of T cells as barriers for virus dissemination. Lüdtke A, Ruibal P, **Wozniak DM**, Pallasch E, Wurr S, Bockholt S, Gómez-Medina S, Qiu X, Kobinger GP, Rodríguez E, Günther S, Krasemann S, Idoyaga J, Oestereich L, Muñoz-Fontela C. Sci Rep. 2017 Mar 3;7:43776

2016

Protective and Pathogenic Roles of CD8+ T Lymphocytes in Murine *Orientia tsutsugamushi* Infection. Hauptmann M, Kolbaum J, Lilla S, **Wozniak DM**, Gharaibeh M, Fleischer B & Keller CA. (2016) PLoS Negl Trop Dis 10(9): e0004991. https://doi.org/10.1371/journal.pntd.0004991

Ebola Virus Disease Is Characterized by Poor Activation and Reduced Levels of Circulating CD16+ Monocytes. Lüdtke A, Ruibal P, Becker-Ziaja B, Rottstegge M**, Wozniak DM**, Cabeza-Cabrerizo M, Thorenz A, Weller R, Kerber R, Idoyaga J, Magassouba N, Gabriel M, Günther S, Oestereich L, Muñoz-Fontela C. J Infect Dis. 2016 Oct 15;214(suppl 3):S275-S280.

Unique human immune signature of Ebola virus disease in Guinea. Ruibal P, Oestereich L, Lüdtke A, Becker-Ziaja B, **Wozniak DM**, Kerber R, Korva M, Cabeza-Cabrerizo M, Bore JA, Koundouno FR, Duraffour S, Weller R, Thorenz A, Cimini E, Viola D, Agrati C, Repits J, Afrough B, Cowley LA, Ngabo D, Hinzmann J, Mertens M, Vitoriano I, Logue CH, Boettcher JP, Pallasch E, Sachse A, Bah A, Nitzsche K, Kuisma E, Michel J, Holm T, Zekeng EG, García-Dorival I, Wölfel R, Stoecker K, Fleischmann E, Strecker T, Di Caro A, Avšič-Županc T, Kurth A, Meschi S, Mély S, Newman E, Bocquin A, Kis Z, Kelterbaum A, Molkenthin P, Carletti F, Portmann J, Wolff S, Castilletti C, Schudt G, Fizet A, Ottowell LJ, Herker E, Jacobs T, Kretschmer B, Severi E, Ouedraogo N, Lago M, Negredo A, Franco L, Anda P, Schmiedel S, Kreuels B, Wichmann D, Addo MM, Lohse AW, De Clerck H, Nanclares C, Jonckheere S, Van Herp M, Sprecher A, Xiaojiang G, Carrington M, Miranda O, Castro CM, Gabriel M, Drury P, Formenty P, Diallo B, Koivogui L, Magassouba N, Carroll MW, Günther S, Muñoz-Fontela C. Nature. 2016 May 5;533(7601):100-4.